

Optimal Design and Analysis of Grid-Connected Solar Photovoltaic Systems

Hassan Zuhair Al Garni

A Thesis

In the Department

Of

Concordia Institute for Information Systems Engineering (CIISE)

Presented in Partial Fulfillment of the Requirements

For the Degree of

Doctor of Philosophy (Information & Systems Engineering)

Concordia University

Montreal, Quebec, Canada

July 2018

© Hassan Zuhair Al Garni, 2018

CONCORDIA UNIVERSITY

School of Graduate Studies

This is to certify the thesis prepared

By: **Hassan Zuhair Al Garni**

Entitled: **Optimal Design and Analysis of Grid-Connected Solar Photovoltaic Systems**

and submitted in partial fulfillment of the requirements for the degree of

Doctor of Philosophy (Information & Systems Engineering)

complies with the regulations of the University and meets with the accepted standards with respect to originality and quality.

Signed by the final examining committee:

_____ Chair
Dr. Catherine Mulligan

_____ External Examiner
Dr. Amrish Chandra

_____ External to program
Dr. Fuzhan Nasiri

_____ Examiner
Dr. Abdessamad Ben Hamza

_____ Examiner
Dr. Arash Mohammadi

_____ Supervisor
Dr. Anjali Awasthi

Approved by _____
Dr. Abdessamad Ben Hamza, Director, Concordia Institute for Information Systems Engineering

July 27, 2018

Dr. Amir Asif
Dean, Faculty of Engineering and Computer Science

ABSTRACT

Optimal Design and Analysis of Grid-Connected Solar Photovoltaic Systems

Hassan Zuhair Al Garni, Ph.D.

Concordia University, 2018

Many countries consider utilizing renewable energy sources such as solar photovoltaic (PV), wind, and biomass to boost their potential for more clean and sustainable development and to gain revenues by export. In this thesis, a top-down approach of solar PV planning and optimization methodology is developed to enable high-performance at minimum costs. The first problem evaluates renewable resources and prioritizes their importance towards sustainable power generation. In the second problem, possible sites for solar PV potential are examined. In the third problem, optimal design of a grid-connected solar PV system is performed using HOMER software. A techno-economic feasibility of different system configurations including seven designs of tracking systems is conducted. In the fourth and the final problem, the optimal tilt and azimuth angles for maximum solar power generation are found. Using a detailed estimation model coded in MATLAB software, the solar irradiation on a tilted angle was estimated using a ground measurement of solar irradiation on a horizontal surface. A case study for Saudi Arabia is conducted.

The results of our prioritization study show solar PV followed by concentrated solar power are the most favorable technologies followed by wind energy. Using a real climatology and legislation data, such as roads, mountains, and protected areas, land suitability is determined via AHP-GIS model. The overlaid result suitability map shows that 16% (300,000 km²) of the study area is promising for deploying utility-size PV power plants in the north and northwest of Saudi Arabia. The optimal PV system design for Makkah, Saudi Arabia shows that the two-axis tracker can

produce 34% more power than the fixed system. Horizontal tracker with continuous adjustment shows the highest net present cost (NPC) and the highest levelized cost of energy (LCOE), with a high penetration of solar energy to the grid. At different tilt and azimuth angles, the solar irradiation, potential power, and system revenue were calculated for 18 cities in Saudi Arabia. For Riyadh city (high suitable site), the monthly adjustment increases the harvested solar energy by 4%. It is recommended to adjust the tilt angle five times per year to achieve near-optimal results and minimize the cost associated with workforce or solar trackers for monthly adjustments. The proposed work can be exploited by decision-makers in the solar energy area for optimal design and analysis of grid-connected solar photovoltaic systems.

Acknowledgments

First and foremost, I am grateful to ALLAH who helped and supported me to accomplish this Ph.D. work. I would like to express my heartfelt thanks to my supervisor, Dr. Anjali Awasthi for her academic and emotional support since day one. She assisted me at various stages of the thesis progress and guided me on the right track especially where I had reached the ‘crossroads’. During the most challenging times of writing this thesis, she provided me with moral support and gave full freedom to pursue my research interest. I am also thankful to my Ph.D. committee members for their great support and invaluable advice.

I gratefully acknowledge the financial support from The Royal Commission of Jubail and Yanbu (Jubail Industrial College) under their scholarship program through Saudi Cultural Bureau in Ottawa. This work would not have been possible without the collaboration from King Abdullah City for Atomic and Renewable Energy (K.A.Care) and Saudi Electric Company (SEC) by providing required data for my thesis.

I have special friends to thank: Yasir Alharthi, Faisal Alhumaidi and Mishaal Alkaabi whom I consider my best friends through this journey and beyond. I would like to offer special thanks to my cousin and high-school teacher Mr. Ali Jaber who, although no longer with us, for encouraging me to pursue a Ph.D. degree. He has indeed shaped my career in a positive direction and continues to inspire me by his example and dedication to serving our community. I also would like to thank my father-in-law (Mr. Zuhair Abdullah) and mother-in-law (Mrs. Salhah Abdullah) for their endless support and help towards me and my family.

An exceptional thanks to my mother (Salhah), to the memory of my father (Zuhair) who raised me with a love of science and supported me in all my pursuits. To my brothers and sisters, thank you for all your support. Finally, I would like to thank my family for their everlasting love and

unconditional support. To my dear wife Tahani who has been a constant source of energy and encouragement through thick and thin; and to my playful kids: Muhannad, Hatem, and Reema for their continuous support and unconditional love.

*I dedicate this thesis to my mother, the memory of my father. To my wife Tahani, and my kids:
Muhannad, Hatem, and Reema*

Contents

List of Figures	xi
List of Tables	xiv
Abbreviations	xvi
Chapter 1 Introduction	1
1.1. Overview and Motivation.....	1
1.2. Research Problems	4
1.3. Thesis Approach and Contributions.....	5
1.4. Tools Used.....	8
1.5. Thesis Organization.....	8
Chapter 2 Renewable Energy Selection.....	9
2.1. Introduction	9
2.2. Problem Statement	11
2.3. Renewable Energy Options.....	12
2.3.1. Solar energy	13
2.3.2. Wind energy.....	15
2.3.3. Geothermal energy.....	16
2.3.4. Biomass energy.....	16
2.4. Methodology	17
2.4.1. Alternatives identification.....	18
2.4.2. Analytical hierarchy process model.....	19
2.4.3. Establishing criteria and sub-criteria	21
2.5. Model Application.....	32
2.6. Results and Discussion.....	35
2.7. Sensitivity Analysis.....	39
2.8. Conclusions	43
Chapter 3 Solar PV Power Plant Site Selection.....	46
3.1. Introduction	46
3.2. Problem Statement	47

3.3.	Literature Review	49
3.3.1.	Decision criteria and restriction factors	49
3.3.2.	Methods in solar site selection	52
3.4.	Proposed Methodology	56
3.4.1.	Criteria for site selection	58
3.4.2.	Restrictions for site selection	62
3.4.3.	PV power plants site selection	64
3.5.	Case Study	70
3.5.1.	Screening potential sites	72
3.5.2.	Site selection results	73
3.5.3.	Sensitivity analysis	76
3.6.	Conclusions	80
Chapter 4 Optimal Solar PV System Design		82
4.1.	Introduction	82
4.2.	Problem Definition	85
4.3.	Literature Review	88
4.4.	System under Consideration	92
4.4.1.	Metrological data	93
4.4.2.	Load profile	96
4.4.3.	Grid and renewable energy feed-in-tariff	98
4.4.4.	Optimal design of solar PV grid-connected system	100
4.5.	Results Discussion	104
4.5.1.	Impact of various tracking designs on technical performance	104
4.5.2.	Impact of various tracking designs on system economics	110
4.6.	Conclusions	113
Chapter 5 Determining Optimal Solar PV Orientation		116
5.1.	Introduction	116
5.2.	Problem Statement	117
5.3.	Literature Review	119
5.4.	Methodology	121
5.4.1.	Input data	123

5.4.2.	Solar angles equations.....	123
5.4.3.	Computing the impact of solar irradiation on solar PV	127
5.5.	Results	130
5.5.1.	Annual optimal orientation and energy yield.....	130
5.5.2.	Monthly orientation adjustments	132
5.5.3.	Proposed orientation adjustment scheme.....	135
5.5.4.	Results validation and optimal annual orientation for 18 cities in Saudi Arabia..	141
5.6.	Conclusions	144
Chapter 6 Conclusions and Future Directions		145
6.1.	Conclusions	145
6.2.	Future Work	146
Bibliography		149

List of Figures

Figure 1.1. Distribution of renewable energy technologies in relation to installed capacity [3].....	2
Figure 1.2. Renewable energy share in global power production by the end of 2016 [4].....	2
Figure 1.3. Share of grid-connected and off-grid installations 2000-2015 [7].....	3
Figure 1.4. The general thesis approach	4
Figure 2.1. Electricity consumption per capita in selected countries [7].....	10
Figure 2.2. Average GHI (left) and DNI (right) for Saudi Arabia [22].....	14
Figure 2.3. Proposed approach to evaluate renewable energy resources.....	18
Figure 2.4. Analytical hierarchy process diagram	24
Figure 2.5. Global priority weights of sub-criteria with respect to goal.....	36
Figure 2.6. Local weights of alternatives under each decision criterion	37
Figure 2.7. Priority weight of renewable energy alternatives.....	39
Figure 2.8. Criteria weights and Alternatives ratings considering the proposed approach	40
Figure 2.9. Equal criteria weights scenario and Alternatives ratings	40
Figure 2.10. Performance sensitivity of alternatives with higher economic criteria (40%)	41
Figure 2.11. Evaluation of each sub-criterion by experts' categories.....	43
Figure 3.1. Components of Solar irradiation intercepted by earth surface [132]	51
Figure 3.2. Flowchart of the proposed methodology	57
Figure 3.3. Criteria maps applied in the proposed GIS-MCDM.....	59
Figure 3.4. Protected areas.....	63
Figure 3.5. Restrictions part of the model.....	64
Figure 3.6. Decision criteria considered in solar site selection.....	67
Figure 3.7. The priority weights of the criteria.....	69
Figure 3.8. The annual global horizontal irradiance among selected countries.....	71
Figure 3.9. Restrictions layer map	72
Figure 3.10. Preliminary results of potential sites	73
Figure 3.11. Suitability Index results using AHP weights.....	74
Figure 3.12. Land suitability distribution	76
Figure 3.13. Weights of decision criteria considering different scenarios	77

Figure 3.14. Suitability Index distribution for equal weights scenario.....	78
Figure 3.15. Suitability results: equal weights (left) and higher weights to economic (right)	79
Figure 4.1. Fuel types used in electricity production in Saudi Arabia in 2013.....	82
Figure 4.2. The relation between load demand and GHI in Makkah City.....	88
Figure 4.3. The tilt and azimuth angles of the solar panel [208]	91
Figure 4.4. Proposed steps for optimal sizing of PV grid connected system	93
Figure 4.5. The monthly average GHI in Makkah.....	94
Figure 4.6. The monthly average temperature	95
Figure 4.7. Histogram graph of temperature data of Makkah.....	95
Figure 4.8. The annual average electrical load of Makkah.....	96
Figure 4.9. The monthly average load profile for Makkah.....	97
Figure 4.10. Histogram graph of the load profile	98
Figure 4.11. The grid scheduling rate during the day in each month	99
Figure 4.12. The scheduled rates for different time during the day [193].....	100
Figure 4.13. Design configuration of PV grid-connected system.....	100
Figure 4.14. (a) Horizontal axis, (b) Vertical axis and (c) Two-axis tracking [229]	103
Figure 4.15. The monthly average electric production.....	104
Figure 4.16. PV power output throughout the year and daytime.....	105
Figure 4.17. Solar PV production versus ambient temperature throughout the year.....	105
Figure 4.18. Average daily power graph of the different tracking systems.....	106
Figure 4.19. The excess electricity of different trackers per year.....	107
Figure 4.20. Monthly power generation from various tracking systems	108
Figure 4.21. Horizontal trackers performance from March to July	108
Figure 4.22. The production of PV system along with grid to maintain load demand.....	109
Figure 4.23. Simulation results of net present cost of FT system.....	110
Figure 4.24. Energy purchased from grid and energy sold to grid	111
Figure 4.25. NPC and LCOE for various scenarios of tracking systems.....	112
Figure 4.26. Return on investment with FT as the reference case.....	113
Figure 5.1. Efficiency comparison of some PV technologies.....	117
Figure 5.2. Flowchart of the developed methodology for a maximum solar irradiation	122
Figure 5.3. Monthly average of GHI on a horizontal surface and air temperature for Riyadh...	123

Figure 5.4. The sun's position with solar altitude and azimuth angles.....	124
Figure 5.5. Sun path presents altitude and azimuth angles in standard time for 24.91° N	126
Figure 5.6. The equation of time (E) in minutes as a function of day number (n)	127
Figure 5.7. Irradiation components received by the panel along with angles.....	128
Figure 5.8. Sample of simulation outcome for different azimuth and tilt angles	131
Figure 5.9. The potential annual energy yield versus tilt angles for different azimuth	132
Figure 5.10. Total monthly energy yield versus tilt angle for -20 azimuth angle.....	133
Figure 5.11. The monthly optimum tilt angle for Riyadh.....	134
Figure 5.12. Total monthly solar irradiation in kWh/m ²	135
Figure 5.13. Total monthly energy yield for different azimuth	135
Figure 5.14. Daily GHI of the 15th day of each month	136
Figure 5.15. Proposed monthly azimuth angle for Riyadh	138
Figure 5.16. The orientation variation with respect to the energy yield.....	141
Figure 5.17. Suitability map and solar station sites	143

List of Tables

Table 2.1. Integer values interpretation [52].....	21
Table 2.2. Socio-Political criteria	22
Table 2.3. Technical criteria	23
Table 2.4. Economic criteria.....	23
Table 2.5. Environmental criteria	24
Table 2.6. The selected decision sub-criteria with their data references	26
Table 2.7. Maturity[82]–[84], efficiency [80], [81], mortality [85], [86], and resource availability [21], [31], [74].....	29
Table 2.8. Capital costs [88] , operations and maintenance costs [88] , energy cost [23] and employment creation [87].....	31
Table 2.9. Land requirement [64] and emission level [89].....	32
Table 2.10. Rank numbers of alternatives for capital cost.....	33
Table 2.11. Pairwise comparison of alternatives with respect to capital cost.....	34
Table 2.12. Priority weights of sub-criteria with respect to parent criteria (local weight)	35
Table 3.1. Solar PV site suitability criteria	50
Table 3.2. Restrictions used in solar energy studies	52
Table 3.3. Multicriteria decision-making techniques in solar PV planning	56
Table 3.4. Parameters used in ArcGIS solar analyst tool	60
Table 3.5. Restrictions layers considered for utility-scale PV in Saudi Arabia.....	62
Table 3.6. Random index for different values of number of elements [161].....	66
Table 3.7. Eigenvalue of criteria.....	66
Table 3.8. Comparison matrix of the adopted decision criteria.....	69
Table 3.9. Land suitability index	74
Table 3.10. Land suitability distribution considering different scenarios	80
Table 4.1. Consumption rates for residential category in Saudi Arabia [173]	98
Table 4.2. PV and Converter parameters	102
Table 4.3. Cost inputs for the different tracking systems [229].....	103
Table 4.4. Hourly power production along with comparison to non-tracking system	109

Table 5.1. Symbols and abbreviations	119
Table 5.2. The monthly optimum orientation and their corresponding potential energy yield ..	137
Table 5.3. Proposed solar PV orientation for summer months	139
Table 5.4. Proposed scheme for periodic adjustments and the corresponding energy yield	140
Table 5.5. Annual optimum orientation for 18 cities with energy yield, revenues and suitability	142

Abbreviations

RESs	Renewable energy sources
PV	Photovoltaic
MCDM	Multiple criteria decision-making
GIS	Geographical information system
CBA	Cost-benefit analysis
DMs	Decision-makers
HOMER	Hybrid Optimization of Multiple Energy Resources
NREL	National Renewable Energy Laboratory
GCC	Gulf Cooperation Council
OPEC	Organization of the Petroleum Exporting
REFIT	Renewable energy feed-in tariff
NPC	Net present cost
AHP	Analytical hierarchy process
K.A.CARE	King Abdullah City for Atomic and Renewable Energy
SEC	Saudi Electricity Company
Mtoe	Million tonnes of oil equivalent
GHI	Global horizontal irradiance
DNI	Direct normal irradiance
CSP	Concentrated solar power
IEA	International Energy Agency
MSW	Municipal solid waste
VIKOR	Multicriteria optimization and compromise solution
TOPSIS	Technique for ordered of preference by similarity to ideal solution
ELECTRE	Elimination and choice expressing reality
PROMETHEE	Preference ranking organization method for enrichment evaluation
CR	Consistency ratio
CI	Consistency index
RNA	Rank number of alternative

IRENA	International Renewable Energy Agency
EIA	Energy Information Administration
O&M	Operations and maintenance
SV	Scoring value
DHI	Diffuse horizontal irradiation
NIMBY	Not in my backyard
U.S.	United States
WLC	Weighted linear combination
OWA	Ordered weighted averaging
LSI	Land suitability index
DEM	Digital elevation model
RRMM	Renewable Resource Monitoring and Mapping
SWA	Saudi Wildlife Authority
SSM	Solar PV suitability map
EPA	Environmental protection agency
CRF	Capacity recovery factor
ECRA	Electricity and Cogeneration Regulatory Authority
NASA	National Aeronautics and Space Administration
LCOE	Levelized cost of energy
ROI	Return on investment
DC	Direct current
AC	Alternating current
FT	Fixed system with no tracking system
HMA	Horizontal-axis with monthly adjustment
HWA	Horizontal-axis with weekly adjustment
HDA	Horizontal-axis with daily adjustment
HCA	Horizontal-axis with continuous adjustment
VCA	Vertical-axis with continuous adjustment
TA	Two-axis tracking system
AOI	Angle of incidence
IAM	Incidence angle modifier

ST	Solar time
CT	Civil time
UTC	Universal time
ASHRAE	American Society of Heating, Refrigerating and Air-Conditioning Engineers
NOCT	Nominal operating cell temperature

Chapter 1

Introduction

1.1. Overview and Motivation

Nowadays, most of the energy supplied globally is being generated from fossil fuels such as coal, oil, and natural gas. However, major drawbacks are associated with fossil fuel sources including their fluctuated prices, environmental pollution, and finite resources. Moreover, the worldwide demand for energy continues to increase, led by developing countries, reflecting growing global economy, population growth and a better energy access [1]. In this context, renewable energy sources (RESs) are considered a viable option for integration with conventional fossil fuel power plants to enhance the energy growth and improve the energy reliability. RESs generated from natural, free and inexhaustible sources such as solar, wind and geothermal, are promising to take a significant share in the energy sector. Currently, RESs contribute to an estimated 19% of global final energy consumption [2]. Figure 1.1 presents the distribution of RESs technologies in relative to renewable energy power capacity [3]. Progressively, the RESs penetration is rising in the electricity sector and growing in both capacity and generation aspects, where the largest increase is led by solar photovoltaic (PV), wind, and hydropower [2]. Many countries have set RESs portfolios to prompt a diversified energy sector for a more sustainable, secure, and low-carbon emission future. In 2016, more than 170 countries adopted at least one type of RESs target, an upward trend from only 43 countries in 2005 [4]. Currently, more than 24% of power globally is generated by RES, as shown in Figure 1.2 [4].

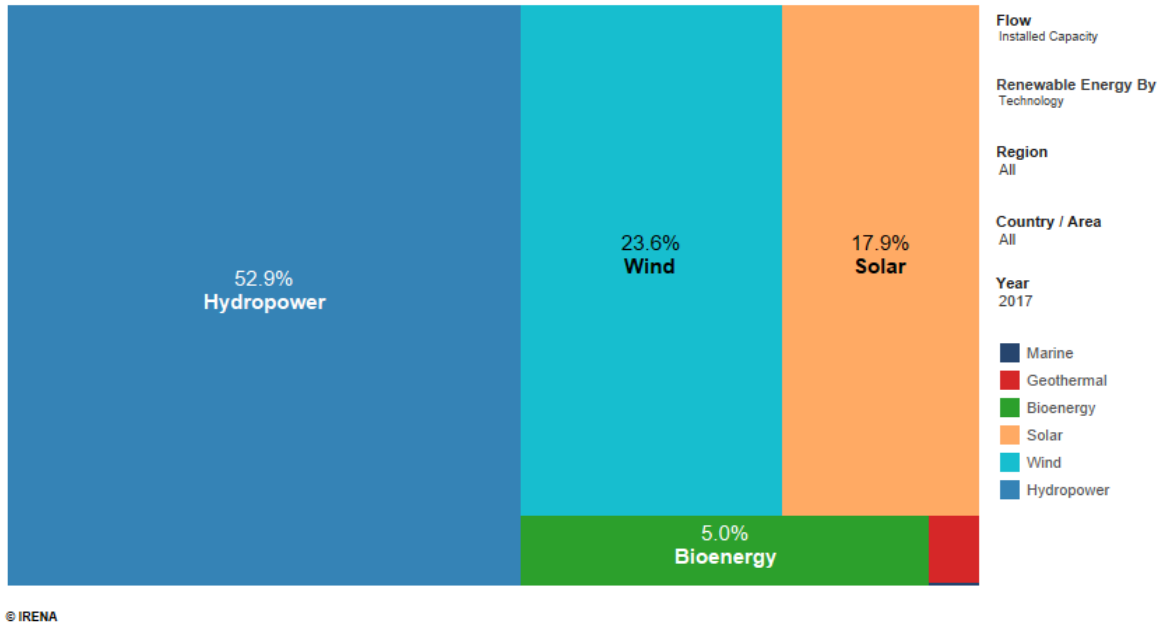


Figure 1.1. Distribution of renewable energy technologies in relation to installed capacity [3]

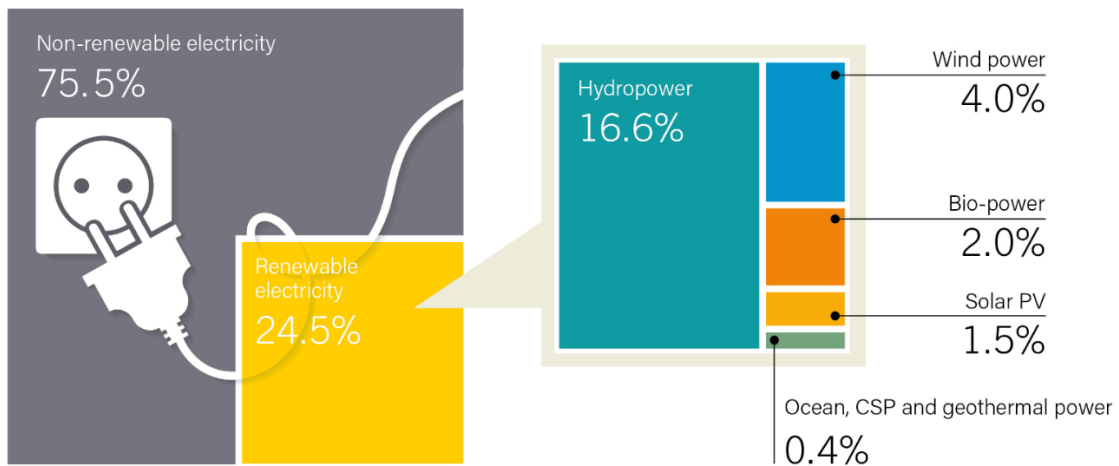


Figure 1.2. Renewable energy share in global power production by the end of 2016 [4]

The integration of fossil fuel with RESs produces a hybrid electrical system that can overcome their limitations of the RESs including the intermittency and the energy quantity. Such hybrid schemes can deliver more reliable, sustainable, and environmentally friendly system. Among the RESs technologies, solar energy technologies demonstrate a significant advancement

and maturity for power generation. Solar PV technology, which converts the sun irradiation directly into electricity, is one of the fastest growing RESs technologies worldwide [5]. This is essentially driven by sharp cost reduction and incentives policies. Recently, the solar PV modules' prices have dropped by 80% and are anticipated to keep falling [6]. Solar PV technologies have improved in efficiency whereas their manufacturing costs have declined over the past few years. In contrast to the concentrated solar thermal technology, PV panels work in the presence of both direct and diffuse solar irradiations.

For the last 15 years, the deployment of grid-connected PV surpasses the off-grid installation of PV worldwide, as shown in Figure 1.3 [7]. The exploitation of utility-size grid-connected solar PV has proven its advantages and has gained favor where vast areas are accessible and where significant amount of solar irradiation is available. It is anticipated that for the next five years (2017-2022), solar PV will represent the principal yearly capacity additions for renewables, further above wind and hydro [5].

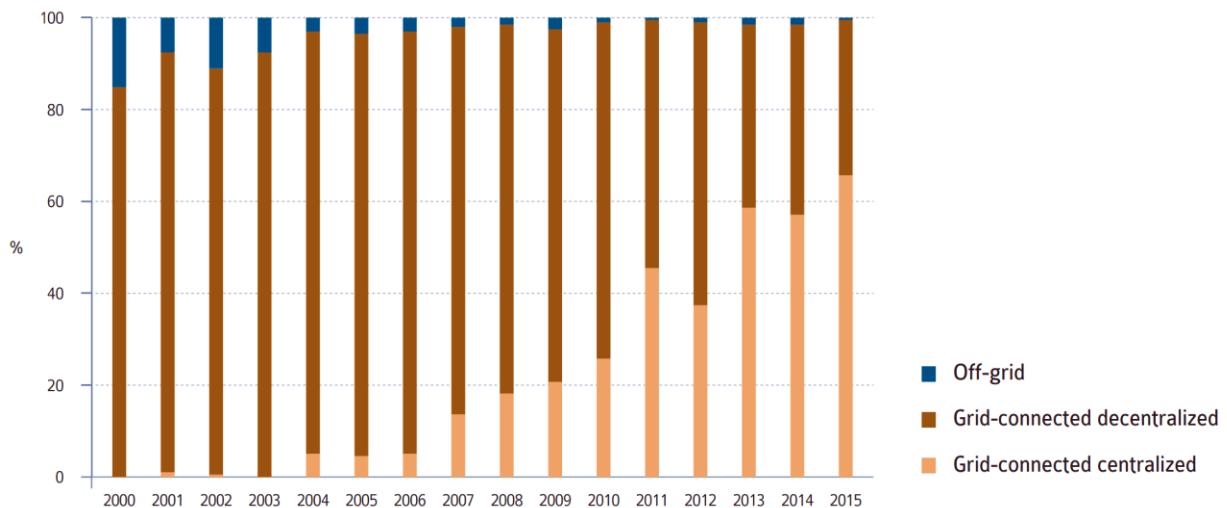


Figure 1.3. Share of grid-connected and off-grid installations 2000-2015 [7]

1.2. Research Problems

As the global economy is continuously growing and the population is increasing rapidly, relying exclusively on fossil fuel to accommodate the potential demand for electricity generation is not a strategic plan. Undoubtedly, such augmentation in demand seeks extra energy resources to encounter this potential, which point-blank a result in increased utilization of finite fossil fuel, environmental pollutions and high lifecycle cost of traditional power systems.

The hybrid electrical system (fossil fuel with RESs) could bring more advantageous environmental friendly system besides dominating the associated shortcomings of alternative energy including the intermittency and the disparity in energy density. Such energy mix targets require an optimal planning of RESs which are more accessible, and which can contribute efficiently to a better energy future. The overall four-phase approach applied in this thesis is illustrated in Figure 1.4.

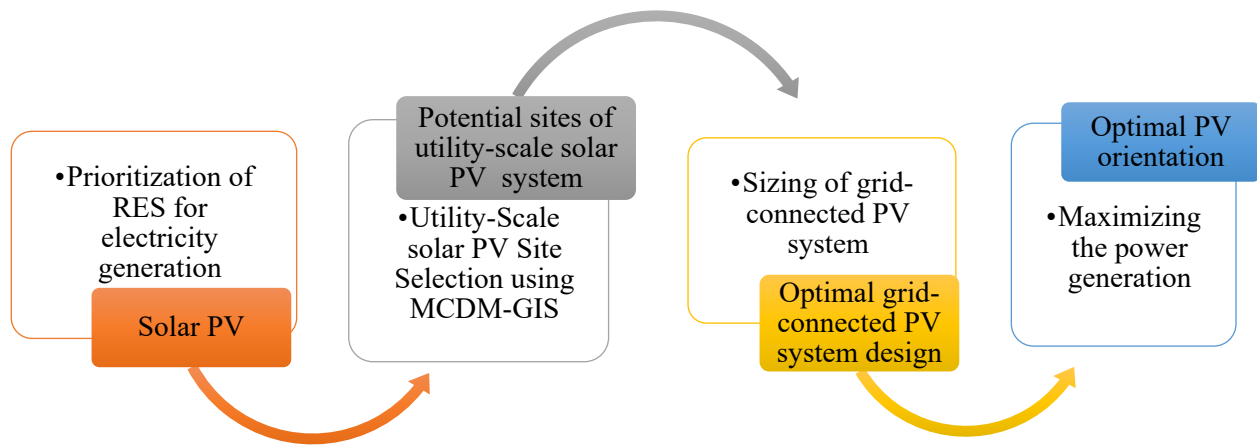


Figure 1.4. The general thesis approach

The first problem deals with prioritization of RESs under different criteria including economic, technical, socio-political and environmental and is covered in Chapter 2. The second problem addresses site selection problem for solar PV power plants (Chapter 3). The third problem investigates the design and analyses of solar PV system with different tracking systems

configurations and is presented in Chapter 4. The combination of site location and climate conditions determines the power generation potential of the system. Thus, understanding and tackling these external factors is essential for improving the solar PV system performance. Chapter 5 deals with optimal orientation problem of solar PV using a detailed solar irradiation model.

1.3. Thesis Approach and Contributions

The main contributions of this thesis can be summarized as follows:

- Chapter 2: A multiple criteria decision-making (MCDM) model for RESs prioritization is presented with application on Saudi Arabia, a major oil-dependent country and one of the world's largest energy supplier and per capita consumer. To authors' knowledge, no previous research has elicited the gulf region's stakeholders' perspectives in a MCDM model for renewable energy mix plan. Moreover, the proposed methodology has presented a systematic procedure through selecting the decision criteria indicated in 20 % or more of the reviewed studies after an extensive literature review, followed by allowing participants to apply modifications to the model for decision criteria validation. This work has resulted in following publications :
 - H. Z. Al Garni, Abdulrahman Kassem, Anjali Awasthi, Dragan Komljenovic, and Kamal Al-Haddad. 2016. "A Multicriteria Decision Making Approach for Evaluating Renewable Power Generation Sources in Saudi Arabia." *Sustainable Energy Technologies and Assessments* 16. Elsevier Ltd: 137–50. <https://doi.org/10.1016/j.seta.2016.05.006>
 - H. Z. Al Garni, and Anjali Awasthi. 2016. "Applying TOPSIS for Setting Priorities for Evaluating the Use of Renewable Power Generation : The Case of Saudi Arabia." In *The Renewable Energy World International 2016*.

Orlando,Florida. <http://events.pennwell.com/rewi2016/Public/Sessions.aspx?SuperTrackId=&TrackId=1757&&SearchEvent=&View=Sessions>

- H. Z. Al Garni and Anjali Awasthi. 2016. “Setting Priorities for Evaluating the Use of Renewable Power Generation using AHP” ICCE 2016: *5th International Conference & Exhibition on Clean Energy*. August 2016 Montreal, Canada.
- Chapter 3: A GIS-AHP based approach for siting utility size PV power plant is presented. A criteria layers model was developed using real atmospheric sensors data and GIS tools. Solar irradiation and air temperature criteria were generated in ArcGIS software and facilitated the AHP process. To the best of author’s knowledge, GIS-based AHP has not been conducted for utility-size PV site suitability study on such scale yet involving economic and technical criteria. This work has resulted in following publications :
 - H. Z. Al Garni and A. Awasthi, “Solar PV power plant site selection using a GIS-AHP based approach with application in Saudi Arabia,” *Applied Energy*, vol. 206C, pp. 1225–1240, 2017. <https://doi.org/10.1016/j.apenergy.2017.10.024> (Impact Factor = 7.5).
 - H. Z. Al Garni and A. Awasthi, “Solar PV Power Plants Site Selection,” in *Advances in Renewable Energies and Power Technologies*, I. Yahyaoui, Ed. Elsevier, 2018, pp. 57–75. <https://doi.org/10.1016/B978-0-12-812959-3.00002-2>.
 - H. Z. Al Garni and A. Awasthi, “A Fuzzy AHP and GIS-based Approach to Prioritize Utility-Scale Solar PV Sites in Saudi Arabia,” in *2017 IEEE International Conference on Systems, Man, and Cybernetics (SMC)*, 2017.
 - H. Z. Al Garni and A. Awasthi, “A Monte-Carlo approach to assess criteria impacts on solar PV site selection,” in *Handbook Of Probabilistic Models For Engineers*

And Scientist, Ed. Elsevier, (Submitted on April 5, 2018).

- Chapter 4: Develop an optimal design of grid-connected solar PV associated with different tracking systems and compare their technical and economic feasibility. As per the authors' knowledge, this techno-economic investigation of the tracking systems with different time adjustment for a grid-connected configuration, represents an original contribution. This work has resulted in following publications :
 - H. Z. Al Garni, A. Awasthi, and M. A. M. Ramli, "Optimal design and analysis of grid-connected photovoltaic under different tracking systems using HOMER," *Energy Conversion and Management*, vol. 155C, pp. 42–57. <https://doi.org/10.1016/j.enconman.2017.10.090> (Impact Factor = 5.59).
 - H. Z. Al Garni and A. Awasthi, "Techno-Economic Feasibility Analysis of a Solar PV Grid-Connected System with Different Tracking Using HOMER Software," in *2017 the 5th IEEE International Conference on Smart Energy Grid Engineering, 2017*, pp.217-222. DOI: <https://doi.org/10.1109/SEGE.2017.8052801>
- Chapter 5: Design and implement a detailed model for optimal orientation angles of solar PV system. Firstly, determining the solar angles and then converting the values of hourly measured solar irradiation components as well as ambient temperature for one year into hourly, monthly and yearly tilted irradiance. These values will be used to find the optimal orientation, consisting of tilt and azimuth, which allow the system to generate the maximum yearly power. This work has resulted in following publications :
 - H. Z. Al Garni and Anjali Awasthi "Optimal orientation angles for maximizing solar irradiation for a fixed solar PV in Saudi Arabia" (Submitted on May 1st, 2018).

1.4. Tools Used

The following tools were used in this thesis:

1. HOMER software was applied for optimal sizing of RES plants and to study the technical and economic performance of the system under different configurations.
2. Matlab R2017b was used to program the optimization algorithm for the solar PV orientation system in Chapter 5.
3. ArcGIS 10.3.1 was utilized in Chapter 3 to overlay all decision criteria and constraints layers as well as to calculate the insolation and air temperature across the entire study area using actual atmospheric parameters.
4. Expert Choice software was used to apply AHP for RESs evaluation and perform sensitivity analysis under different scenarios.
5. MS Excel 2016 was used to validate the results and process all the calculations and matrices manipulations.

1.5. Thesis Organization

This thesis is organized as follows: Chapter 2 presents the multicriteria decision-model for evaluating renewable energy sources for electricity generation. Chapter 3 presents the GIS-AHP based approach for site selection of utility-size PV power plants. Chapter 4 studies a grid-connected solar PV with different tracking systems to identify optimal design. Chapter 5 presents the tilt and azimuth angles for maximizing solar irradiation for a fixed solar PV. Finally, Chapter 6 concludes the thesis and presents the future works.

Chapter 2

Renewable Energy Selection

2.1. Introduction

Nowadays, several countries' economies including United States, Canada, Germany and France are ranked among those with the highest electricity consumption per capita globally as illustrated in Figure 2.1. Likewise, the Gulf Cooperation Council countries (GCC), consist of six-member states: Saudi Arabia, United Arab Emirates, Qatar, Bahrain, Kuwait and Oman, are placed high compared to other countries. In recent decades, these countries have experienced significant economic growth due to the wealth generated from plentiful hydrocarbon reserves. This development has been combined with unparalleled increase in urbanization, infrastructure, and industrial expansion. Since 1970, the region's population has grown by six-fold including migrant workers from Asian and other countries [8]. The Kingdom of Saudi Arabia is one of the world's largest oil producers and exporters, producing an estimated average of more than 11 million barrels per day (bbl/d) and exporting an estimated 8.6 million bbl/d in 2012. Saudi Arabia is also the largest oil-consuming country in the Middle East; in 2012, it consumed more than 3 million bbl/d of oil, essentially for electricity generation, water desalination, and transportation [9]. According to the Organization of the Petroleum Exporting Countries (OPEC), petroleum exports accounted for 90% of total Saudi export revenues in 2011.

Due to a rapidly growing population and economic development along with subsidized prices of gas, water, and electricity in Saudi Arabia, the overall demand for energy used in power, transportation, and desalination is estimated to increase dramatically from 3.4 million bbl/d in 2012 to 8.3 million bbl/d of oil equivalent in 2028, unless alternative energy initiatives are

deployed and energy efficiency is improved [10]. Such progressively high-energy consumption led to establish Saudi Energy Efficiency Centre in 2010 to publicize rationalization awareness and enhance energy consumption efficiency which will support and preserve the national wealth of energy resources [11].

Furthermore, the Kingdom’s leaders are well aware of the fact that heavy dependence on oil is not a good strategic decision; therefore, the King Abdullah City for Atomic and Renewable Energy (K.A.CARE) was established to introduce sustainable development and make remarkable diversifications in terms of energy resources. Saudi Arabia has pushed back its long-term RESs plans to 2040 instead of 2032 due to the need for more time to decide which domestic RESs to use for the portfolio based on Bloomberg report [12].

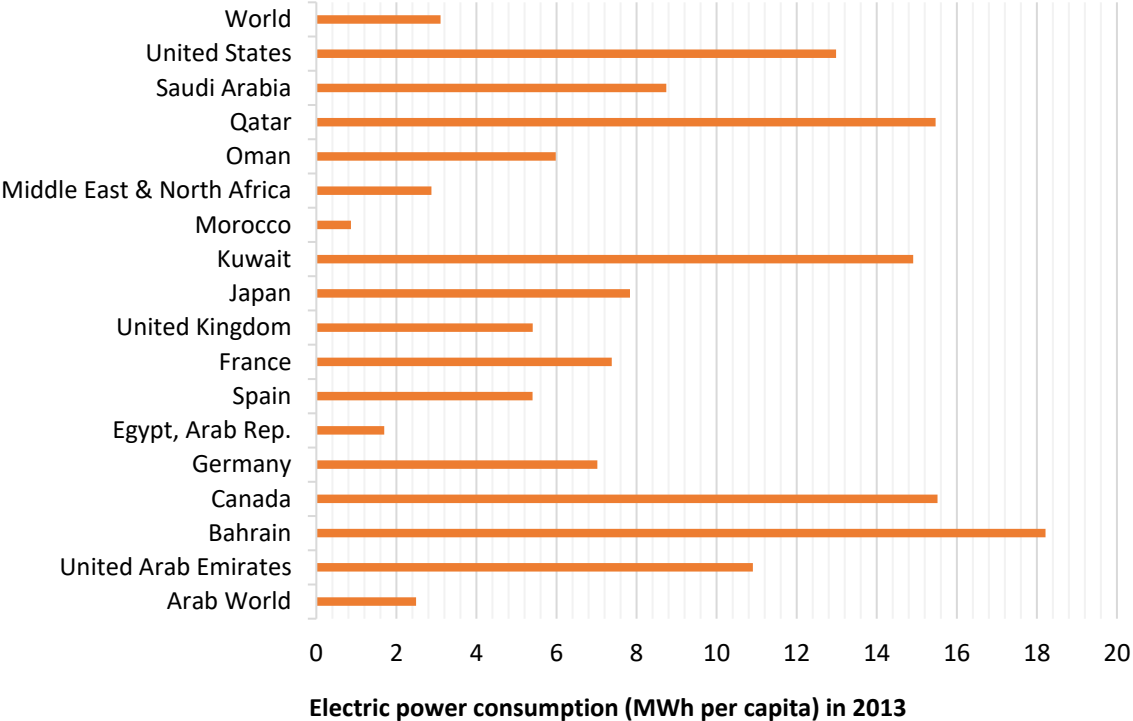


Figure 2.1. Electricity consumption per capita in selected countries [7]

A roadmap based on extensive and comprehensive research is needed to evaluate and justify the extent to which each alternative energy technology could contribute to the mix of energy

sources for electricity generation. As an initial stage in proper planning for sustainable development and the deployment of RESs in the electricity production sector, different RESs and the technologies for their exploitation should be evaluated and ranked, to identify their contribution to the sustainable energy mix profile. To accomplish this, multiple criteria must be considered. The literature lacks a comprehensive overview of the significant criteria that should be considered in the evaluation of RESs including economic, technical, socio-political and environmental criteria.

2.2. Problem Statement

RESs planning involves multiple quantitative and qualitative attributes (often conflicting), which cannot be adequately addressed by a single-phase evaluation such as cost-benefit analysis (CBA). Given the fact that several criteria can influence the selection of RES and the sites of the generation plants, using MCDM can facilitate the decision making related to the evaluation of RESs.

The objectives of this chapter are the following:

- To evaluate and prioritize five renewable power generation sources, namely: solar PV, concentrated solar power, wind energy, biomass, and geothermal with application for Saudi Arabia, an oil-dependent and developing country.
- The decision framework should evaluate the relative suitability of the five RESs and rank them for potential project investment, by considering the relevant technical, socio-political, economic, and environmental criteria. Apply the decision framework to a case study.
- Assess the available RESs for the case country towards prioritizing them to facilitate decision makers in deciding the portions and the extent to which each of the technologies can form the mix of renewable energy portfolio for the country.

To the best of our knowledge this is the first work prioritizing RESs from different aspects including economic, technical, socio-political and environmental criteria in the context of Saudi Arabia. Moreover, this chapter identifies to what extent each alternative energy technology contributes to the sustainable energy mix profile. Different resources were used to define the criteria in the model, including a literature review, stakeholders' inputs, and the Saudi vision for the energy diversification announced by K.A.CARE.

2.3. Renewable Energy Options

The total available power generation capacity in the Kingdom reached 69,761 MW in 2013 [13]. The power generated is based 100% on fossil fuels (oil and gas). The number of customers increased from 4.5 million in 2004 to 7 million in 2013 for Saudi Electricity Company (SEC) which is the major electricity supplier (74%) in the country [13]. SEC spends more than 40 billion riyals on energy projects annually [14]. Owing to the population increase, strong economic and industrial growth, and high levels of price subsidization, the electricity demand is projected to grow significantly. According to government estimates, the anticipated electricity demand in the Kingdom is expected to increase from 80 GW by 2020 to more than 120 GW by 2030 [7]. K.A.CARE has recommended the utilization of renewable and atomic energy progressively to meet the expected demand, such that half of all electricity production would come from non-fossil fuels in 2032 [15].

Saudi Arabia is one of the most enriched countries with natural resources and has the potential to take advantage of abundant RESs to meet a significant share of the Kingdom's energy needs and provide an efficient energy future [17]. In addition, harnessing RESs to supply electricity to consumers in Saudi Arabia will have significant environmental benefits. The following sub-

sections provide details of potential RESs, including solar energy, wind energy, geothermal energy, and biomass energy, with their potential for electricity generation in Saudi Arabia.

2.3.1. Solar energy

The Kingdom has significant potential to exploit solar energy owing to its location, large unused area, and daily solar radiation availability. Solar radiation in the Kingdom is considered to have one of the highest rates globally with an average global horizontal irradiance (GHI) of 2 MWh/m²/year, which is higher than the average global solar radiation in one of the leading countries in solar energy, Spain (1.6 MWh/m²/year) [18], [19]

Rahman et al. [20] studied long-term mean values of sunshine duration and global solar radiation on horizontal surfaces over 41 cities in the kingdom. The results show that the overall mean of yearly sunshine duration in the kingdom is 3,248 hours and the GHI varies between a minimum of 1.63 MWh/m²/year at Tabuk in the northwest of the kingdom and a maximum of 2.56 MWh/m²/year at Bisha in the southwest. However, the minimum solar radiation is higher than the average GHI in Germany and many other European countries. Furthermore, the pattern of global solar radiation intensity and sunshine duration follows the electricity demand pattern, which could be the most favorable RESs generation option to meet demand, especially during the summer season when the demand peak is highest due to significant rises in domestic demand for air conditioning [19]. Since 1960, significant experience has been gained and lessons learnt in the area of solar energy from different studies and research programs conducted in the kingdom [19], [21]. Figure 2.2 depicts the long-term annual average GHI and direct normal irradiance (DNI) obtained from the SolarGIS database [22].

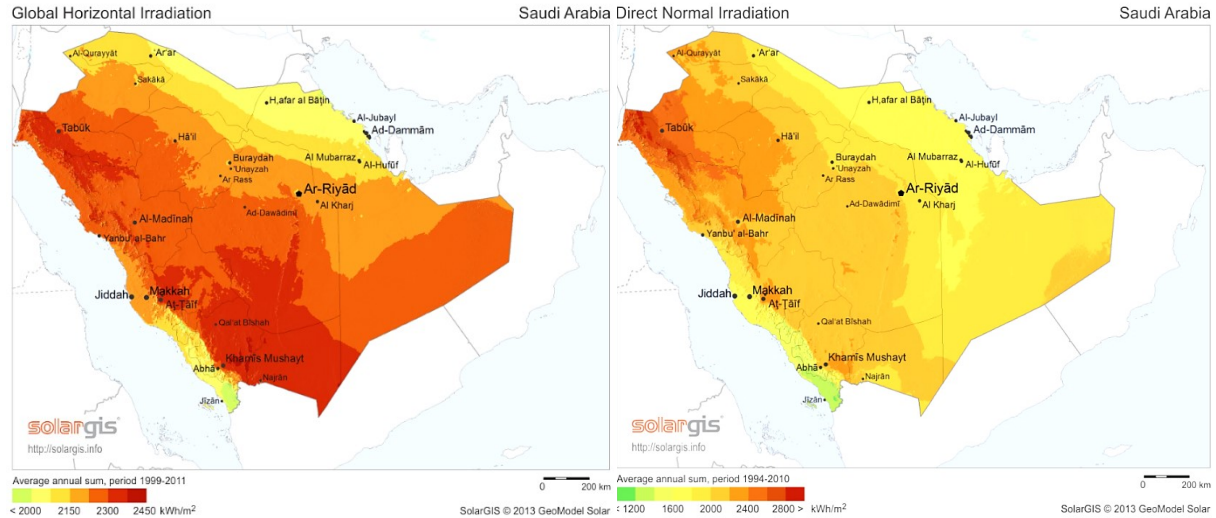


Figure 2.2. Average GHI (left) and DNI (right) for Saudi Arabia [22].

Two solar energy technologies are considered in this study, including solar PV and concentrated solar power (CSP), also known as concentrated solar thermal. CSP technology deploys reflectors or mirrors in order to concentrate solar radiation to heat transfer fluid that is used to generate electricity. On the other hand, solar PV technology utilizes a PV-effect phenomenon existing in semiconductor material in order to convert solar energy directly into electricity. Unlike CSP, PV technology works in the presence of both direct and diffuse solar irradiation. Solar PV is commercially more mature technology than CSP with total installed capacity of 175 GW compared to 4 GW for CSP worldwide [23]. Due to massive scale production and technology advancement, the upfront cost of PV system has significantly decreased in the past few years while the upfront costs of CSP are considerably high. Since the end of 2010, the electricity cost generated from PV has halved while PV module costs have decreased by 80 % [6], [24]. In addition, the maintenance costs associated with PV power plants are minimal compared to other power utility systems as a result of the absence of mechanical parts. It is essential to note that for arid environments, the impact of dust on PV modules efficiencies should be considered. Al-Jawah [25] assessed the cleaning systems for PV power plants in Saudi Arabia. PV is suitable to cover peak demand during

sun hours. However, storing energy through batteries is expensive for large-scale utilities. CSP on the other hand is anticipated to witness increase levels of installation in the coming decades. The International Energy Agency (IEA) anticipates that the installed capacities of PV will keep increasing to cover peak demands before the significance of cheap thermal storage associated with CSP systems play its role to facilitate CSP covering 11% of total global installed capacities of all generation sources in 2050 [26]. In addition, CSP technology is suitable for hybridization in which CSP could be combined with steam generation sectors of existing or new conventional power plants. This also serves the ability of these systems to take advantage of backup fossil fuels to cover base loads and reduce fluctuation [27].

2.3.2. Wind energy

By end of 2017, the total installed capacity of wind energy reached 530 GW globally. China accounted for almost 190 GW followed by the US and Germany [28]. Many researchers have proposed wind energy as a potential source of energy in Saudi Arabia as in many locations, the annual mean wind speed exceeds 4 m/s at a height of 20 m [29]. Site selection of wind farms can play a major role in output power. The research outcomes of an economic feasibility study by Shaahid et al. [30] indicate that the western region has a relatively better wind speed, with monthly average speeds ranging from 3.1 to 4.8 m/s at a height of 10 m. The kingdom has very long coastal areas in the west and the east with large desert areas in the center. Hence, there is potential to develop wind power in the western coastal region, including at Al-Wajh, Jeddah, Yanbu, and Jizan. Yanbu has shown relatively better potential for wind power deployment compared to other locations [30]. Eltamaly et al. [29] studied five locations in Saudi Arabia and found that the best place to install wind turbines is Dhahran at a cost of 5.85 US cents/kWh. The estimated wind energy potential in Saudi Arabia is around 20 TWh/year [23].

2.3.3. Geothermal energy

The total installed capacity of geothermal energy reached 12.8 GW in January 2015 in 24 countries worldwide [33]. The outcome of research indicates that the kingdom has sufficient geothermal energy to contribute towards many direct applications. Sedimentary aquifers, hot springs, and rock geothermal systems are the main geothermal resources in the kingdom. In the eastern province, there are deep-seated aquifers that are confined and could be reached only by oil wells. The hot springs and volcanic areas along the western and southwestern coastal parts of the Red Sea have been considered in many studies to hold potential for geothermal energy in the kingdom [25]. Currently, existing geothermal resources remain untapped for electricity generation, heating, or other purposes. Further research is needed, and exploration projects are required to bring this technology into the kingdom's energy mix plan.

2.3.4. Biomass energy

The exploitation of biomass energy in Saudi Arabia remains idle despite estimated potential of 3 Mtoe/year. The kingdom had a waste-to-energy potential estimated to be 1.75 kg per capita per day in 2012 owing to high municipal solid waste (MSW). Moreover, a huge amount of organic waste is being produced by such businesses as dairy producers, bakeries, and olive oil plants, which could use anaerobic digestion treatment. In addition, there is a limited agricultural residue from crops and animal waste that could offer potential for biomass energy [38]. The significant growing population and urban development will increase the biomass availability, in particular, MSW. A huge amount of biomass could be transformed into usable energy for more sustainable electricity generation.

2.4. Methodology

RESs planning problems include multiple quantitative and qualitative attributes which cannot be always adequately covered by single phase evaluation indicators such as CBA. Cavallaro [39] and Shattan [40] discussed the deficiency of considering mere financial indicators such as CBA and net present cost (NPC) for such complex problems. CBA requires quantitative values for analysis, however, in energy planning problems there are several criteria that cannot be measured as monetary values such as social acceptance and effect on human health. As a result, MCDM techniques have gained high popularity in recent years to tackle problems involving long-term energy source ranking as opposed to the classic single-dimensional index. Several stakeholders are involved in the process of planning for sustainable development, including consumers, investors, policymakers, academics, and environmental and public interest groups. They share diverse viewpoints and interests with regard to RESs projects. Indeed, the process of selecting RESs for sustainable development encompasses multiple contradictory objectives from different stakeholders. This leads to the need for development of a framework that is capable of combining tradeoffs since no one resource satisfies all criteria simultaneously [41]. MCDM is used to evaluate the overall system mix for power suppliers to establish the best proposed alternative for sustainable development [42]. The proposed model takes into account technical, financial, environmental, political, and social considerations. This study adopts RESs technologies announced by K.A.CARE as potential alternatives for the RESs portfolio plan of Saudi Arabia.

The main steps of any MCDM are as follows: defining the problem, setting goals for solving the problem, selecting the appropriate method, generating alternatives, establishing criteria, assigning criteria weights, construction of an evaluation matrix, and ranking of the alternatives [41]. Figure

2.3 illustrates the proposed approach of evaluating RESs for Saudi Arabia. The various steps are described in detail as follows:

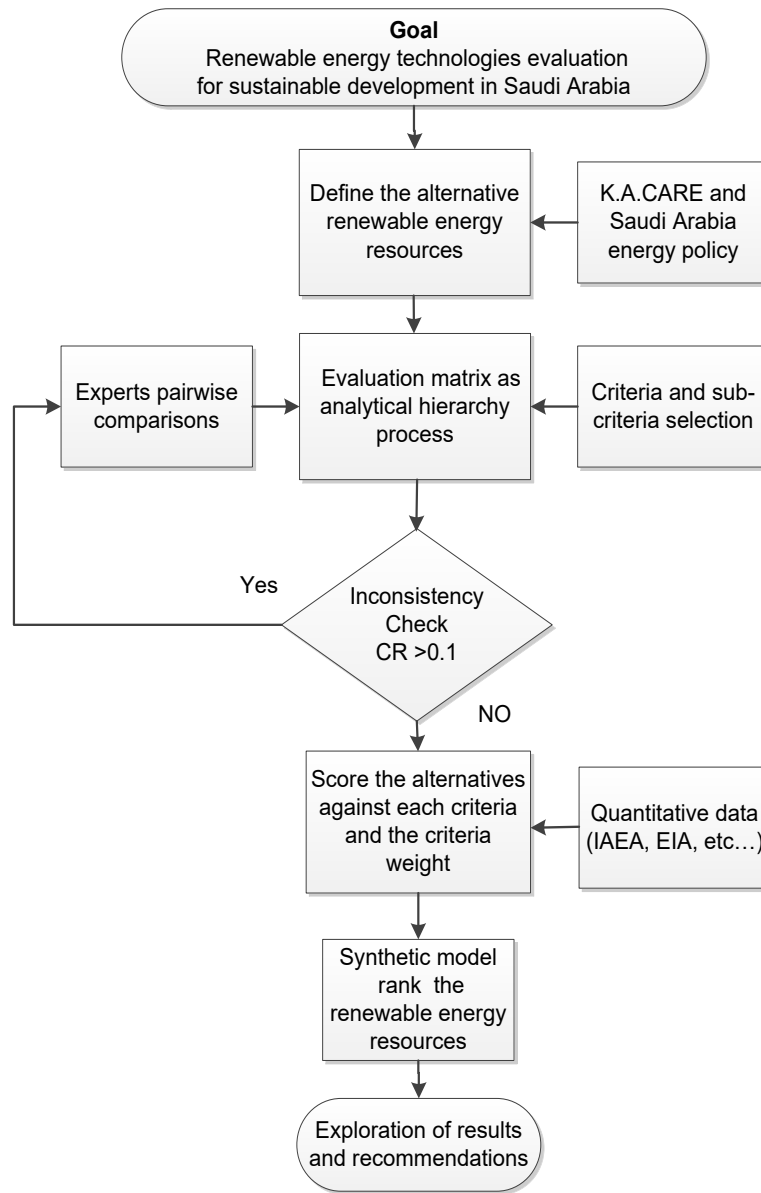


Figure 2.3. Proposed approach to evaluate renewable energy resources

2.4.1. Alternatives identification

This study proposes a model for the prioritization of a RESs portfolio for Saudi Arabia. The country has the potential to invest hugely in the alternative energy sector for electricity generation

and water desalination. Thus, a roadmap based on extensive and comprehensive research has to be considered to evaluate and justify the extent to which each alternative energy technology could contribute to the mix of energy sources.

The K.A.CARE evaluation of RESs concludes with the proposal to use nuclear, solar, wind, biomass, and geothermal in the energy mix in 2032 although fossil fuel will remain a key element.

The considered alternatives in this study are solar thermal, solar PV, wind, waste-to-energy, and geothermal as they are endorsed by K.A.CARE [15].

2.4.2. Analytical hierarchy process model

Several MCDM approaches have been reported in literature. The common ones are optimization and compromise solution (VIKOR), the AHP, the technique for order of preference by similarity to ideal solution (TOPSIS), elimination and choice expressing reality (ELECTRE), and preference ranking organization method for enrichment evaluation (PROMETHEE). Kaya & Kahraman applied VIKOR with AHP for renewable energy planning in Turkey. Amer & Daim [43] and Ahmed & Tahar [44] adopted AHP for ranking renewable energy sources in Pakistan and Malaysia. Streimikiene et al. [45] employed TOPSIS for prioritizing sustainable electricity production technologies. Georgopoulou et al. [46] adapted ELECTRE for energy planning problem. Beccali et al. [47] used it for renewable energy diffusion technologies at regional scale. Diakoulaki & Karangelis [48] utilized PROMETHEE to examine electricity development scenarios in Greece. Goletsis et al.[49] propose a hybrid approach based on PROMETHEE and ELECTRE for ranking energy sector projects in Armenia. Good literature review on application of MCDM approaches in the renewable energy field can be found in Pohekar & Ramachandran [50], Mateo [41], and Wang et al. [51].

AHP method developed by Saaty [52] facilitates the ranking of alternatives by introducing a framework that is capable of dealing with multiple objectives and provides the best compromise solution when objectives are contradictory. The top level of the hierarchy comprises the main goal to be achieved, whereas the bottom level represents the alternatives, and the intermediate levels are the criteria and sub-criteria. This framework supports the assessment process in which stakeholders are requested to appraise each level parameter in a pairwise comparison with respect to their parent node.

The utilization of AHP analysis for the decision-making process has been carried out using the following key steps. First, the decision problem is structured into a hierarchal model. In our case, the problem as defined in Section 2.2 involves defining the RESs portfolio and evaluation of alternatives for sustainable development in the context of Saudi Arabia. This goal represents the top level of the hierarchy, while the alternatives, defined in Section 2.3, represent the bottom level. The second key step is to obtain the weights of each level of the hierarchy with respect to its immediate upper level. Pairwise comparison between each two parameters is undertaken utilizing the nine-integer value scale suggested by Saaty [52] to compare parameters (A) and (B) with respect to their parent node, as shown in Table 2.1. There are different families of comparison methods as well as scales, each one of them has advantages and disadvantages, and their selection depends on decision makers' rationality. Elliott [7] reviewed several scales to examine the accuracy of converting subjective expressions into numerical values. He concluded that no single scaling approach is suitable for capturing the preferences of all individuals and it is dependent on individual rationality. In this chapter, the scaling method is adapted in order to encourage invited stakeholders to participate in the questionnaire through asking them fewer questions.

The third key step in carrying out AHP is to calculate eigenvectors to obtain priority weights and to check for inconsistency. The consistency control is a point of strength for AHP since pairwise comparison could be subjective. A consistency ratio (CR) is given by CI/RI , in which RI is the random consistency index that varies according to the number of elements in a comparison (n). CI is the consistency index, which equals $(\lambda_{max} - n)/(n-1)$. Here, λ_{max} are the maximum eigenvalues of the comparison matrix. The fourth key step to apply AHP is to calculate the scores of each criterion, sub-criterion, and finally, each alternative. This process is explained in Section 2.5 after the criteria are obtained and the model is formulated.

Table 2.1. Integer values interpretation [52]

Intensity of Importance (Value of A to B)	Definition
1	Objectives A and B are of equal importance
3	Objective A is slightly more important than B
5	Objective A is moderately more important than B
7	Objective A is strongly more important than B
9	Objective A is extremely more important than B
2,4,6,8	Intermediate values between judgment values

2.4.3. Establishing criteria and sub-criteria

Exploitation of RESs options is an interdisciplinary field that single-criteria decision-making methods are incapable of handling. Instead of the traditional focus on the cost versus efficiency of projects, many parameters can be considered from technical, economic, environmental, social, and political viewpoints. Technical and economic aspects have been, are, and will continue to be of importance for decision making in strategic energy planning. Environmental aspects have gained strong interest in recent years for sustainable development. Finally, social and political attitudes towards RESs are related and influential in the decision-making process.

In order to define the decision criteria, a comprehensive assessment of the literature is conducted to collect the most utilized attributes in developing sustainable energy planning. Hence, the most common criteria are selected to form the second and third levels of the model. Thereafter, this list of criteria and sub-criteria is modified when needed to suit the characteristics of a developing country that is a world leader in the energy supply sector. In addition, it is considered that the scope of the study is its evaluation of declared alternative RESs, in which reviewed studies include comparisons among renewable, conventional, and nuclear energy sources. Table 2.2 to Table 2.5 present the four main criteria: technical, socio-political, economic, and environmental. The sub-criteria are listed for these four main criteria. It is important to note that these four tables represent the most common sub-criteria considered in the reviewed literature for evaluating energy sources (renewable and conventional). Thereafter, to construct the AHP model, two steps are carried out. First, omitting sub-criteria that are non-influential when comparing renewable energy sources (e.g. fuel cost and need of waste disposal). Second, utilize sub-criteria that are considered by at least 20% of the reviewed studies. Applying these steps, we obtained 14 sub-criteria categorized under four main decision criteria. The resulting AHP model is illustrated in Figure 2.4. Metrics for the 14 sub-criteria and the alternatives values are presented in subsections (2.4.3.1) – (2.4.3.4).

Table 2.2. Socio-Political criteria

D.C	No.	Sub-criteria	References
Socio-political	1	Employment creation	[41], [42], [55]–[59], [43]–[47], [51], [53], [54]
	2	Social and political acceptance	[41], [42], [60]–[64], [43], [44], [49], [51], [53]–[55], [59]
	3	Impact on human health	[45], [56], [57], [63], [65]
	4	Feasibility	[47], [49], [53], [58]
	5	Compatibility with the national energy policy	[46], [49], [53], [54]
	6	National energy security/energy independency	[42], [43], [45], [48], [54], [56], [57], [63], [65]
	7	Maintain leading position as energy supplier	OWN

Table 2.3. Technical criteria

D.C	No.	Sub-criteria	References
Technical	1	Technology maturity	[41], [43], [47], [51], [53], [54], [59], [61], [64]
	2	Efficiency	[41], [43], [67]–[70], [44], [51], [54], [57]–[60], [66]
	3	Reliability	[71]–[73].
	4	Deployment time	[43], [44], [49], [53]
	5	Expert human resource	[43], [59]
	6	Resource reserves	[43], [44], [46], [57], [58], [61], [67]
	7	Safety of energy system	[41], [45], [51], [53], [55], [57], [59]
	8	Electricity supply availability	[45], [48], [66], [68]
	9	Ease of decentralization	OWN
	10	Safety in covering peak demand	[42], [45], [46]
	11	Network stability	[46], [63]

Table 2.4. Economic criteria

D.C	No.	Sub-criteria	References
Economic	1	R&D cost	[43]
	2	Capital cost	[41], [42], [54], [56]–[59], [62], [66], [67], [69], [70], [43]–[46], [48], [49], [51], [53]
	3	Operations and maintenance (O&M) cost	[41], [42], [67], [43], [45], [46], [51], [56], [57], [59], [66]
	5	Energy cost	[41]–[43], [51], [59], [62], [63], [69], [70]
	6	Operational life	[41], [44], [45], [51], [59]
	7	Cost of grid connection	[45]
	8	Fuel cost	[42], [45], [51], [56], [59], [66], [67]
	9	Market maturity (commercial competitiveness)	[47], [53], [61]
	10	Site advantage	[58], [68]
	11	Availability of funds	[49], [53]
	12	National economic development	[42], [43], [56], [58], [63], [64], [67]

Table 2.5. Environmental criteria

D.C.	No.	Sub-criteria	References
Environmental	1	Land requirement	[41], [43], [59], [64], [70], [44]–[46], [51], [53], [55], [56], [58]
	2	Emission reduction	[41], [42], [58], [59], [62], [63], [65], [67], [69], [70], [43]–[45], [48], [53], [54], [56], [57]
	3	Impact on environment	[44], [48], [49], [60], [64]
	5	Need for waste disposal	[45], [53], [62]
	6	Disturbance of ecological balance	[45], [46], [57], [58], [65]

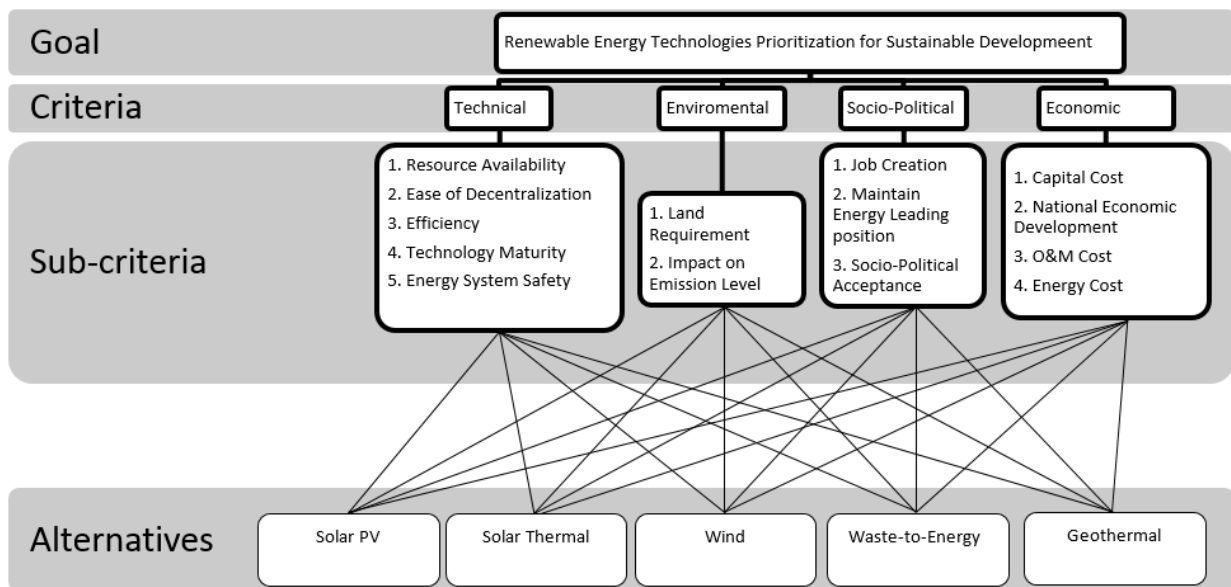


Figure 2.4. Analytical hierarchy process diagram

The strength of AHP comes from the ability to include quantitative and qualitative data in one model. The priority is to use quantitative data whenever possible for alternatives evaluation. However, unmeasurable data such as social acceptance is obtained from experts qualitatively. Stakeholder' evaluation was fully considered in two steps while in the third step a combination of experts' evaluation and quantitative data was used as follows:

First, the assessment of the four main decision criteria was done with respect to goal; and then the assessment of sub-criteria with respect to their parent criteria based on experts' evaluation; third,

the assessment of alternatives with respect to each sub-criterion was derived quantitatively whenever possible or qualitatively otherwise through survey instrument. Table 2.6 presents the selected sub-criteria with their data references.

In this study, the survey instrument is answered by 20 experts in the energy sector. Participants' panel consists of energy sector stakeholders from academic, research, government, and industrial sectors. Participants received a questionnaire containing a summary of the study goal and methodology at the beginning. They were subsequently requested to review the list of evaluation parameters. Then, participants evaluated criteria and sub-criteria in a hierarchical manner, while they evaluated alternatives with respect to sub-criteria if and only if there is no data available.

Afterwards, the geometric mean is calculated for each evaluation received from experts. Accordingly, the rank number of alternative (RNA), which is a scale method based on the geometric mean, is conducted following Eq. 2.2. Thereafter, the pairwise comparison is carried out according to Eq. 2.3 following AHP approach, which will be elaborated in Section 2.5. The Expert Choice software is utilized for generating local weights, global weights, and alternatives prioritization. The following subsections present detailed definitions, metrics, and the acquired data for each sub-criterion used in the model.

Table 2.6. The selected decision sub-criteria with their data references

Sub-criteria	Reference
Efficiency	U.S. Energy Information Administration (EIA) and literature
Capital cost	U.S. Energy Information Administration (EIA)
O&M cost	
Job creation	Literature
Land requirement	
Safety	
Energy cost	IRENA Data and Statistics
Resource availability	
Maturity	International Energy Agency (IEA) and United Nations Environment Program
Impact on emission	International Energy Agency (IEA)
Decentralization	Experts inputs
Leading position	
National economic development	
Social & political acceptance	

2.4.3.1. Technical (Tech.)

- *Resource availability (SC₁₁)*

Resource availability reflects the weight for each RESs technology. Several studies have discussed the availability of sun irradiation and wind for electricity generation in Saudi Arabia. On the other hand, there is a lack of studies considering geothermal and biomass estimation for electricity generation, as stated by the K.A.CARE and International Renewable Energy Agency (IRENA) databases. Consequently, this study carried out qualitative estimations through eliciting responses from experts to obtain their knowledge about the availability of RESs in Saudi Arabia. Subjective comparisons, the K.A.CARE vision, and studies about hot spring availability in Saudi Arabia and available waste-for-energy conversion were reviewed to obtain assumptions for geothermal and biomass estimation for electricity generation. All the aforementioned sources have led us to believe

that geothermal followed by biomass represent the lowest level of resources, far behind even wind, for massive production (equal to or more than 1 GW). Biomass and geothermal electric generation were estimated as 200 kWh/m²/year and 100 kWh/m²/year, respectively. Table 2.7 compares resource availability among the considered alternatives [31], [74].

- ***Ease of decentralization (SC₁₂)***

An important advantage of some RESs is that they support decentralized distribution of energy supplies. Distributed energy resources are built closer to consumers, which helps to reduce transmission and distribution bottlenecks and losses, improve voltage profiles, and delay the need for huge investment of large-scale generation systems [75], [76]. Decentralization supports the electrification of rural areas that are not connected to the grid. The above mentioned benefits of decentralizing RESs power plants make this a parameter of importance by means of measuring which RESs technology acquires higher weight. Further details about decentralization are discussed [77]–[79]. Decentralization is considered as a qualitative parameter that reflects the ability to build more distributed plants closer to users supporting the long-term adaptation of smarter grids with lower energy losses.

- ***Efficiency (SC₁₃)***

This criterion depicts how efficient a RESs technology is in converting its primary energy source into electricity. The ideal efficiency is 100%, yet in practice, it is always less owing to losses. Efficiency reflects the percentage of output to input energy to show the usefulness with which a certain RESs technology can acquire electricity from an energy source. The efficiency index uses quantitative data of different RESs technologies obtained from the annual energy report of the US Energy Information Administration (EIA) [80] while the efficiency of biomass is obtained through [81]. A comparison of the efficiency of the alternatives is introduced in Table 2.7. The efficiencies

shown in this table are notional efficiencies, which each technology might achieve under normal operation range and may vary based on site-specific technology and environmental factors.

- ***Technology maturity (SC₁₄)***

The technical maturity parameter reflects the level of a given technology being widespread locally and internationally and being available commercially. A technology is regarded as mature if it is tested and used for a long enough period in real world applications for it to overcome its preliminary faults and inherent difficulties through enhancement. The comparison of RESs technologies from a maturity point of view is discussed in [82]–[84] and presented in Table 2.7.

- ***Energy system safety (SC₁₅)***

Energy system safety is a critical parameter that exposes the degree to which a certain RESs technology results in loss of human lives. It is measured quantitatively indicating the normalized number of fatal accidents at power plants, whether in the establishment phase or during operations, over specific time periods. Burgherr et al., [85], [86] present a broad comparison of energy technologies considering accident and fatality risks by GW year based on the Energy-Related Severe Accident Database as well as contributions of available data, modeling, and expert judgments. Table 2.7 presents a comparison of mortality for the RESs alternatives.

Table 2.7. Maturity[82]–[84], efficiency [80], [81], mortality [85], [86], and resource availability [21], [31], [74]

Alternative	Maturity	Efficiency (%)	Mortality	Resource Availability (kwh/m ² /year)
Solar PV	Moderate maturity	12	Lowest mortality	2130
Solar Thermal	Least mature	21	Low mortality	2200
Wind	High maturity	35	Moderate mortality	570
Geothermal	Very high maturity	16	Moderate mortality	100
Biomass	Most Mature	25	Highest mortality	200

2.4.3.2. Socio-political (Soc-pol.)

- *Employment creation (SC₂₁)*

Employment creation demonstrates the potential for jobs to be created in association with energy supply system creation, from construction to decommissioning, including operations and maintenance (O&M). The employment creation data of the RESs alternatives are presented by Wei et al., [87]. The index of the parameter is measured in jobs-years per GW-hour, where a job-year is equivalent to full-time employment for one person in 1 year as shown in Table 2.8.

- *Maintain leading position as energy supplier (SC₂₂)*

This is a qualitative sub-criterion that reflects the utilization of RESs to facilitate a nation's independence through supporting greater national energy security and reducing the need to import energy from foreign countries. Energy dependency to support national energy security is an important attribute in considering alternative energy sources [42], [45], [54], [56], [57], [65]. However, as a world leader in energy supply and with the largest oil reserves, Saudi Arabia is more interested in maintaining its leading position as an energy supplier. The country is entirely dependent on its own oil for electricity generation. Hence, Saudi Arabia could benefit from the surplus oil that would be reserved through generating electricity from alternative resources by

selling it to foreign countries. Furthermore, with the abundance of RESs, like solar radiation and heat, Saudi Arabia could sell excess electricity generated from RESs.

- ***Social and political acceptance (SC₂₃)***

This parameter qualitatively indicates the anticipated level of satisfaction of the public and politicians and their opinions toward each RESs technology. The parameter has a possible impact on the duration of commissioning a power plant and the logistic support that different RESs projects may receive.

2.4.3.3. Economic (Eco.)

- ***Capital cost (SC₃₁)***

Capital cost significantly influences the economic viability of the energy supply project and electricity. It comprises expenditure to establish a power plant, including the costs of land, equipment, wages, installation, and infrastructure. A comparison of the capital cost for the RESs alternatives is conducted through an EIA report on both capital and O&M costs [88]. Consequently, pairwise comparisons are obtained and the data are depicted in Table 2.8.

- ***National economic development (SC₃₂)***

National economic development is considered a qualitative parameter that reflects the extent to which the national economy benefits from each technology considering local manufacturing share and job localization [42]. In addition, in the case of Saudi Arabia, it includes the additional national income from selling oil for local electricity production.

- **Operations and maintenance cost (SC_{33})**

O&M costs comprise, on the one hand, operation costs, including salaries additional to the expenditure on energy production and services. On the other hand, it also consists of maintenance costs, which are the funds spent to ensure reliable plant operations and to avoid failure and damage. This index is measured in dollars per kWh and the data are shown in Table 2.8.

- **Energy cost (SC_{34})**

This parameter evaluates the expected cost of electricity produced by a power plant over its lifetime. A lower generation price of a RESs technology is reflected in a higher weight. Energy cost is a quantitative index. The energy cost data of each technology is obtained from the IRENA database, which is collected from different sources as depicted in Table 2.8 [23].

Table 2.8. Capital costs [88] , operations and maintenance costs [88] , energy cost [23] and employment creation [87]

Alternative	Capital cost (USD /MW)	Operations and maintenance cost (USD /kW-year)	Energy cost (USD/kWh)	Total Job- Year/GWh
Solar PV	3,873	39.55	0.270	0.87
Solar Thermal	5,067	67.26	0.230	0.23
Wind	2,213	24.69	0.08	0.17
Geothermal	6,243	132	0.07	0.25
Biomass	8,312	460.47	0.05	0.21

2.4.3.4. Environmental (Env.)

- **Land requirement (SC_{41})**

Land use reflects the required occupation of land for plant installation, which differs according to the RESs technology for a given installed capacity. The land requirements for plants of each RESs

technology depend on the intensity of resource availability and efficiency. A comparison of the land requirement of the RESs alternatives is shown in Table 2.9 [64].

- **Impact on emissions level (SC_{42})**

This parameter concerns the impact of a power plant on the environment and society in terms of emission reduction and ecological system disturbance owing to air emissions. It depends mainly on CO_2 reduction and further reflects the impact on the ozone layer and global warming. The impact on emission level is a quantitative parameter. Data are acquired from an IEA report of policy considerations for deploying RESs in Organization for Economic Co-operation and Development countries [89]. A comparison of alternatives in terms of impact on emission level is shown in Table 2.9 .

Table 2.9. Land requirement [64] and emission level [89]

Alternative	Land use average (m^2/GWh)	Emissions (tCO_2 equivalent/ MWh)
Solar PV	150	0.07
Solar Thermal	40	0.02
Wind	200	0.04
Geothermal	100	0.04
Biomass	25	0.1

2.5. Model Application

The data on preliminary criteria and sub-criteria was specified and collected from 20 stakeholders. The responses are represented by giving weights to criteria and sub-criteria, as well as by carrying out weighting for alternatives against sub-criteria that are not measurable or that lack data. In addition, participants are asked to add any parameters they believe are important and to remove criteria that they believe must not be considered. These modifications to the criteria are considered in the sensitivity analysis.

Sub-criteria are given as qualitative and quantitative parameters. Quantitative data are obtained objectively through international databases (e.g., the IEA), the literature, or from the data of developed countries where similar projects have been implemented. On the other hand, qualitative data are obtained subjectively by means of expert weighting. Subjective judgment is needed in the case of non-measurable parameters (e.g., social acceptance).

Classical AHP pairwise comparison is replaced by evaluation on a nine-level scale owing to the abundance of considered parameters. Using rank number of alternative (RNA) scale method (Eq. 2.2), the nine-level scale evaluations are converted into pairwise comparisons. This replacement of classic direct pairwise comparison between each of the two parameters has reduced the number of questions for participants.

Owing to uncertainty and lack of data associated with new technology planning in some developing countries, data collected from stakeholders are considered in order to prioritize the decision criteria and sub-criteria. Participants were asked only to evaluate criteria against each other with respect to the goal, as well as the sub-criteria of each criterion against each other with respect to their parent criterion. This gives the weight of each sub-criteria locally (i.e., with respect to the parent criterion) and globally (i.e., with respect to the goal). For quantitative parameters and sub-criteria where the alternative with minimum values is preferred such as the capital cost of each alternative, the transformation into RNA is presented in Table 2.10.

Table 2.10. Rank numbers of alternatives for capital cost

Alternative	Capital cost (\$/MW)	RNA (i)
Solar PV	3,873	6
Solar Thermal	5,067	4
Wind	2,213 (O_{\min})	9
Geothermal	6,243	3
Biomass	8,312 (O_{\max})	1

Authors mapped these values into the AHP scale using the following steps [90] :

1. Find the step value (h):

$$h = \frac{O_{\max} - O_{\min}}{9} \quad \text{Eq. 2.1}$$

Where O_{\max} and O_{\min} are the maximum and minimum values, respectively, among all investigated alternatives.

2. According to the AHP numerical scale Table 2.1, the $RNA_{(i)}$ is calculated and attained for the integer value. The RNA of alternative i is presented as follows:

$$RNA_{(i)} = \begin{cases} \text{int} \left(9 - \frac{O_i - O_{\min}}{h} \right), & \text{if } O_{\min} \text{ is the best} \\ \text{int} \left(\frac{O_i - O_{\min}}{h} \right), & \text{if } O_{\max} \text{ is the best} \end{cases} \quad \text{Eq. 2.2}$$

The maximum capital cost O_{\max} achieves the minimum allowable score ($RNA_{(i)} = 1$) whereas O_{\min} provides the maximum $RNA_{(i)} = 9$. For instance, wind energy has the minimum capital cost, which leads to the highest $RNA_{(i)}$, while biomass has the maximum energy cost among the analyzed alternatives and obtains the minimum score ($RNA_{(i)} = 1$) according to Eq. 2.2.

3. To adapt the rank numbers of alternatives into the AHP scale, a pairwise comparison between two alternatives (A and B) is obtained using scoring value (SV) in Eq. 2.3 below. Table 2.11 shows the pairwise comparison of alternatives obtained for the capital cost.

Table 2.11. Pairwise comparison of alternatives with respect to capital cost

	Solar PV	Solar thermal	Wind	Geothermal	Biomass
Solar PV	1	3	1/4	4	6
Solar thermal	1/3	1	1/6	2	4
Wind	4	6	1	7	9
Geothermal	1/4	1/2	1/7	1	3
Biomass	1/6	1/4	1/9	1/3	1

$$SV_{A \rightarrow B} = \begin{cases} (1/(RNA_{(B)} - RNA_{(A)} + 1)) , & RNA_{(A)} - RNA_{(B)} < 0 \\ (RNA_{(A)} - RNA_{(B)} + 1) , & RNA_{(A)} - RNA_{(B)} \geq 0 \end{cases} \quad Eq. 2.3$$

As a qualitative input, each alternative is evaluated under each sub-criterion. For example, the social acceptance indicator that varies from one society to another is considered. Then, the geometric mean is calculated from stakeholders' evaluations to form the $RNA_{(i)}$. Accordingly, the pairwise comparison can be obtained using the scoring value Eq. 2.3.

2.6. Results and Discussion

The results in Table 2.12 show the 14 sub-criteria categorized into four main criteria for evaluating five RESs alternatives for electricity generation. After acquiring data from different resources (i.e., international databases, literature, and stakeholders), the evaluation matrix of AHP is formulated according to the following steps. First, the AHP pairwise comparison of the four main decision criteria is conducted with respect to the main goal of the study. Second, the AHP technique discussed in Section 2.4 is used to prioritize weights of decision criteria with respect to the goal. The assessment model indicates that the economic and technical criteria are the most important with respect to the goal; their relative priority weights are each 35.1%. The socio-political aspect is the third most important criteria with a score of 19% whereas the environment is the least important with a weight of 11%.

Table 2.12. Priority weights of sub-criteria with respect to parent criteria (local weight)

Technical (0.351)	Socio-political (0.189)	Economic (0.351)	Environmental (0.11)
$\begin{bmatrix} SC_{11} = 0.333 \\ SC_{12} = 0.167 \\ SC_{13} = 0.167 \\ SC_{14} = 0.167 \\ SC_{15} = 0.167 \end{bmatrix}$	$\begin{bmatrix} SC_{21} = 0.333 \\ SC_{22} = 0.333 \\ SC_{23} = 0.333 \end{bmatrix}$	$\begin{bmatrix} SC_{31} = 0.227 \\ SC_{32} = 0.227 \\ SC_{33} = 0.122 \\ SC_{34} = 0.424 \end{bmatrix}$	$\begin{bmatrix} SC_{41} = 0.333 \\ SC_{42} = 0.667 \end{bmatrix}$

Third, a pairwise comparison is conducted for each list of sub-criteria with respect to their parent node (i.e., decision criterion) and local priority weights are obtained, as depicted in Table 2.12.

The global priority weights of sub-criteria with respect to the overall goal of the decision framework are depicted in Figure 2.5. The results show that the energy cost sub-criterion under the economic criterion has by far the highest importance with a global weight of 14.9% whereas the resource availability sub-criterion under the technical criterion has the second highest global weight of 11.7% with respect to the overall goal.

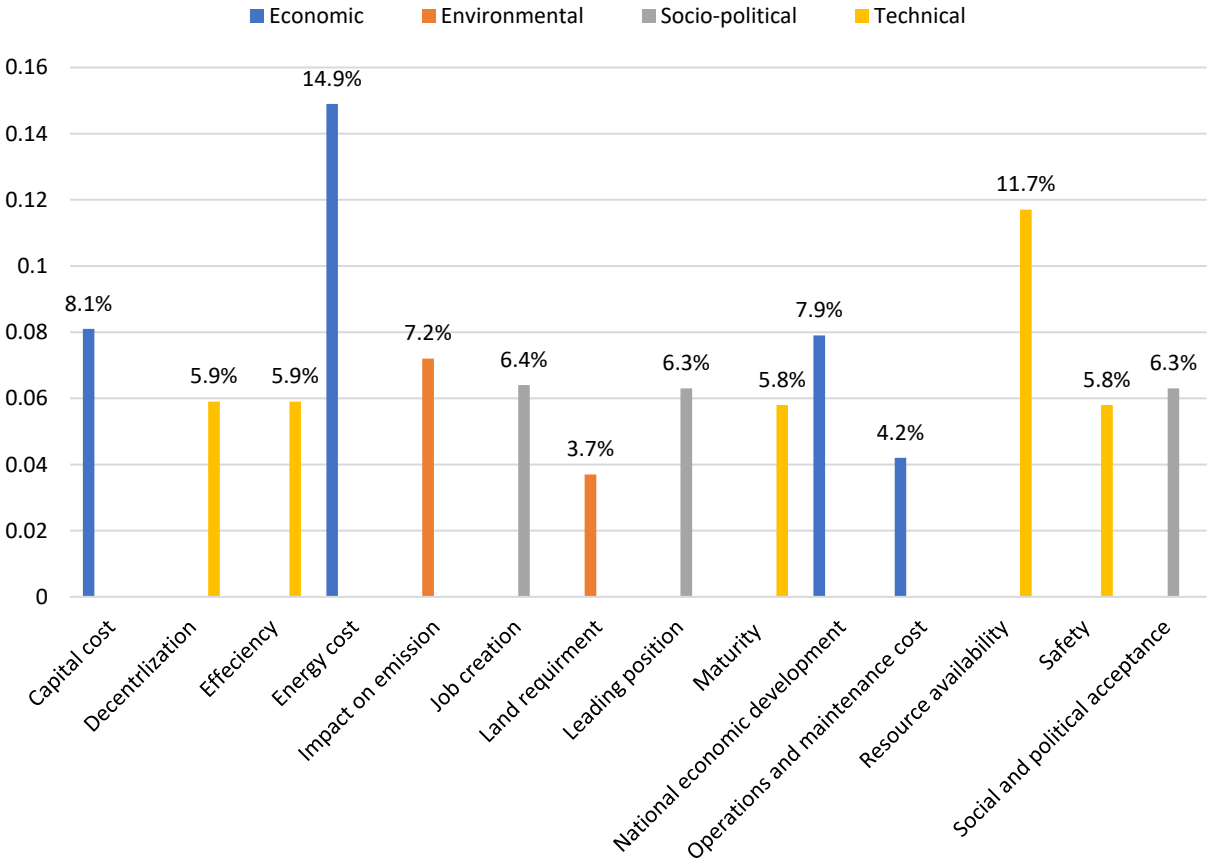


Figure 2.5. Global priority weights of sub-criteria with respect to goal

Capital cost and national economic development are the third most important sub-criteria, each with a weight of almost 8%. Due to the vast unused land in the kingdom, the land requirement

turns out to be the least important sub-criteria in evaluating any RESs alternative, with a weight of only 3.7%.

Fourth, the pairwise comparison of alternatives with respect to each sub-criterion is conducted through data for quantitative indexes, and through stakeholders' inputs for qualitative data. The priority weights obtained from this step formulate a matrix, which is multiplied by the priority weights of sub-criteria with respect to each criterion, resulting in priority weights of alternatives with respect to each criterion. These weights represent the local weights of alternatives under each decision criterion. As illustrated in Figure 2.6, the analysis of RESs alternatives by end-node criteria presents the performance of each alternative in each criterion that has influenced the score of the RESs alternatives toward the goal. From an economic aspect, wind energy ranked top owing to its lower capital cost, average energy cost, and potential major contribution to national economic development.

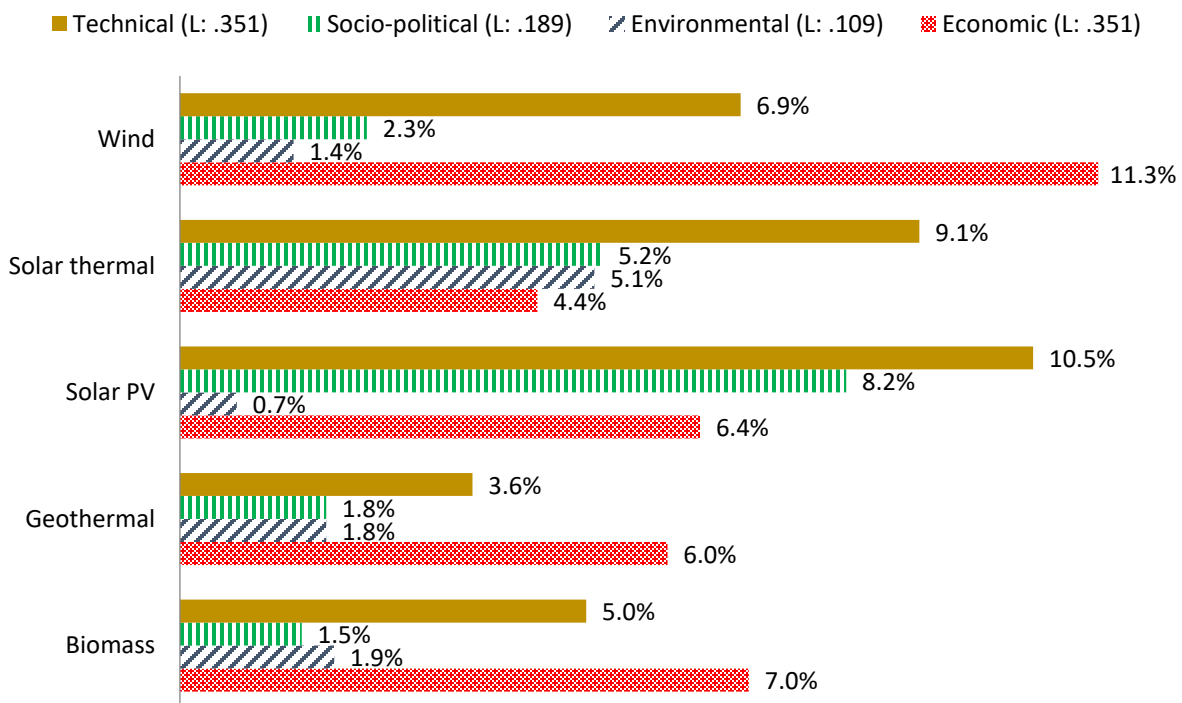


Figure 2.6. Local weights of alternatives under each decision criterion

Compared to other alternatives, solar PV performed best in technical aspects because of the high resource availability of solar energy in Saudi Arabia. On the other hand, it obtained the lowest score under the environmental criterion owing to the high life-cycle CO_2 emissions involved in the production phase of PV technology.

Finally, the results from the previous phase formulate a matrix that is multiplied by the priority weights of the decision criteria with respect to the goal in order to obtain the final ranking of RESs alternatives with respect to the goal, as shown in Eq. 2.4 below.

$$\begin{matrix} & [Tech. & Soc-pol. & Eco. & Env.] & [Wc] & [Alternative ranking] \\ \left[\begin{matrix} Solar\ PV \\ Solar\ thermal \\ Wind \\ Geothermal \\ Biomass \end{matrix} \right] & \begin{bmatrix} 0.298 & 0.429 & 0.182 & 0.059 \\ 0.258 & 0.275 & 0.124 & 0.462 \\ 0.201 & 0.121 & 0.321 & 0.135 \\ 0.102 & 0.095 & 0.172 & 0.166 \\ 0.141 & 0.08 & 0.202 & 0.179 \end{bmatrix} & * & \begin{bmatrix} 0.351 \\ 0.189 \\ 0.351 \\ 0.109 \end{bmatrix} & = & \begin{bmatrix} 0.256 \\ 0.236 \\ 0.221 \\ 0.132 \\ 0.155 \end{bmatrix} & Eq. 2.4
 \end{matrix}$$

The results show that solar PV is the most promising RESs technology, followed by solar thermal, wind, biomass, and geothermal, as presented in Figure 2.7. Based on the priority weights of PV technology in resource availability, contribution to economic development, higher employment opportunity, strong social acceptance, and ease of decentralization, the PV alternative has the highest weight of 25.6%. PV technology offers higher decentralized electricity production, which contributes to reduced losses in transmission lines and serves rural areas in a large desert country such as Saudi Arabia (the second largest by land area in the Arab world).

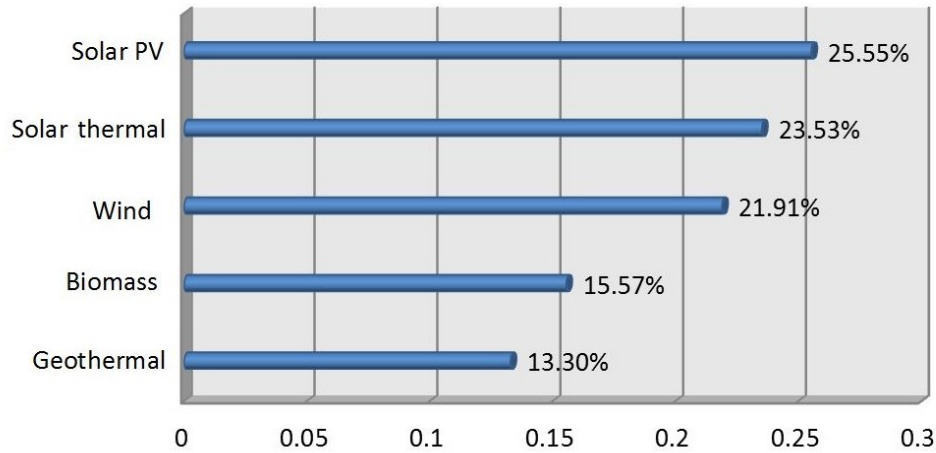


Figure 2.7. Priority weight of renewable energy alternatives

Solar thermal has the second highest priority weight of 23.5% as it has the highest resource availability, lowest carbon emissions, and higher social acceptance; it has a major potential contribution to make to the kingdom maintaining its leading global energy position. Wind energy performed significantly in economic and technical aspects. It obtained the third highest priority weight of 22%. Its moderate performance with regard to resource availability compared to solar energy (PV and thermal) and ease of decentralization reduces the overall relative weight of wind energy. Biomass and geothermal have modest weights for resource availability, lower maturity, and higher energy cost compared to the other alternatives. Their overall scores are 15.6% and 13.3%, respectively. In the proposed model the inconsistency ratio did not exceed 0.05 for any of the conducted pairwise comparison. This value is within the accepted range proposed by the AHP consistency which has a maximum of 0.1.

2.7. Sensitivity Analysis

Since there is subjective evaluation in this study, sensitivity analysis is essential to observe how the overall rankings of RESs alternatives change with respect to changes in the priority weights of the criteria or sub-criteria. Expert Choice software is used to obtain the results and perform

sensitivity analysis under different scenarios. Figure 2.8 presents the default results for the proposed model.

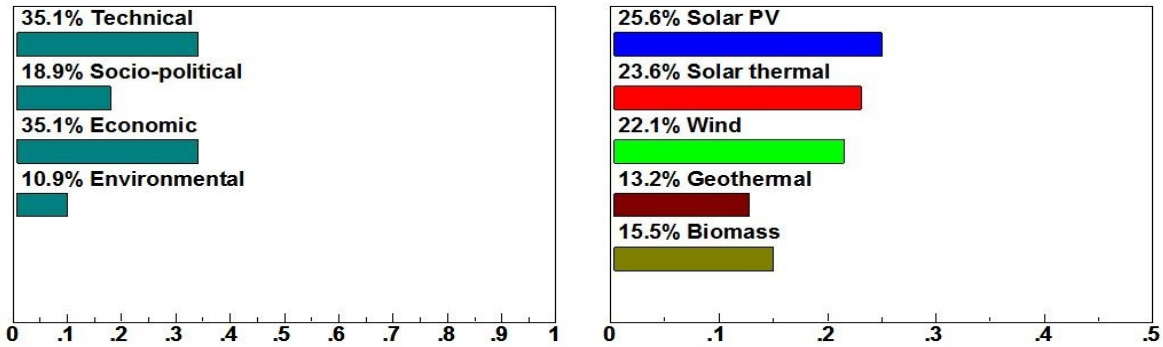


Figure 2.8. Criteria weights and Alternatives ratings considering the proposed approach

Considering equal weights scenario (25% for each criterion), results show that solar thermal has the highest score (28%) among other alternatives. The solar PV has the second highest score (24.2%) while the other alternatives ranking remains in the same order compared to the default scenario. This is mainly due to the exceptional performance of solar thermal in all decision criteria. The equal weight scenario's output is shown in Figure 2.9.

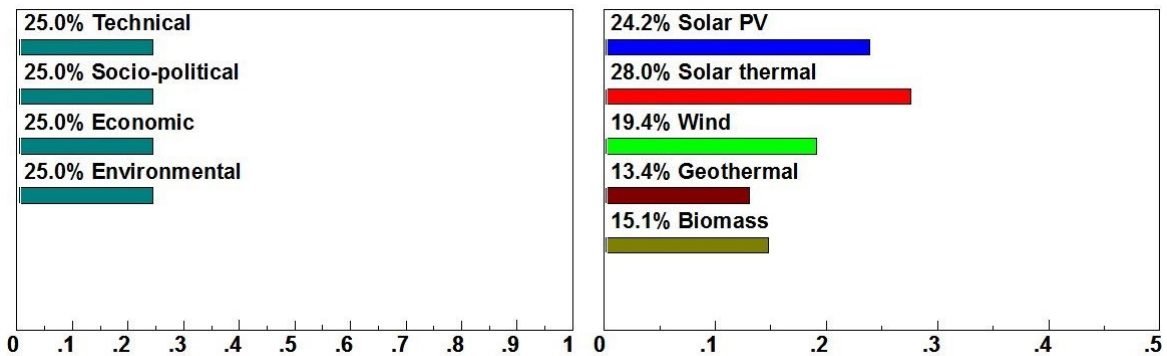


Figure 2.9. Equal criteria weights scenario and Alternatives ratings

Since the kingdom is heavily dependent on fossil fuel for electricity generation, switching to RESs should enable it to continue maintaining national economic development and strong economic and industrial growth. Increasing the economic criterion weight to 40% and maintaining equal weight

(20%) for the other criteria gives the same priorities as the scenario of equal weight criteria as depicted in Figure 2.10.

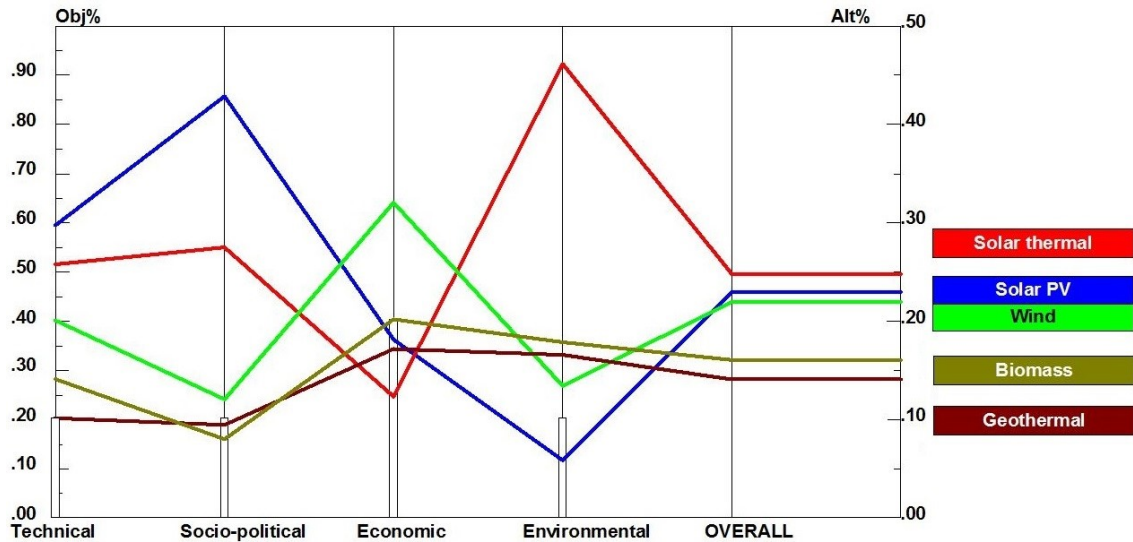


Figure 2.10. Performance sensitivity of alternatives with higher economic criteria (40%)

The results obtained from this scenario are in line with the initial energy mix plan for RESs generation in Saudi Arabia proposed by K.A.CARE (i.e., 25 GW of solar thermal, 16 GW of solar PV, 9 GW of wind, 3 GW of waste-to-energy, and 1 GW of geothermal).

Heterogeneity is essential in the decision-making process to ensure different opinions are involved and various perspectives are considered. The expert panel for the AHP model is composed of participants from different sectors involved in energy planning and road mapping for the country. Participants can be categorized in the academic, industrial, energy research, and decision-making sectors.

In this section, we highlight the variation of weights given to the main decision criteria considering the category orientation. This helps to understand the impact of bias derived from participants' backgrounds, and highlights the importance of heterogeneity in obtaining balanced outputs. Participants from the research and government sectors weighted the economic criterion as the

highest, followed by the technical criterion. On the other hand, the academic sector participants weighted the socio-political criterion the highest, while the economic and technical criteria were rated equally. The academic, government, and research sector participants weighted the environmental criterion the lowest. Meanwhile, the industrial sector participants presented a different distribution in which technical, economic, and environmental criteria scored similar weights, while the socio-political criterion achieved the lowest score.

Figure 2.11 shows the analysis of sub-criteria local weights per different categories of the stakeholders. Research, government, and academic experts considered energy cost and resource availability as the highest priority weights. This points to the fact that RESs alternatives with high potential for resource availability and low energy cost are preferred for sustainable power generation projects. Furthermore, participants from the research, government, and academic sectors considered land requirements as a lower weighted sub-criterion. Technology maturity, efficiency, and national economic development were considered to be of high importance by experts from industries.

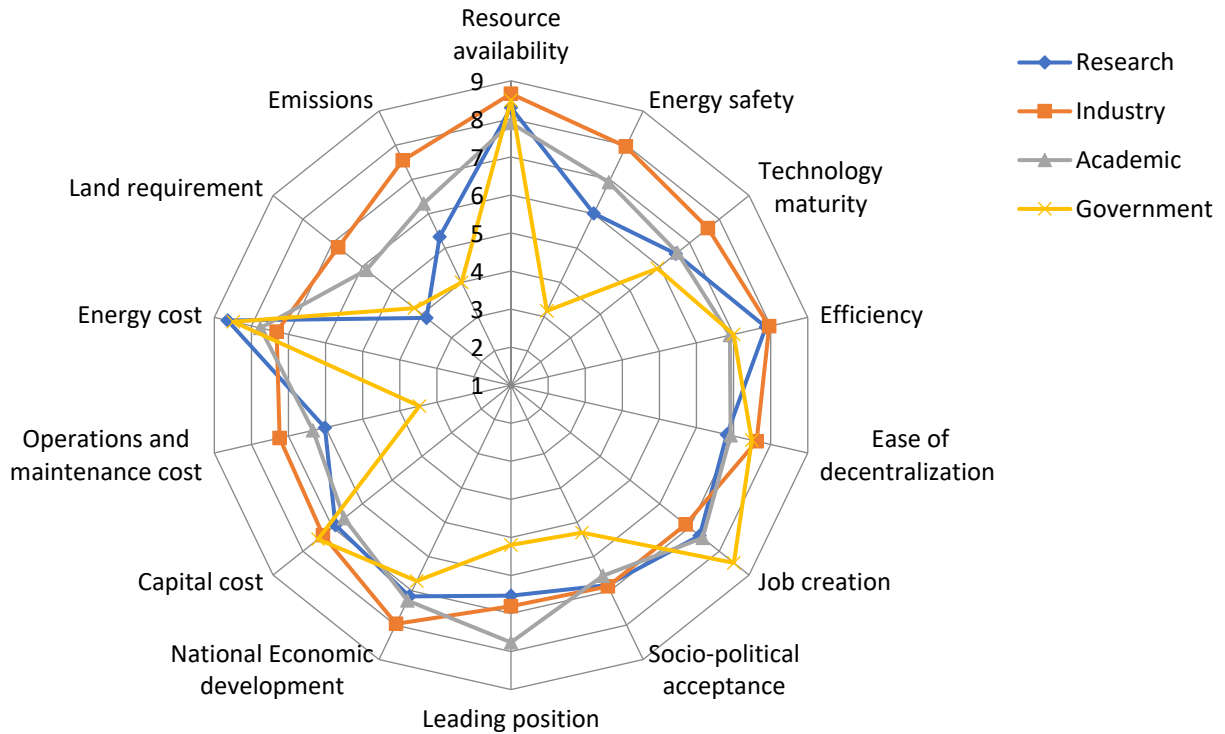


Figure 2.11. Evaluation of each sub-criterion by experts' categories

As a result of the high unemployment rate in Saudi Arabia (11.7%) [91], government experts took into account the number of employment opportunities generated from RESs alternative projects by giving job creation the highest priority weight over the other categories. Looking into the prioritization based on participants' categories, one realizes those governmental sector participants rating resulted in higher preference for PV compared to other alternatives. This preference reflects the low concerns they showed with regard to safety and O&M cost parameters (as illustrated in Figure 2.11) since these are insignificant for PV systems.

2.8. Conclusions

In energy mix planning, tackling the dilemma of which source to prioritize from one perspective only presents a major inadequacy owing to the complexity and multidimensional aspects of energy. Therefore, this study carried out prioritization and assessment of five RESs by developing an AHP

decision model for power-generation purposes in an oil-based and developing country. It presented a case study set in Saudi Arabia to demonstrate the effectiveness of the proposed model. An evaluation of solar PV, solar thermal, wind, biomass, and geothermal energy resources was determined with respect to technical, economic, socio-political, and environmental criteria. These criteria were sub-divided further into clusters of 14 sub-criteria for which each alternative was evaluated. The criteria and sub-criteria were elicited from experts, the literature, and the country's energy policy. Qualitative and quantitative data were integrated for the overall synthesis. The MCDA prioritization model shows PV technology to be the most promising RESs followed by solar thermal. This was mainly owing to their high performance in most of the criteria. Moreover, the results ranked wind energy third in the RESs technologies on the strength of its performance in economic and technical aspects. Compared to other RESs, biomass and geothermal had modest weights for energy cost, technology maturity, and resource availability causing these two technologies to be ranked the lowest. The proposed model shows that energy cost and resource availability are the most important sub-criteria in the economic and technical criteria, respectively. The major advantages of RESs deployment in Saudi Arabia are sustainable power generation, lower fossil fuel consumption, and maintaining the kingdom's leading global position in the energy sector. It is recommended that the country invests more in solar energy technologies (PV and thermal), which would significantly promote the sustainable development of Saudi Arabia. One caveat is that, owing to the country's vast deserted area, there is a high chance of dusty weather, which may limit the performance of solar PV panels. The study limitations are associated with the number of participants, which could be elaborated by considering higher number of experts and the limited local data for the alternatives comparisons with respect to sub-criteria.

The findings of this study have several policy implications including:

- The energy policy road mapping process involves several critical factors which interplay and contribute substantially to the shaping of sustainable energy sector. Instead of cost benefit analysis, developing a MCDM framework would facilitate inclusion of social, political, and environmental criteria in the decision making process towards promoting the use of renewable energy resources.
- The proposed methodology supports the involvement of different stakeholders standpoints in the decision making process thereby has increased consensus, acceptability, fair share of responsibility and results credibility.
- By implementing energy mix policy, Saudi Arabia can preserve its finite energy resources for the future or export the surplus to back its strong economic and industrial growth, which also leaves more energy available for other developing countries.

Chapter 3

Solar PV Power Plant Site Selection

3.1. Introduction

Utility-size solar PV technology has promising potential for deployment in vast land areas where the amount of solar irradiation per year is very high. However, one of the barriers in solar power development is the inconsistency and variability of solar irradiation which can be geographically dissimilar from one site to another. Site selection has a direct impact on the potential RESs projects in many different ways including technical, economic and environmental aspects. Accordingly, the identification of potential sites will rise to the forefront as a crucial phase to devote fostering sustainable projects. Site selection for the utility-scale grid-connected PV system is a critical issue due to its direct impact on the output power, project cost, environmental, social and infrastructures influences. The location of such project could be more technically feasible, economical, and further environmental friendly if interrelated factors are involved in the site selection process.

To select a site for a PV installation, it is essential to investigate the location suitability for this purpose. The solar plant site selection plays a vital role in maximizing solar energy received and the generated output power. It could reduce project costs and assist in planning future infrastructure projects including roads, power lines, etc. Given the fact that several factors can influence the site selection for utility-scale grid-connected solar PV systems, employing MCDM integrated with GIS facilitates the decision by considering the multiple key factors in the decision process. The utility-scale solar PV power plant site selection based on extensive information, especially from GIS, offers significant advantages [92]:

- Improving the solar project performance by ensuring a high level of solar irradiation and moderate temperature.
- The orientation of the site can be optimized when the project is installed on flat ground, towards the south and without a large shadow.
- Minimizing the losses from transportation, power transmission, and production by choosing the sites near these utilities and near urban areas, which are the main consumption points.
- Reducing the environmental, social and infrastructure impacts.
- Excluding the protected areas and unsuitable sites from the study areas.
- The findings of potential site solar suitability studies can support new development of transportation and transmission lines to be near those locations to promote the utilization of renewable energy.

3.2. Problem Statement

To select a site for such an installation, certain aspects must be investigated, such as how good the PV power plant location is, and how to minimize the total cost of the project concerning proximity to existing infrastructures while maximizing power output from the solar panels. Performing a comprehensive solar site analysis is a strategic step towards ensuring a cost-effective and well-performing solar project. MCDM integrated with a geographical information system (GIS) can be used to evaluate the land suitability in site selection for grid-connected solar plants. A comprehensive site analysis is a primary stage in ensuring a cost-effective and well performing solar PV project. The plans for sustainable solar energy exploitation can take advantage of optimization tools such as MCDM to avoid some of the inherent obstacles and to enhance the outcomes of the solar energy projects.

Given the fact that several criteria can influence site selection, applying MCDM methods can help facilitate site selection for utility-scale grid-connected PV solar energy systems by considering key factors in the decision process. The utility-scale PV can be defined as large-scale PV projects which can generate at least 5 MW [93], [94]. MCDM methods have been successfully applied in many energy-planning projects. Pohekar and Ramachandran [50], Mateo [41], and Wang et al. [51] provide an excellent literature review on application of MCDM approaches in the RES planning.

In recent years, the GIS has become increasingly popular for various site selection studies, particularly for energy planning [95], [96], [105]–[109], [97]–[104]. Screening possible sites for PV projects is a prime strategic process as suggested by several studies and strategic organizations such as National Renewable Energy Laboratory (NREL) [94], [110]–[112]. The decision-making process for site selection can be structured into the following general phases [102]:

- Development of decision criteria and restriction factors for the site selection study;
- Model-based prioritization of selected potential sites;
- Sensitivity analysis to draw insights into the relevance of decision criteria.

Evaluation of renewable sources in Chapter 2 shows that considering 14 criteria, solar PV technology is the most favorable option. This chapter facilitates site selection for utility-scale grid-connected solar PV projects by proposing a decision model that integrates AHP as a MCDM technique with data on sites from the GIS. Such combination technique will provide further insights into various subjective and conflicting factors which can aid DMs in the process of site selection. The aim of this chapter is to define and analyze optimal locations for utility-scale grid-connected solar PV projects. The site selection should ensure maximum power output and minimize the potential project cost. For this, develop a MCDM model to consider different

economic and technical factors, and use real data such as those on climate, roads, mountains, protected areas and other relevant data. Apply the developed model to the case of Saudi Arabia.

The following points are the main contributions of this chapter:

- Presents an original approach of developing criteria layers using real atmospheric sensors data in siting utility size PV power plant using GIS tools. Solar irradiation and air temperature criteria were generated in the ArcGIS software and facilitated for AHP process.
- To the best of author's knowledge, GIS-based AHP has not yet been conducted for utility-size PV site suitability study on such scale involving economic and technical criteria.
- Currently, no solar farm studies are applying GIS-MCDM within Saudi Arabia. This research is the first contribution in this direction.

The remainder of the chapter is organized as follows. Section 3.3 presents the literature review. Section 3.4 presents the proposed methodology for site selection of PV power plants. In Section 3.5, a case study for Saudi Arabia is provided. Finally, Section 3.6 concludes the chapter.

3.3. Literature Review

3.3.1. Decision criteria and restriction factors

In this chapter, the decision criteria are derived based on the existing literature, the study objective, and accessibility to the geo-referenced database. Solar irradiation is an essential criterion for large-scale PV solar power projects. High amounts of solar energy play a major role in producing more electrical power from available resources. Solar irradiation is considered as one of the most important decision criteria in majority of solar site suitability studies, as shown in Table 3.1.

Table 3.1. Solar PV site suitability criteria

Criteria	Sub-criteria	Reference
Environmental	Land use	[113]–[117]
	Agrological capacity	[98], [118], [119]
Location	Distance to urban areas	[96], [98], [122], [99], [111], [113], [114], [118]–[121]
	Distance to substations	[98], [99], [118], [119]
	Land Cover	[96], [114]
	Population density	[96], [116], [117], [123]
	Distance to main roads	[96], [98], [124]–[126], [99], [113], [114], [117]–[119], [121], [122]
	Distance to power lines	[96], [98], [121]–[124], [126]–[128], [99], [111], [113], [114], [117]–[120]
	Distance to historical areas	[122] [114]
	Distance to wildlife designations	[122]
Economic	Land cost	[123]
	Construction cost	[123]
Climatic	Solar irradiation	[96], [98], [120]–[129], [99], [130], [131], [111], [114]–[119]
	Average temperature	[98], [99], [118], [119], [124], [125], [128], [131]
Orography	Slope	[98], [99], [113]–[115], [118]–[121], [125]
	Orientation (aspect angles)	[98], [99], [115], [118], [119], [121], [130]
	Plot area	[98], [99], [118], [119]

In the context of solar irradiation, the GHI is the sum of DNI, diffuse horizontal irradiation (DHI) and ground-reflected irradiation as depicted in Figure 3.1. The DNI is the amount of directed sunlight while DHI is the irradiation components scattered by clouds or another object in the atmosphere; however, the irradiation reflected from ground is considered lesser compared to the other components and could be neglected. The PV technology works in the presence of both DNI and DHI solar irradiation, unlike CSP technology which works using only DNI [24].

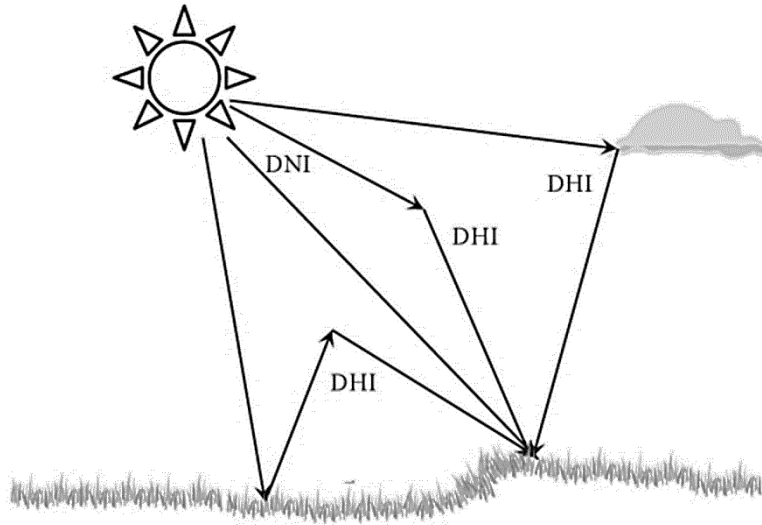


Figure 3.1. Components of Solar irradiation intercepted by earth surface [132]

Close proximity to utilities prompts sufficient accessibility and aids to avoid high cost of infrastructure construction as well as harmful consequences to the environment. Moreover, minimizing the distance to electric transmission lines is an economical way to avoid the high cost of establishing new lines as well as minimizing power loss in the transmission. Certain studies [96], [98], [113] consider locations that are further away from cities more suitable for RES development to avoid negative environmental impact on urban development and to avoid not in my back yard (NIMBY) opposition. On the other hand, studies [120], [121] indicate that sites nearby cities have more economic advantages. To obtain more accurate results, the study area could be screened to eliminate infeasible locations that pose hindrance to the installation of a utility-scale PV plant. Unsuitable locations which prohibit the deployment of such facilities will be discarded using the GIS. Table 3.2 presents the most common restrictions applied for solar site suitability.

Table 3.2. Restrictions used in solar energy studies

Layers of restrictions	Reference
Urban lands	[98], [99], [113], [119], [121], [122], [124], [125], [131]
Protected land	[96], [98], [113], [119]–[121], [123], [131]
Cultivated land	[121], [122] [116] [126]
Area with high landscape	[96], [98], [99], [113], [119]–[123]
Water infrastructure	[99], [116], [119], [129]
Military zones	[98], [113], [118], [119]
Cattle trails (wildlife areas)	[98], [113], [118], [119]
Cultural heritage	[96], [98], [118], [119], [122], [124]
Archaeological sites	[96], [98], [99], [113], [118], [119], [123], [124]
Paleontological sites	[98], [118], [119]
Roads and railroad network	[98], [99], [113], [119], [121], [124]
Sand dunes	[124], [125]
Natural disaster (Flood Area etc.)	[123], [124]
Area with higher slope (>5°)	[122]–[124], [131]
Mountains	[118], [119]
Soft soil	[123]
Community interest sites	[98], [118], [119], [123]
Dams	[124], [126]
Flight security	[120]
Biological significant areas	[113]
Watercourses and streams	[119] [126]
Special protection area for birds (SPA)	[119], [122]
Coast	[119]
Land aspects	[122]

3.3.2. Methods in solar site selection

MCDM techniques aid DMs to select the best option among several alternatives in the coexistence of various criteria. These techniques have been frequently deployed in the planning of RES, especially for site selection under environmental, technical, and economic factors. Furthermore, multiple DMs could have different opinions regarding the specific criteria or alternatives that

should be involved in the decision framework. The selection of sites for RES based merely on one criterion is inadequate [133]. Huang et al. [134] and Loken [133] propose site selection to be suitably handled through the use of MCDM, particularly for energy planning complexity. Recently, the integration of the GIS with MCDM has become increasingly popular for various siting applications, such as landfill site selection [135], [136], urban planning [137], [138], and the planning of RES sites [50], [104], [129], [139], [140].

The GIS has demonstrated its principal role in exploiting geographical information for developing a spatial decision support system for locating solar facilities. Extensive information from the GIS offers significant advantages for determining site suitability for utility-scale solar PV power plants [92]. These include the following:

- Improved performance of the solar project by ensuring a high level of solar irradiation and moderate air temperature;
- Optimization of the orientation of the site when the project is installed on a flat ground placed towards the south in regions with no large shadows;
- Minimizing loss from transportation, power transmission, and production by considering sites near these utilities as well as nearby urban areas, which are the main consumption points;
- Reducing environmental, societal and infrastructural impacts;
- Excluding protected areas and unsuitable sites from the study areas;
- Using GIS extensive information to develop decision support system for locating solar facilities could support new infrastructure development near those locations to promote utilization of free energy.

Therefore, incorporating both fields of GIS and MCDM yields mutual benefits and can offer a more reliable decision for solar site selection. A study conducted by the NREL on feasibility assessment of concentrated solar thermal potential in the southwestern United States (U.S.) utilized GIS screening techniques [141]. After interpreting several constraints, such as protected areas, slope, and distance from the transmission, solar resource maps were generated and potential areas for project development were highlighted.

Various MCDM methods are available in the literature; however, research on GIS-MCDM has utilized relatively few approaches, such as the weighted linear combination (WLC) [120], TOPSIS [142], AHP [113], [118], [119], [121], [122], [124], grey cumulative prospect theory [103], and ELECTRE [98]. Jankowski [143] clarified the role of the GIS and MCDM methods in supporting spatial decision making and presented a framework for their integration. Greene et al. [144] provided an overview of MCDA and its spatial extension using the GIS. The authors suggested improving the integration of MCDA with GIS software for increasing accessibility.

Chandio et al. [137] investigated land suitability for solar energy sites using a GIS-based AHP approach. A variety of criteria have been considered, including solar irradiation, slope, land orientation, urban areas, protected areas, transmission lines, and road accessibility. Rumbayan and Nagaska [129] employed MCDM methods with the GIS to prioritize RES (solar, wind, and geothermal) in 30 provinces in Indonesia considering the availability criteria. Sánchez et al. [98] optimized solar farm locations using ELECTRE and the GIS. Effat [121] used the GIS and remote sensing tools with an AHP to calculate the criteria weight of a spatial model. Uyan [113] applied a GIS-based solar farm site selection in Konya, Turkey.

In their work on optimal placement of PV solar power plants in the area of Cartagena, Spain, Sánchez et al. [118] used AHP for weighting decision criteria, whereas TOPSIS was applied for

assessment of alternatives. Sánchez et al. [119] applied fuzzy TOPSIS for the installation of solar thermoelectric power plants on the coast of Murcia, Spain. AHP was used to weigh the criteria, whereas results were validated using ELECTRE-TRI methodology.

Charabi and Gastli [124] conducted an evaluation of land suitability for the implementation of large PV farms in Oman. They combined AHP with ordered weighted averaging (OWA), using fuzzy quantifiers in GIS. Aydin et al. [120] proposed fuzzy decision-making procedure that deploys the OWA algorithm for aggregating multiple objectives and prioritizing the most feasible locations for hybrid solar PV-wind systems. Janke [96] applied a multi-criteria GIS to identify areas for the installation of wind and solar farms in Colorado. A large area of Southern England was assessed for the suitability of wind and solar farms by Watson and Hudson [122] using AHP and GIS. A recent study by Liu et al. in [103] investigated the site selection of PV power plants to support decisions in optimal installation site by using grey cumulative prospect theory. Table 3.3 summarizes the applications of MCDM techniques in different studies for RES site selection. It can be noticed that AHP has been frequently utilized for the planning of renewable and conventional energy, the allocation of energy resources, the management of building energy, and the planning of electricity utilities [50] [127].

Table 3.3. Multicriteria decision-making techniques in solar PV planning

No.	MCDM Technique	RES	Location	Reference
1	AHP	Solar PV-wind-geothermal	Indonesia	[129]
2	ELECTRE	Solar PV	Southeast of Spain	[98]
3	AHP	Solar PV and CSP	Ismailia, Egypt	[121]
4	AHP	Solar PV and CSP	Konya, Turkey	[113]
5	AHP – TOPSIS	Solar PV	Southeast Spain	[118]
6	AHP–Fuzzy TOPSIS and ELECTRE	CSP	Murcia, Spain	[119]
7	AHP-Fuzzy OWA	Solar PV and CSP	Oman	[124]
8	Fuzzy OWA	Wind-solar PV	Western Turkey	[120]
9	WLC	Wind-solar PV and CSP	Colorado, USA	[96]
10	AHP	Wind-solar PV and CSP	Central England	[122]
11	Grey Cumulative Prospect Theory	Solar PV	Northwest China	[103]
12	TOPSIS-ELECTRE	Solar PV	Southeast of Spain	[99]
13	AHP	PV	Serbia	[145]
14	AHP-Fuzzy TOPSIS	PV	India	[146]
15	Fuzzy ANP and VIKOR	PV	Taiwan	[147]
16	WLC	PV-CSP-Wind	Afghanistan	[148]
17	AHP	PV-CSP	Tanzania	[149]
18	FAHP	PV	Ulleung, Korea	[150]
19	ELECTRE-II	PV-Wind	China	[151]
20	AHP	PV	Morocco	[152]

3.4. Proposed Methodology

The proposed methodology is depicted in Figure 3.2. This study aims to provide an evaluation of site alternatives for the sake of discovering the most suitable sites for utility-scale PV projects in Saudi Arabia. The raw data of this chapter is collected from different resources including governmental agencies, open sources, and related literature. A four-stage analysis is performed to facilitate decision support for PV solar farm site selection.

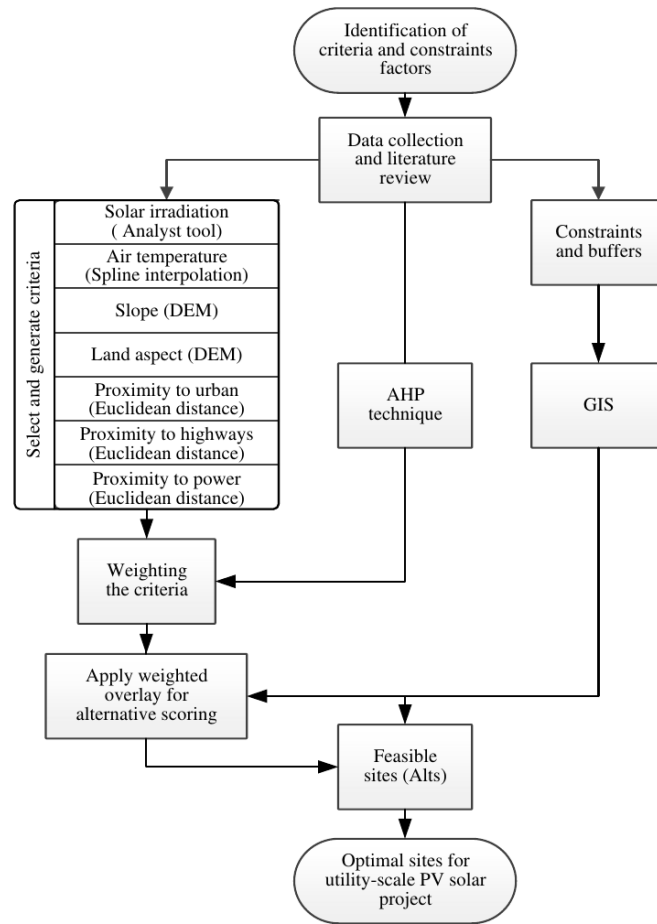


Figure 3.2. Flowchart of the proposed methodology

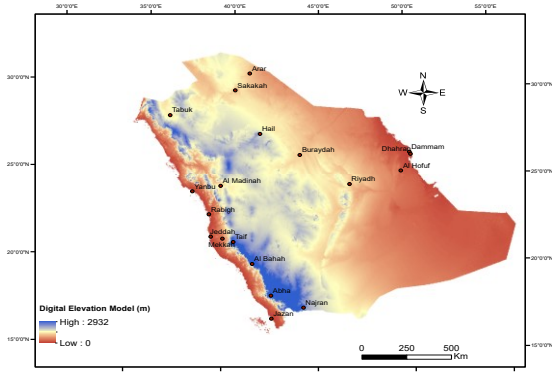
- In the first stage, a GIS map overlay technique is applied taking different constraints and restrictions into consideration to rule out unsuitable sites.
- In the second stage, an AHP technique is applied to determine the relative importance and priority weight of each criterion.
- In the third stage, overall evaluation of the candidate site is performed by applying weighted sum overlay approach using the ArcGIS tool. The main concept of this technique involves overlaying several criteria maps with consideration of the input criteria and their relative weights obtained from AHP to create an integrated analysis. The weighted sum overlay receives the scaled data inputs, weights the input layers, and adds them together.

- Finally, the unfeasible sites generated in the first stage are excluded from potential areas for the selection of solar PV sites. A land suitability index (LSI) is developed to demonstrate the suitability distribution of the potential sites and to visualize their spatial allocation on the suitability map [153]. A reclassification is performed to achieve the LSI map and the results are grouped into five scales from 1 (least suitable) to 5 (most suitable). Depending on the chosen PV technologies, the required area per 1 MW can vary. Assuming a PV system on 18,000 m² generates approximately 1 MW of power, the potential areas were limited to utility size areas to ensure that the total system size is large enough to be considered for a utility-scale project [93], [94].

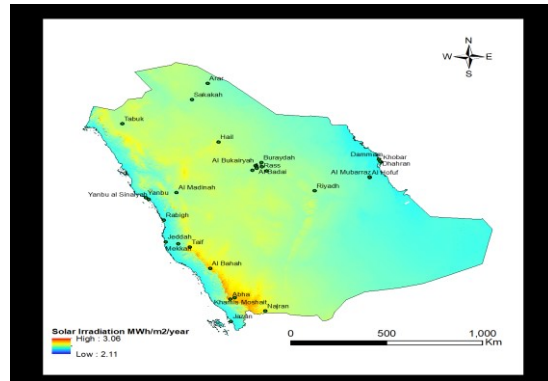
3.4.1. Criteria for site selection

The location of utility-scale PV projects involves technical feasibility criteria, which directly affect the performance of the solar power plant. These include the amount of solar irradiation and the average of the air temperature criteria. Economic factors express the impact of the placement of solar farms on the project cost. These include proximity to urban areas, proximity to highways, proximity to power lines, slope, and the aspect of the land criteria (Figure 3.3). The two technical feasibility criteria are explained in detail as follows:

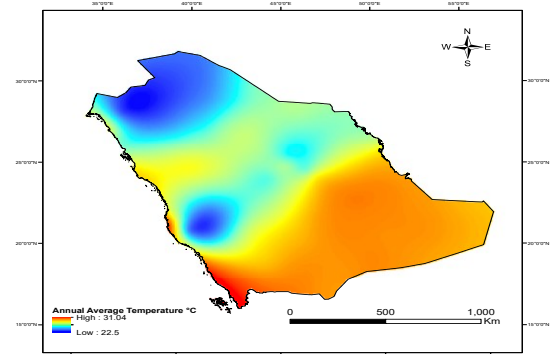
- **Solar irradiation (C1)** (kWh/m²): The solar analyst tool in the ArcGIS software supports solar irradiation mapping and analysis for specific areas or points and specific time. It has been chosen because it is viable for modeling solar irradiation for a field with diverse terrain as it considers local factors such as orientation, slope, and weather conditions [154].



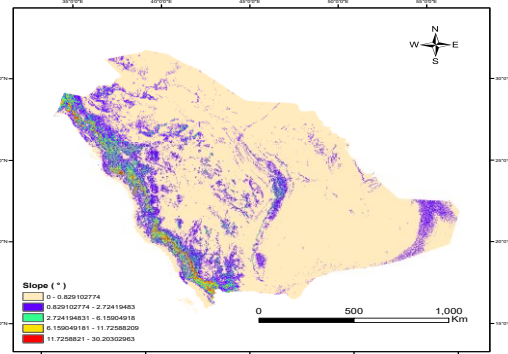
Digital Elevation map



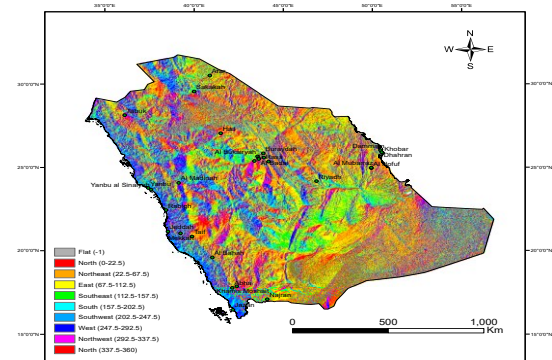
C1. Solar irradiation



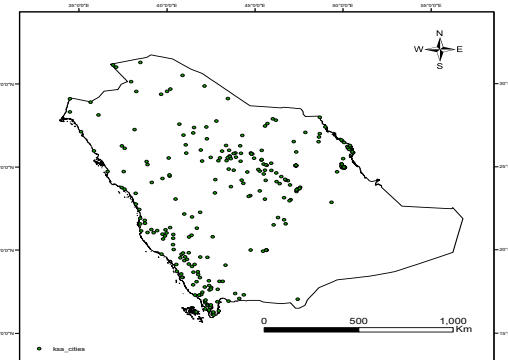
C2. Annual average temperature



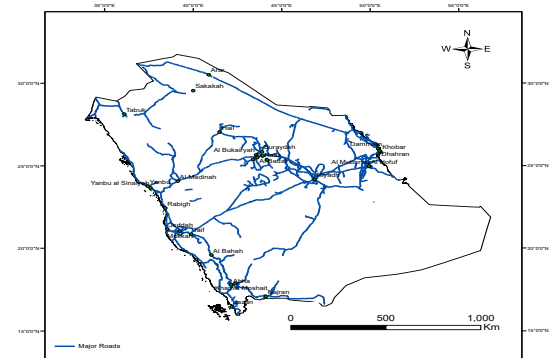
C3. Slope map



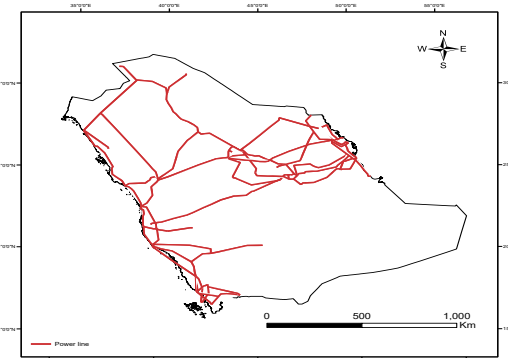
C4. Land aspects



C5. Cities



C6. Major roads distribution



C7. Power lines distribution

Figure 3.3. Criteria maps applied in the proposed GIS-MCDM

In addition, the solar analyst tool uses the digital elevation model (DEM) as input, which was used to generate slope and land aspects layers. This will result in a perfect match between the incorporated layers. Three map layers were used internally in the model for calculating the solar irradiation. These include viewshed map, sky map, and sun map. The value of diffuse proportion variable ranges from 0 to 1, where higher values indicate a less clear sky [155]. The diffuse proportion considered in this study was elicited from a K.A.CARE study that used twelve months of data from 30 stations distributed across the country based on one-minute measurements of GHI and DHI [156]. The transmittivity is the property of the ratio of energy that is received by the earth's surface to the amount received by the upper limit of the atmosphere, and its values range from 0 (no transmission) to 1 (complete transmission). This study considers a value of 0.65, which has been applied in several studies that have similar arid regions [124], [157]. The parameters applied in ArcGIS solar analyst are presented in Table 3.4.

Table 3.4. Parameters used in ArcGIS solar analyst tool

Parameter	Value	Parameter	Value
DEM	Resolution of 90m	Slope Aspect Input Type	DEM
Latitude	24.1 (Auto)	Calculations Directions	32
Sky Size	200 (Default)	Zenith Divisions	8
Time Configuration	Whole Year (2014)	Azimuth Number	8
Day Interval Hour	14 (Default)	Diffuse Model Type	Uniform_Sky
Hour Interval	0.5 (Default)	Diffuse Proportion	0.36
Z Units	1	Transmittivity	0.65

- **Average temperature (C2) (°C):** New network monitoring systems have been installed in Saudi Arabia as part of the Renewable Resource Monitoring and Mapping (RRMM) program initiated by K.A.CARE to provide more reliable and real-time measurements for large-scale

deployment of RES technologies. A study by Zell et al. [156] summarizes the analysis of the measurement data used in 30 stations spread across the country. At each site during the study period, the annual average based on 24 hours of data for each day's temperature is recorded. In this study, real measurements are utilized for interpolating the yearly average temperature for the entire study area. The spatial analyst tool in ArcGIS 10.3.1 employs several interpolation tools that can generate a surface grid from points data. Natural Neighbors, Trend methods, Topo to Raster, Inverse Distance Weight, Spline, and Kriging are available interpolation methods. The Spline interpolation tool can estimate the values very smoothly using a mathematical model which minimizes the overall surface curvature. It can predict valleys in the data, and it is the best interpolation tool for smoothing varying phenomena such as temperature [158], [159]. The tension spline type was used to obtain higher values for the weight parameter resulting in a coarser surface (weight=10, No. of points=4).

- **Slope (C3) and land aspects (C4):** Flat areas or mild steep slopes will help to avoid the high construction cost required in high slope areas. Flat terrain is essential for large-scale PV farms; as such, high slope areas are not preferable for such projects due to low economic feasibility. A south-facing slope is an ideal orientation for solar farm sites and must be less than 5° in this study. Higher slope areas such as valleys and steep lands should be avoided. Using the DEM, the aspects of the survey area have been generated.
- **Proximity to urban areas (C5), proximity to highways (C6), and proximity to power lines (C7) (m):** In this study, the proximity to residential areas is considered as a favorable factor. A buffer of 1.5 km from urban cities and a maximum radius of 50 km are considered, where close proximity to the city is preferable. The Euclidean distance is used to calculate the closest source based on straight-line distance with a maximum of 50 km. Proximity

factors to such utilities are crucial in creating a distributed generation network and for grid-connected PV solar power.

3.4.2. Restrictions for site selection

For suitability analysis, aspects such as urban areas, protected land, major road networks and higher slope lands ($>5^\circ$) have been selected as restriction factors. These four constraints are commonly applied in similar solar site suitability studies. In addition, these factors were available as a dataset for the study area and serve the objective of this chapter. The protected areas include wildlife sanctuaries, national parks, industrial cities, and sacred places. According to the Saudi wildlife authority (SWA), there are 75 wildlife-protected areas in Saudi Arabia to encourage sustainable rural development and preserve wildlife, 62 of which are wilderness areas and 13 of which are coastal and marine areas as shown in Figure 3.4. The thematic layers of protected areas in this study are obtained from governmental agencies while the buffer distances have been adopted from the literature as shown in Table 3.5. The total area of the existing and proposed protected lands is approximately 10.42% of the country's total area.

Table 3.5. Restrictions layers considered for utility-scale PV in Saudi Arabia

Restriction	Data Source	Accessed on	Buffer	Reference
Protected lands	Renewable Resource Atlas of Saudi Arabia	Feb 9, 2014	<1000 m	[122]
Major roads	http://faculty.ksu.edu.sa/falmutlaq/pages/gis_data.aspx	Oct. 15, 2015	<500 m	[160]
Slope	Renewable Resource Atlas of Saudi Arabia	Feb 9, 2014	$\leq 5^\circ$	[124]
Urban areas	Renewable Resource Atlas of Saudi Arabia	Feb 9, 2014	<1000 m	Modified from [113], [122]

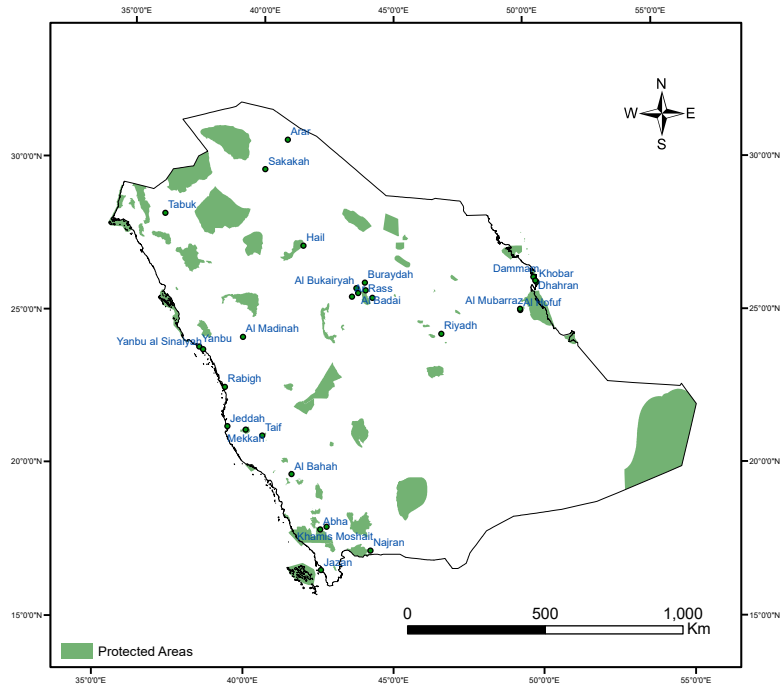


Figure 3.4. Protected areas

High slope areas are not viable for solar PV projects due to low economic feasibility. Based on the data from various literary works [113], [121], [122], [124], the slope factor for this study should be less than or equal to 5°. Higher slope areas including valleys and steep slopes were eliminated. Moreover, to limit the feasibility analysis, urban areas, highway networks, developed areas, and major roads were discarded due to the high density of population and buildings in addition to traffic safety issues.

The restriction layers shown in Figure 3.5 were integrated into one layer including the necessary buffers. They were then assigned a binary scale (1 and 0), where “one” indicates the absence of the allocated constraint indicating that the development of the project is possible, whereas “zero” indicates the presence of limitations, indicating that the development of the project is impossible. The initial resulting layer was reclassified as exploitable areas attributed by one. Once the

constraints layer was converted to binary, the multiplication of this layer with the criteria layer in Subsection 3.4.1 was performed to generate the preliminarily suitable sites map.

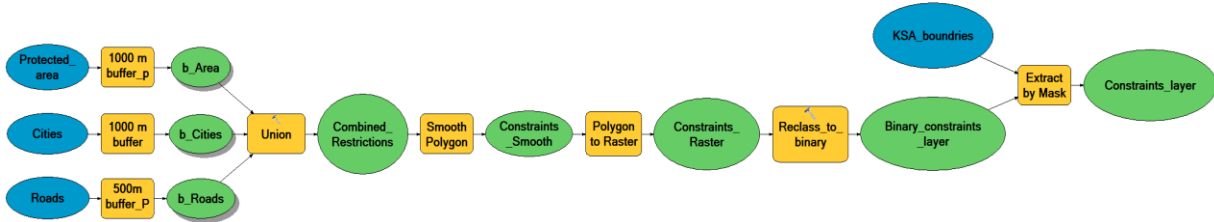


Figure 3.5. Restrictions part of the model

3.4.3. PV power plants site selection

3.4.3.1. GIS-AHP based approach

The basics and procedure of AHP introduced in Section 2.4. AHP has been accepted by the international scientific community as a robust and flexible MCDM technique for solving complex decision problems [61]. The top level of the AHP hierarchy encompasses the primary goal, whereas the middle and bottom levels represent the decision criteria and the alternatives, respectively. The DMs assess each level parameters in pairwise comparisons against their parent node. The AHP decomposes a large problem into smaller sub-problems in hierarchical levels and assigns weights to the decision-making criteria. GIS-AHP applications are among the most often used approaches for integrating AHP with other decision support techniques.

Following steps demonstrate how to generate solar PV suitability map using AHP for n number of criteria [161]:

- 1) Form a pairwise comparison matrix $m = (n * n)$ for several criteria. Let P_{ij} reveal the preference score of criteria i to criteria j using the nine-integer value scale suggested by Saaty [161], as presented in Table 2.1. P_{ij} denotes the entry in the i th row

and the j th column of matrix m . The entries of preference score P_{ij} and P_{ji} must satisfy the following constraint in Eq. 3.1:

$$P_{ij} \cdot P_{ji} = 1 \quad \text{Eq. 3.1}$$

- 2) Second, to establish a normalized pairwise comparison matrix \bar{m} , the sum of each column must equal to 1. This can be obtained using Eq. 3.2 to calculate \bar{P}_{lj} for each entry of the matrix \bar{m} .

$$\bar{P}_{lj} = \frac{P_{lj}}{\sum_{l=1}^n P_{lj}} \quad \text{Eq. 3.2}$$

- 3) Then, the average across rows is computed to obtain the relative weights using Eq. 3.3. For each element, the relative weight is within the range of 0 to 1; a higher weight shows a greater influence of the element to the solar PV power plant site.

$$w_i = \frac{\sum_{l=1}^n \bar{P}_{lj}}{n} \quad \text{Eq. 3.3}$$

- 4) Finally, to obtain the solar PV suitability map (SSM), Eq. 3.4 has been applied for each pixel of study area layer. If restriction (r) exists, then $r = 0$ which leads to the SSM value of an unsuitable site. Otherwise SSM could be obtained by finding the summation of each criteria value (x_i) multiplied by corresponding criteria weight (w_i).

$$SSM = \sum_{i=1}^n x_i \cdot w_i \cdot r \quad \text{where } r \in \{0,1\} \quad \text{Eq. 3.4}$$

- 5) The present study has seven elements associated with decision criteria or $n = 7$. The CR and RI equations are presented in Subsection 2.4.2. The random consistency index varies according to the number of comparison criteria (n) as shown in Table 3.6. Accordingly, $RI = 1.32$ and $CR = 0.02$ which is in acceptable range.

Table 3.7 presents the eigenvalue obtained by pairwise comparisons of criteria with respect to the goal of selecting the best site for solar PV.

Table 3.6. Random index for different values of number of elements [161]

n	2	3	4	5	6	7	8	9	10	11	12
RI	0	0.58	0.90	1.12	1.24	1.32	1.41	1.45	1.49	1.51	1.48

Table 3.7. Eigenvalue of criteria

Criteria	Eigenvalue
C1	0.350
C2	0.237
C3	0.159
C4	0.106
C5	0.032
C6	0.046
C7	0.070
Total	1.000

- 6) If $CR \leq 0.10$, the degree of consistency is considered satisfactory; otherwise, there are serious inconsistencies in the pairwise comparison. Therefore, the AHP may not return meaningful results [161].

The original high-level maturity and advanced embedded features enable the GIS to be a powerful tool for strategic planning of energy development projects, including solar technologies [94] [95]. In the present chapter, ArcMap 10.3 was utilized to perform spatial processes and manipulation for both vector (points, lines, or polygons) and raster (pixels or cells) files of the

study area's dataset. It has been used to overlay the different layers to create composite map results and smart visualizations for insightful decision-making.

3.4.3.2. Steps in determining best sites

The key steps in determining the best sites for deploying solar PV plants are as follows:

- First, the decision problem was structured into a hierarchical model as shown in Figure 3.6.

The goal represents the top-level of the hierarchy, which is to select the most suitable site to install utility-size PV power plants. The decision criteria are represented in the second level of the model.

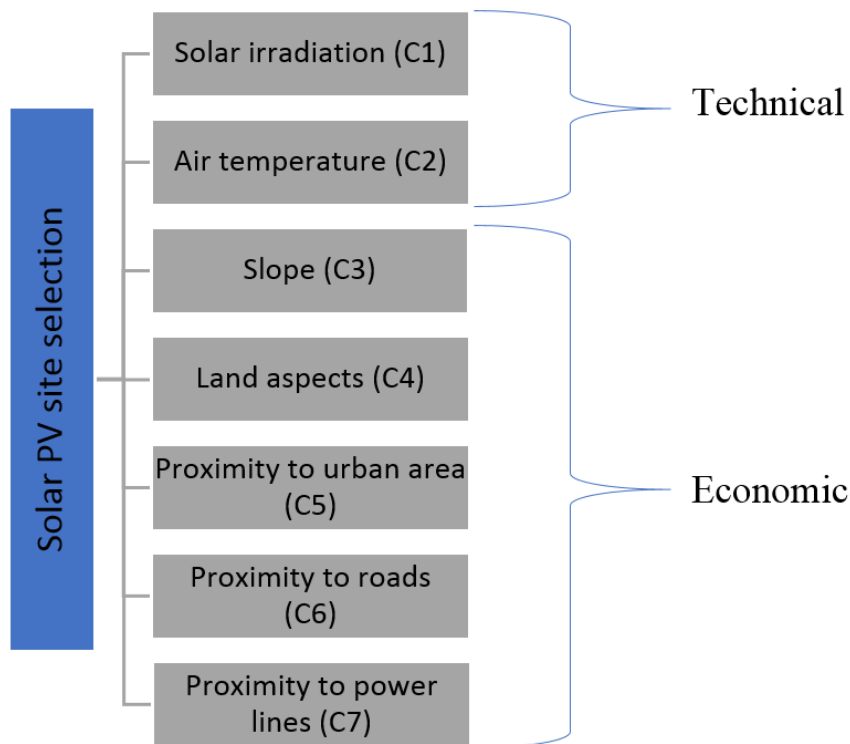


Figure 3.6. Decision criteria considered in solar site selection

- The second key step is to obtain the comparison matrix of criteria including solar irradiation, yearly average temperature, slope, land aspects, proximity to an urban area, proximity to the main road, and proximity to power lines, all of which are elements towards

the goal of the study in the proposed decision framework. Aran et al. [92] introduced an approach to obtain a pair-wise comparison matrix and determined the priority weights of the criteria. Several points highlight the rationale behind the criterion weighting. First, the climate criteria, including solar irradiation and the yearly average temperature, are considered the most important criteria as they define the output power of the PV power plant. In subsequent order of importance are the slope and the land aspects criteria, as they determine the amount of irradiance received by the solar panels. Their importance essentially depends on the steepness or mildness of the slopes and the orientation of the area. Milder slopes and south aspect areas are considered high importance factors. From an economic perspective, the distance to the electricity grid, major roads, and cities follow in importance, as they determine the infrastructure and transmission cost of installation.

- Based on the above reasoning, and considering the criteria weights presented in similar solar site suitability studies [119], [124], [153] the pair-wise comparison matrix was established, as shown in Table 3.8. The importance of such criteria is also emphasized by strategic organizations such as the NREL and the environmental protection agency (EPA) in U.S. [92], [96], [110], [124].
- The third key step is to calculate the priority weights and to check for inconsistencies. The eigenvector, which indicates the priority weight of each criterion, was computed and the sum of all weights is equal to one as represented in Figure 3.7. To verify the weighted values of each criterion, the CR was calculated ($CR=0.02$); as it is less than 0.10, the value judgments are considered to be acceptable [161].

Table 3.8. Comparison matrix of the adopted decision criteria

Criteria	C1	C2	C3	C4	C5	C6	C7
C1	1	2	3	4	7	6	5
C2	1/2	1	2	3	6	5	4
C3	1/3	1/2	1	2	5	4	3
C4	1/4	1/3	1/2	1	4	3	2
C5	1/7	1/6	1/5	1/4	1	1/2	1/3
C6	1/6	1/5	1/4	1/3	2	1	1/2
C7	1/5	1/4	1/3	1/2	3	2	1

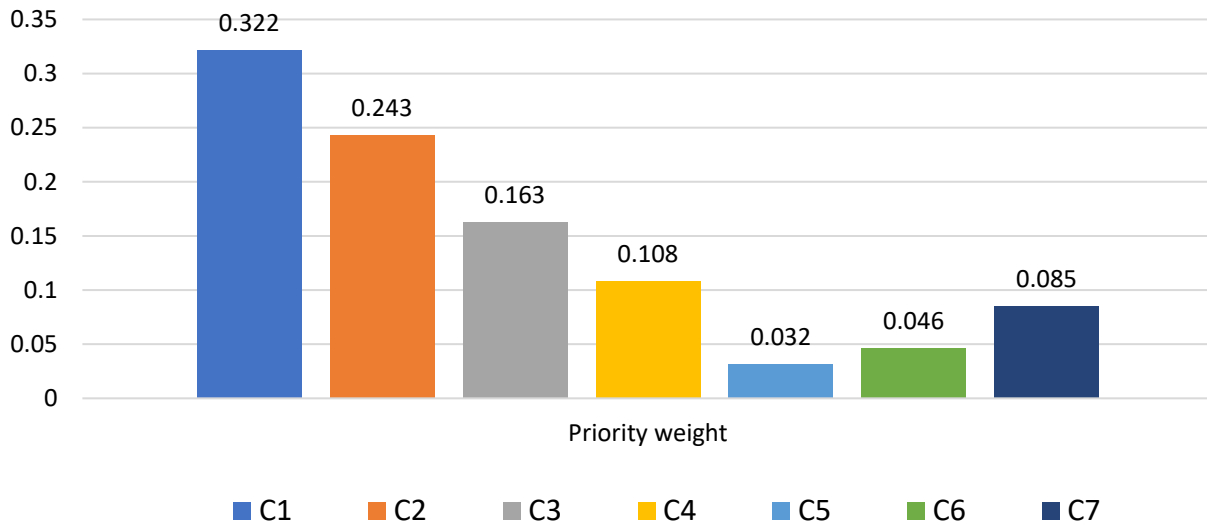


Figure 3.7. The priority weights of the criteria

At this point, seven layers of the considered criteria with their corresponding weights (gained from the AHP tool) were obtained. Using the weighted sum overlay tool in the GIS, the PV site selection is tackled as follows [162]:

1. Since the input layers are in different values and ranges, each criterion must be brought to a common scale in order to integrate them in one layer. Subsequently, values in the input maps were reclassified into a common preference scale of suitability ranging from 10 to 100 (with 100 being the most suitable).

2. Each criteria layer is multiplied by the criteria's weight or importance according to the AHP.
3. The resulting cell values were added together to generate the ultimate combined layer. Therefore, the alternatives are the potential sites generated through the GIS which takes into account the criteria weights obtained from AHP technique.

3.5. Case Study

The field of our study includes Saudi Arabia, which encompasses most of the Arabian Peninsula. The country is located in the southeast of Asia with an area greater than 2 million km². The main cities are Riyadh (capital city), Jeddah, Mecca, Medina, and Dammam. The country is majorly arid terrain except the Asir province in the southwest that is influenced by monsoons of the Indian Ocean. Most of the country is dominated by a desert climate with extreme heat during the day and an abrupt drop in temperature at night. The Kingdom's location, massive unused areas, and amount of daily solar irradiation are all factors that offer profound potential for exploiting solar energy in Saudi Arabia. The solar irradiation in the Kingdom is considered one of the highest rates worldwide with an average GHI of 2 MWh/m²/year as shown in Figure 3.8 [163] [164].

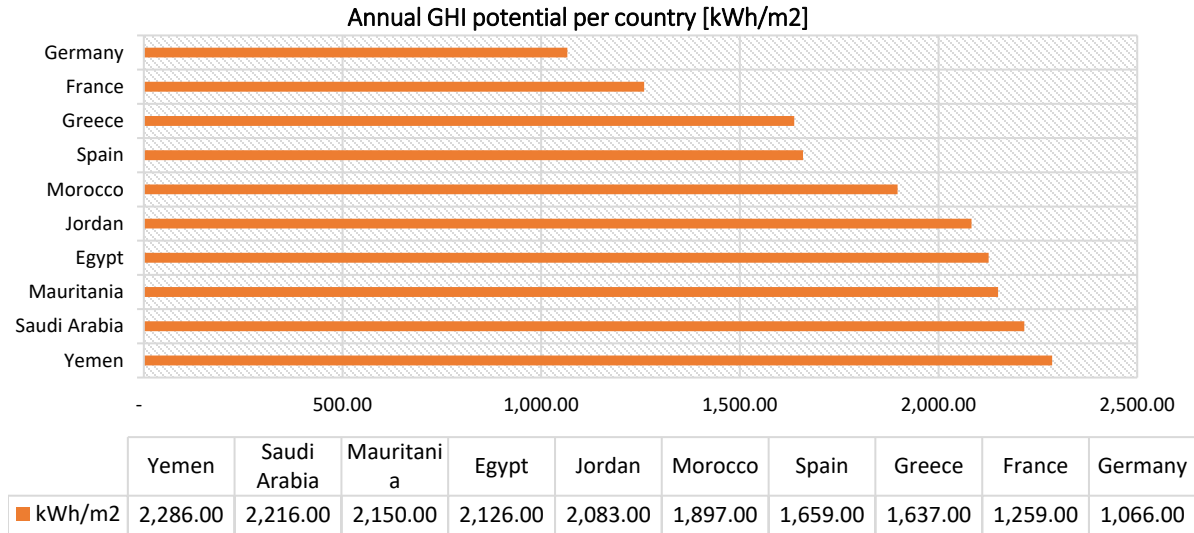


Figure 3.8. The annual global horizontal irradiance among selected countries

Rahman et al. [20] studied long-term mean values of sunshine duration and global solar irradiation on horizontal surfaces of over 41 cities in the kingdom. Results showed that the overall mean of yearly sunshine duration in the Kingdom is 3,248 hours, and the GHI varies between a minimum of 1.63 MWh/m²/year at Tabuk, a northwestern region of the Kingdom, and a maximum of 2.56 MWh/m²/year at Bisha, a southwestern region of the Kingdom. The minimum solar irradiation is higher than the average GHI in Germany and many other European countries. Furthermore, the pattern of global solar irradiation intensity and sunshine duration follows that of electricity demand. Solar energy could be the most desirable RES option to encounter the required power, especially during the summer season when demand peak reaches its highest, mainly due to air conditioning systems [19]. Saudi Arabia gained significant experience in the area of solar energy from different studies and research program [21] [19].

Solar PV has great potential for deployment in the kingdom where vast areas of land are available and the amount of global solar irradiation is very high. Currently, Saudi Arabia plans to produce

9.5 gigawatts from renewables, mainly solar and wind power, by 2023 as a part of Kingdom's 2030 vision [165].

3.5.1. Screening potential sites

The proposed methodology was applied to a study area of Saudi Arabia for site selection of utility-scale solar PV power plants. The final map of unsuitable areas indicates that most of the study area does not fall under any restrictions and does not belong to any protected areas, as illustrated in Figure 3.9. The seemingly suitable areas are large zones across the study area, which can be exploited to implement utility-size solar PV power plants.

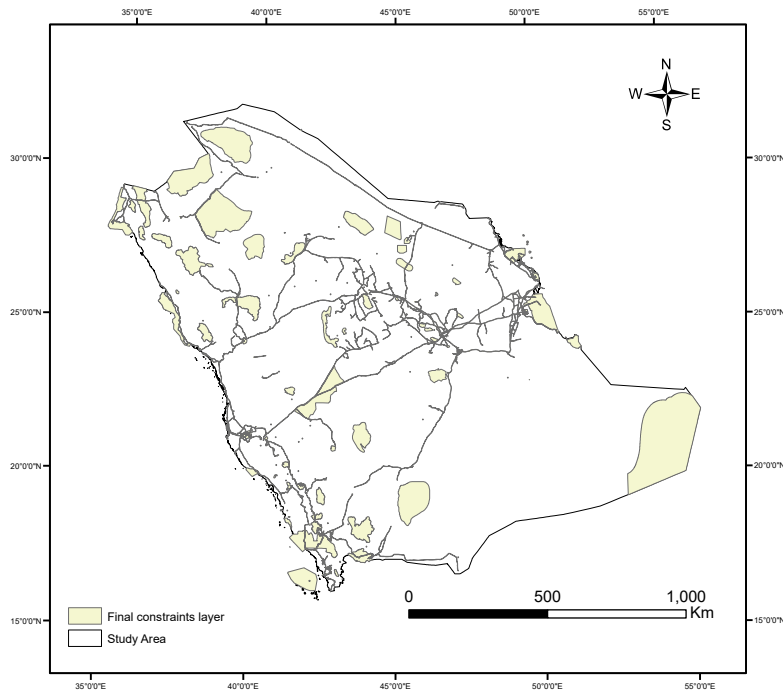


Figure 3.9. Restrictions layer map

As a result of MCDM-GIS integration, the overlaid result map showed that 16% (300,000 km²) of the study area is promising and suitable for deploying utility-size PV power plants as depicted in Figure 3.10. The central part of Saudi Arabia has shown more areas that are appropriate for utility-size PV power plants, mainly due to their favorable high solar irradiance, mild slope, and proximity

to major roads, grid lines, and urban areas. It has also been found that few sites are suitable north and northwest of the study area. The east and west coasts presented a few strips of suitable sites. The southeast region, which contains the largest contiguous sand desert (known as Rub' al Khali), is mostly unsuitable for installing such a facility due to relatively high air temperature and low density of main roads, power transmission lines, and urban areas.

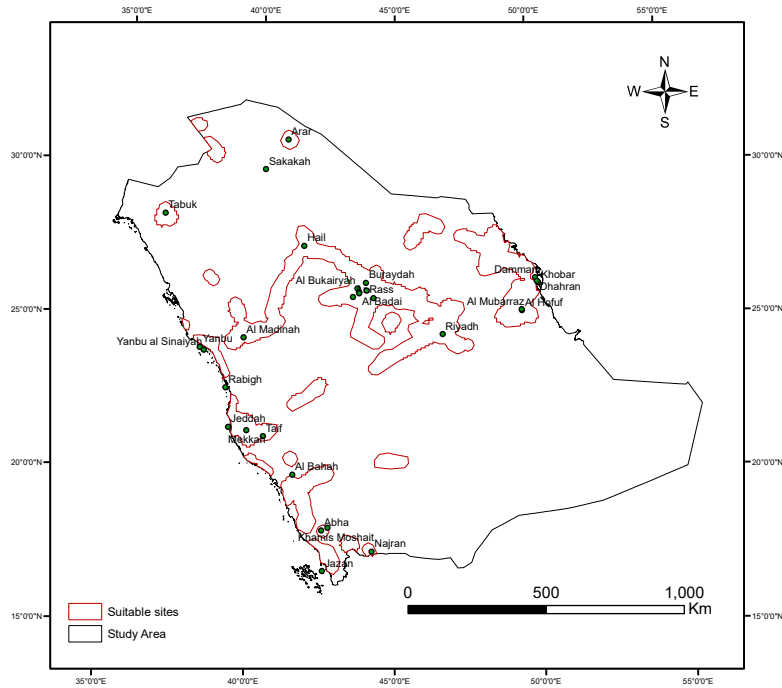


Figure 3.10. Preliminary results of potential sites

3.5.2. Site selection results

For better demonstration and insight, the LSI is proposed. The LSI defines the degree to which each site is suitable for the placement of PV plants according to the associated criteria and excluding all restrictions. The resulting data indicates that most of the overlaid values range from 30 to 80 with a mean of 60 considering the common suitability scale (10-100). For this distributed data, the suggested LSI values are shown in Table 3.9.

Table 3.9. Land suitability index

Scale values	Land suitability index
1 - 40	1 (least suitable)
40 - 50	2 (marginally suitable)
50 - 60	3 (moderately suitable)
60 - 70	4 (highly suitable)
70 - 100	5 (most suitable)

According to the LSI analysis, many of the highly suitable locations are in the central region as illustrated in Figure 3.11. The most suitable areas are located north to northwest, mainly due to higher solar insolation and lower air temperatures in that region. Along the southwest and west coasts, lands have lower LSIs due to major steep slopes, including the mountain range (Sarawat Mountains) which runs parallel to the west coast. The eastern region of the study area shows moderate to high LSIs since it has adequate infrastructure combined with the high density of high solar irradiation.

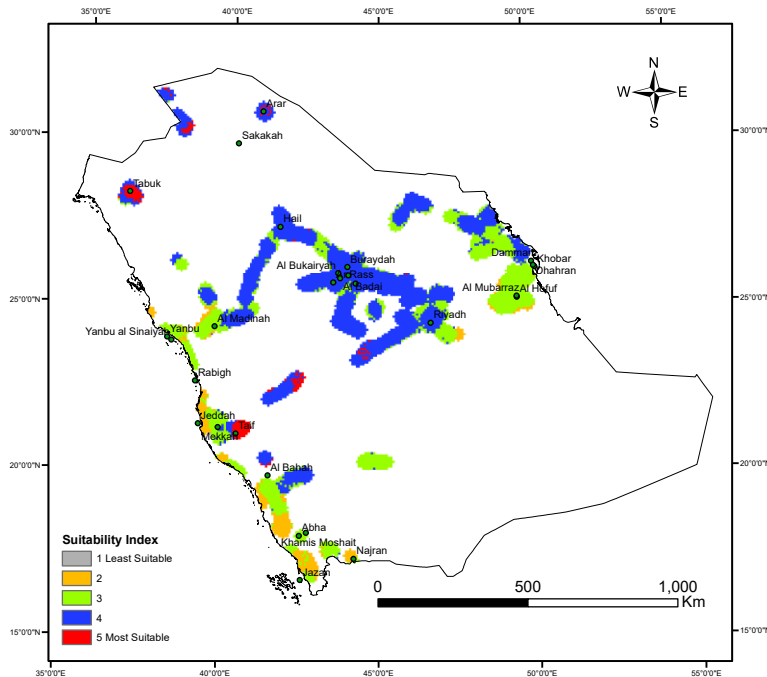


Figure 3.11. Suitability Index results using AHP weights

Based on the model results, Tabuk and Arar cities located in the North, besides Taif city in the West would be the most suitable sites to implement solar PV on a utility-size scale. While these locations account for only 3% of all the suitable areas, they offer a potential for high performance solar PV projects in terms of power generation and associated infrastructure costs. On the other side, the largest contiguous sand desert located to the East and South East (known as Rub' al Khali) is unsuitable for such projects due to relatively high air temperature and low density of infrastructure.

The suitability distribution for Saudi Arabia developed in this study can support decision-makers in selecting the most suitable sites for utility-size solar PV projects. Recently, Saudi Arabia has planned to build 300 MW of solar and wind plants in several locations [166]. Al-Jouf city which is located in the North (East from Tabuk as shown in Figure 3.11) has been designated for a 50 MW solar PV project. Such a location which is near the most suitable sites is favorable to the PV technology and offers a high potential for ultimate performance of a solar PV system. Likewise, considering the high suitability sites in central areas, which comprise 50% of the suitable areas, is significant for grid-connected utility-scale PV power plants, since these areas are near the most populous city, Riyadh. Lastly, this suitability distribution map can benefit the decision makers by helping them to be proactive in the solar PV development and can aid to achieve the Saudi 2030 diversified energy targets.

Figure 3.12 outlines the land suitability distribution based on the previous suitability index analysis. We found that more than 80% of the suitable areas had a moderate to high LSI. It has been found that suitable lands are following the pattern of the approximate range of the proximity to main roads, transmission lines, and urban cities. Therefore, there is great potential to have more suitable sites in the north and northwest of Saudi Arabia by improving the efficiency of power

lines and major road networks and utilizing these sites to generate power from their abundance of solar energy. However, no sites had a score of 100 in the study results, which indicates that no location is perfect across all of the criteria.

To validate the model, the results obtained are compared with a performance study of solar resources in Saudi Arabia conducted in [167]. Based on real-time solar radiation and air temperature from monitoring sensors, the author reviewed the performance of a pilot photovoltaic across 32 sites in Saudi Arabia. Results are consistent with suitability index map resulting from the proposed GIS-AHP model. For instance, due to the lower air temperature in Tabuk and Taif cities (with yearly average temperature $\approx 30^{\circ}\text{C}$) and high solar irradiation (annual average of GHI $\approx 6.3 \text{ kWh/m}^2$), they show a high energy productivity compared to other sites (generated energy $\approx 210 \text{ MWh}$). Also, Najran site gives the highest generated energy (218.5 MWh) due to the highest solar irradiation compared to all locations (6.8 kWh/m^2). Nevertheless, in our study it has low suitability index due to low distribution of power lines, major roads, and urban areas.

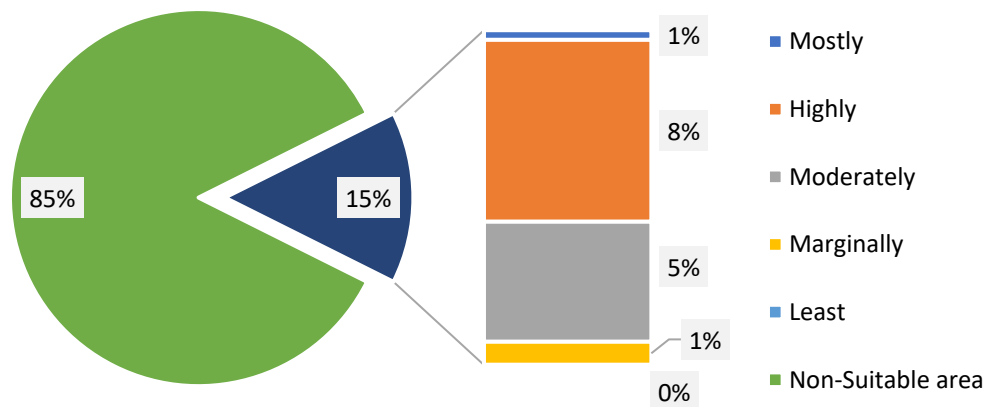


Figure 3.12. Land suitability distribution

3.5.3. Sensitivity analysis

For conducting sensitivity analysis, different criteria weight scenarios were considered and their overall impact on land suitability index was assessed. In addition to the criteria weights assigned

using AHP technique, two scenarios including equal weights and higher economic weight have been examined in this study. In the case of equal weights scenario, the weight of 14.28% has been assigned to each criterion to ignore the relative importance of each criterion. This approach is the simplest decision-making method for avoiding risk. On the other side, the economic criteria including slope, land aspect, proximity to urban areas, to power lines and to major roads are given higher weights than others (each 16%) in order to study the influence of economic factors. Figure 3.13 depicts the criteria weight used in AHP, equal weights, and higher economic weight scenario.

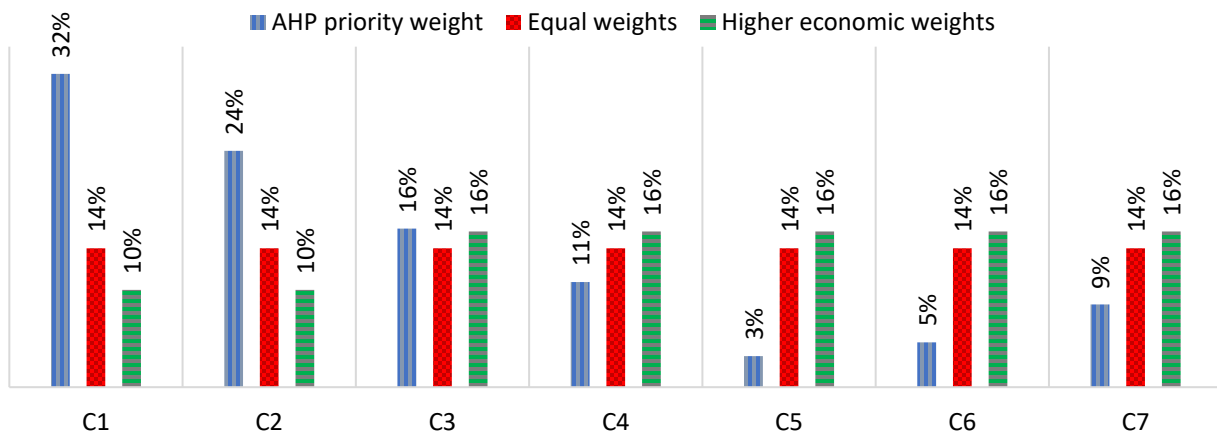


Figure 3.13. Weights of decision criteria considering different scenarios

Alternative sites were assessed and ranked to develop utility-scale solar PV projects using equal weights for associated criteria. This scenario will prompt the even measurement of the influence of the criteria on the resulting suitability layer and will lead to a greater understanding of the importance of each criteria weight. Compared to AHP methodology, the overall suitable area of this scenario has decreased by 0.64% (1,825.55 km²) of the study area. This is essentially attributable to the decision criteria that offer more weights (14.3%) to economic factors including proximity to major roads, grid lines, and urban areas. Similar to the AHP approach, the result of the similar weight scenario shows that there are vast areas with a high LSI for approximately 48%

of the suitable area. On the other hand, marginal LSIs and moderate LSIs have increased from 1.02% to 1.22% and from 5.29% to 5.9% respectively around the whole study area, as shown in Figure 3.14.

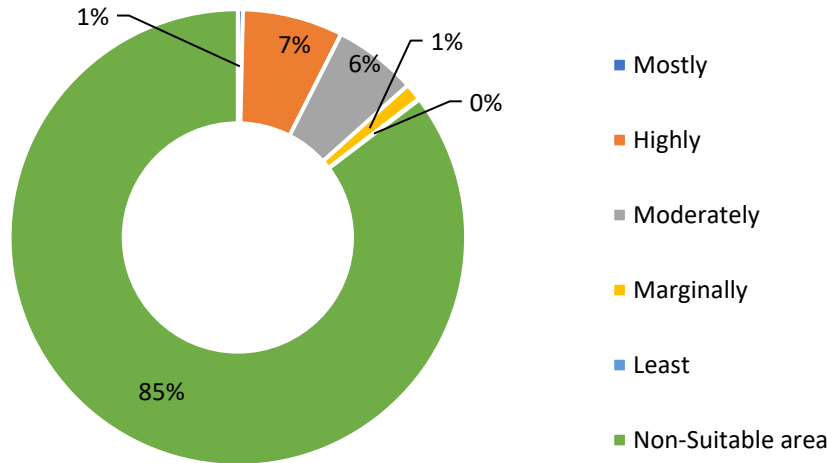


Figure 3.14. Suitability Index distribution for equal weights scenario

The most suitable LSI showed a slight decline from 3% to 2.5% of the suitable area (from 0.4% to 0.35% of the study area) when considering equal weightings for all criteria. Most of the moderate to high LSI areas are spread near the central province of Saudi Arabia, as depicted in Figure 3.15. More moderate and high LSI sites exist where mountains stretch from the southwest along the west coast, since the slope weights have decreased by 2% (from 16.3% to 14.3%). In the east, the moderate LSI improved to highly suitable and most suitable due to higher weights to the proximity to economic factors and lower weights to the temperature criteria. As solar PV systems present a high initial cost and require relatively large areas of land to produce energy, the land construction costs turn out to be more of an issue, whereby proximity to the national grid, major roads, and urban areas could have significant economic costs which outweighs the electricity generated from the solar farm [168]. Selecting sites on the basis of slope and orientation as well as installation near existing infrastructures will be more pertinent for solar developments.

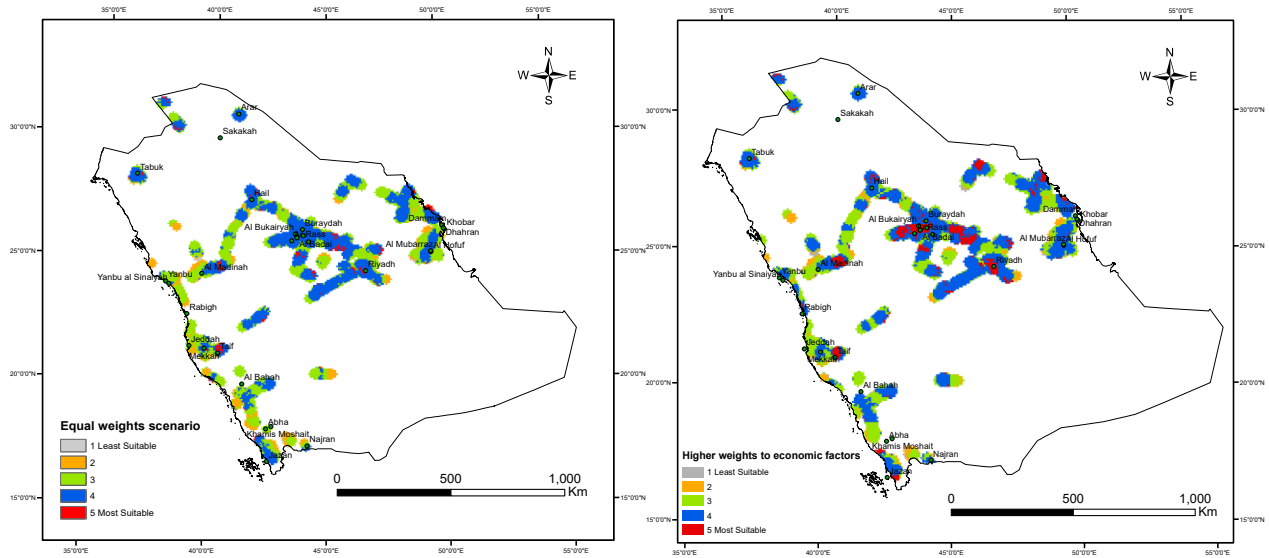


Figure 3.15. Suitability results: equal weights (left) and higher weights to economic (right)

Assigning higher weights to economic criteria including slope, land aspects, proximity to urban areas, roads, and proximity to power lines could be a viable option. When assigning higher weights to economic factors, the results reveal that the most suitable areas are approximately three times superior compared to equal weight and AHP scenarios as depicted in Figure 3.15.

The central region where the necessary infrastructure exists demonstrates high density of the most suitable LSI areas. The least LSI has increased slightly, whereas the moderate and marginal LSI dropped compared to the same weight scenario.

The results of different scenarios have proven sensitivity to the criteria weights and offer various land suitability distribution. Table 3.10 illustrates the final results obtained by varying the criteria weights, thus demonstrating that both economic and technical factors are influential in the evaluation of the study area.

Table 3.10. Land suitability distribution considering different scenarios

Scenario	Weights	Land suitability distribution (%)				
		5 (Most suitable)	4	3	2	1 (Least suitable)
AHP	Tech. = 0.57	0.42	8.01	5.29	1.02	0.01
	Eco. = 0.43					
Equal weights	Tech. = 0.5	0.36	7.12	5.90	1.22	0.06
	Eco. = 0.5					
Higher economic weights	Tech. = 0.2	1.25	7.67	4.85	0.86	0.08
	Eco. = 0.8					

3.6. Conclusions

RESs such as solar energy can contribute to electricity generation with a sustainable, secure, and low-carbon emission future. This chapter presents an original approach of developing criteria layers including solar irradiation and air temperature using real atmospheric sensor data in siting utility size PV power plants. As an initial stage of installing PV power plants, the identification of suitable sites can save DMs a great deal of time and money and can promote future infrastructure developments. The integration of the GIS with MCDM methods has emerged as a highly useful technique to systematically deal with rich geographical information data as well as manipulate criteria importance towards introducing the best sites for solar power plants. Furthermore, by incorporating associated criteria into the decision-making process, we could offer better results and make the solar project more economically and technically feasible.

This chapter offers a high-level overview of the potential of site suitability of utility-scale PV technology in the study area based on integration of the geographical information system and multi-criteria decision-making tool. The AHP technique is used to evaluate the importance of each decision criterion in selecting the best site for utility-scale solar PV power plants. Technical and economic factors considered in the proposed model include the amount of solar irradiation, yearly

average temperature, slope, land aspects, and proximity to power lines, major roads, and urban sites. The methodology successfully generates a land suitability index for potential sites where implementing utility-size grid-connected PV power plants are ideal. Our study for Saudi Arabia case indicates that most suitable areas are found north and northwest of the study area as well as west of Taif city near the west coast. High suitability areas comprise 50% of the suitability areas and are mainly spread around the central region. This location will be important to consider for grid connected utility-scale PV power plants since it is one of the most populated areas in Saudi Arabia. The eastern region of the study area shows moderate to high LSIs since it has a decent infrastructure together with the high density of high solar irradiation. More detailed survey for each region will be a direction for future work. These techniques can help Saudi Arabia and other countries to achieve their RES portfolio goals towards a more sustainable energy future.

The proposed approach exploits the existing resources and infrastructure to provide needed power to the cities in harmony with the environment. The solar analyst modeling in ArcGIS used to generate solar irradiation maps is a very powerful tool due to its flexibility to embed real atmospheric parameters. In addition, actual temperature measurements are considered from sensors spread across the country, and the average yearly temperature is interpolated using the spline tool in ArcGIS. Considering a small number of points for the temperature interpolation process could be a limitation of our study which may reduce the accuracy of the temperature layer. Currently, research is actively being conducted on solar resources; however, our results describe for the first time the solar site suitability in Saudi Arabia employing MCDM methods.

Chapter 4

Optimal Solar PV System Design

4.1. Introduction

Oil-dependent countries including Saudi Arabia, which is a major oil producer and exporter, and the country with highest oil consumption in the Middle East, have an arduous task ahead concerning energy production and consumption [169]. Nowadays, 100% of the power in Saudi Arabia is generated from fossil fuels, as shown in Figure 4.1. Saudi Arabia consumes more than 3 million barrels/day of oil, primarily for power generation, water desalination, and transportation [170]. The growing power demand is burdening the country, as generating more power means burning more fossil fuel. Recently, the Electricity and Cogeneration Regulatory Authority (ECRA) highlighted the power gap as high as 25% between the supply by the SEC, the main electricity provider, and the peak loads in central and southern provinces [171]. Furthermore, according to The World Bank, the CO₂ emissions in Saudi Arabia were around 18.1 metric tons per capita in 2013, which places it in the top 10 countries in CO₂ emissions worldwide [172].

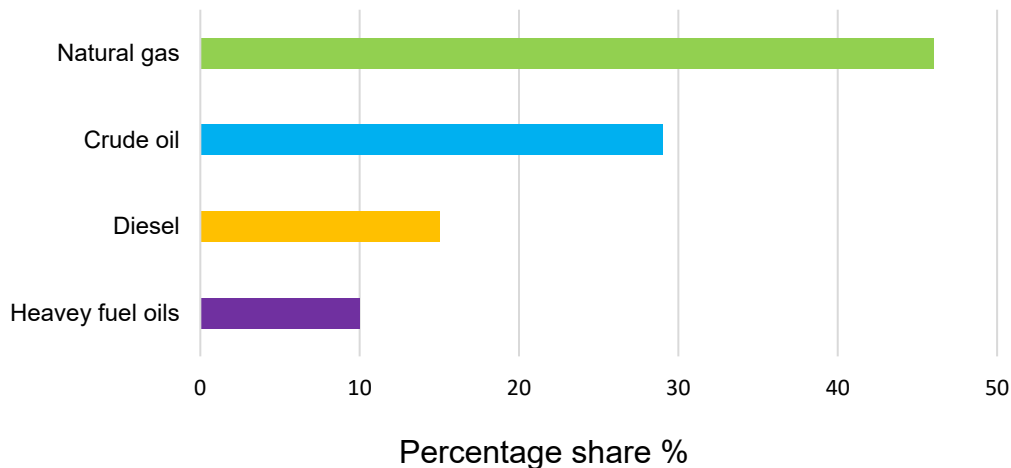


Figure 4.1. Fuel types used in electricity production in Saudi Arabia in 2013

The prolonged hot weather during summer is causing a significant usage of air conditioning, which consumes more than 60% of the total power generated in the country [173]. To tackle the high power consumption issue, several measures have already been taken by the decision makers, including the establishment of the Saudi Energy Efficiency Centre in 2010 to publicize the rationalization awareness and to boost power consumption efficiency, in order to preserve the national wealth of energy resources [174]. Furthermore, K.A.CARE was established, to improve the diversification of energy resources. In June 2016, the government removed subsidies for power generation and made a new adjustment to the consumption tariffs, which caused an increase in the cost of energy of more than 60% in some service categories [173]. Such policy measures were intended to encourage commercial and industrial solar energy applications in the country. Currently, Saudi Arabia plans to produce 9.5 gigawatts from renewables, mainly solar and wind power, by 2023 as a part of the Kingdom's 2030 vision [165].

Due to the variability of solar irradiation, electricity prices, renewable energy feed-in tariff (REFIT) and load demand, the optimal planning of RESs components is becoming an important issue that considers different aspects including technical, economic and environmental performance. The optimal sizing and planning would provide a system that requires minimum investment and operation and maintenance costs while meeting the technical and emission constraints [175]. The assessment of different solar tracking system designs is significant because the use of solar trackers is highly efficient and has become more mainstream and accepted by the solar energy developers. One of the most powerful tools for this purpose is HOMER software. Considering such relevance of the grid-connected solar energy technologies, the objective of this chapter is to examine the grid-connected solar PV systems propped by different tracking systems, and particularly to examine their performance under different time adjustments. It aims at

designing a system that requires the lowest investment among the alternatives available while providing a highly efficient solar PV system.

The PV tracking system configurations considered in this study include seven tracking systems. The actual data required by the model, including solar irradiation, air temperature, load profile, and cost of energy, have been collected in Makkah, Saudi Arabia. Makkah city experiences some of the highest average daily and peak electricity demands. The design should include the decisions on different sun tracking systems and REFIT. The optimal design should consider the technical performance as well as economic metrics including NPC, levelized cost of energy (LCOE) and return on investment (ROI) of the system.

As per the authors' knowledge, this is the first study examining different tracking designs for a grid-connected configuration with their impact on the system cost. Furthermore, this is an original techno-economic study of solar PV tracking systems in GCC countries (i.e. Bahrain, Kuwait, Oman, Qatar, Saudi Arabia, and the United Arab Emirates) to date, which entailed a detailed investigation of the local conditions. This objective requires a comprehensive investigation, and the technologies examined have a high potential deployment in this region. Recently, several software were developed to evaluate hybrid energy system performance, which help the user to plan, design, and examine the integration of renewable sources with conventional power generators. Hybrid Optimization of Multiple Energy Resources (HOMER) software, developed by NREL, is the easiest to use and the fastest in evaluating the RESs.

This chapter is organized as follows. Section 4.2 reviews the related studies about grid-connected PV and tracking systems. In Section 4.3, the problem definition and the case study are presented. Then in Section 4.4, the proposed system designs and the associated model inputs are defined. The

results and discussion of various cases considering tracking designs are presented in Section 4.5. Finally, the conclusion associated with this chapter are presented in Section 4.6.

4.2. Problem Definition

Ultimately, the dilemma of the project viability including economic and technical potential could be tackled by optimal design and planning of solar energy system. Such design depends on several factors including realistic inputs of the site such as metrological data, load consumption of the community and components cost. The techno-economic assessment of energy systems could be carried out using reliable and advanced commercial simulation tools as an alternative to the complex and lengthy algorithms and to the costly physical experiments. Currently, there exist several software to design, optimize and simulate RES, primarily aiming at technical and economic assessment. HOMER, RETScreen, PVSyst, Hybrid2, iHOGA, and TRNSYS are among the most popular and the most frequently reported software tools in the literature. Due to the nature of the problem, which includes 1-hour time-step data of load profile and air temperature, HOMER has been selected for this study, as it is superior to other software in handling this type of input. Moreover, HOMER demonstrates high capability to handle different simulation scenarios, including various tracking schemes, and to perform optimization and sensitivity analysis. Also, it is user-friendly and offers powerful graphical presentations. Computer tools used for the integration of renewable energy into various energy systems with different objectives were analyzed and compared by Connolly et al. [176]. According to a recent study of 19 software associated with RES sizing and planning, Sinha and Chandel [177] concluded that HOMER is the easiest to use and the fastest in evaluating the RES. Moreover, Bahramara et al. [175] presented a comprehensive review of papers which used HOMER exclusively for optimal planning in the area

of RES. The study showed that HOMER software is the most popular tool considered by many researchers and applied widely in the developing countries.

The primary economic metrics used to rank various energy system configurations are the NPC and the levelized cost of energy (LCOE). The NPC computes the present cost of installation and operation of the entire system over the project lifetime minus the present revenues, and it can be expressed by Eq. 4.1, whereas the LCOE calculates the average cost per kWh of electrical energy in the system and is calculated using Eq. 4.2.

$$NPC = \frac{C_{ann,tot}}{CRF(i, N)} \quad Eq. 4.1$$

Where $C_{ann,tot}$ is the total annualized cost, i is the annual interest rate, N is the project lifetime, and CRF is the capacity recovery factor, given by $CRF(i, N) = \frac{i(1+i)^N}{(1+i)^N - 1}$

$$LCOE (\$/kWh) = \frac{C_{ann,tot}}{R_{prim} + R_{tot,grid,sales}} \quad Eq. 4.2$$

Where R_{prim} is the primary load (kWh/year) and $R_{tot,grid,sales}$ is the total grid sales (kWh/year). When making such important decisions, alternative economic performance measures could be considered. Along with NPV and LCOE, the return on investment (ROI) represents the amount of return on an investment relative to a reference system. HOMER calculates ROI using Eq. 4.3:

$$ROI = \frac{\sum_{i=0}^N C_{i,ref} - C_i}{N (C_{cap} - C_{cap,ref})} \quad Eq. 4.3$$

Where:

- $C_{i,ref}$ = reference system nominal annual cash flow
- C_i = current system nominal annual cash flow
- C_{cap} = current system capital cost

- $C_{cap,ref}$ = reference system capital cost

Beyond the original approach presented in this chapter, the case of the Makkah, Saudi Arabia is investigated as a case study. Makkah is the capital city of the western region with the highest number of consumers (more than 2.7 million), and it had a maximum energy sale of 84,264,000 MWh in 2014 [171]. Makkah has an extremely hot summer season and it hosts millions of visitors every year during various religious occasions. Consequently, the power grid experiences a high-power consumption, mainly due to air-conditioning. A recent study by Al Garni and Awasthi in [178] investigated the most suitable sites towards deploying a utility-size solar PV in Saudi Arabia. This study found Makkah city as a highly suitable site for such a project considering several technical and economic factors.

A significant drawback of the solar energy lies in its unpredictable nature, as it depends on weather conditions. Nevertheless, the high demand in Makkah quite often coincides with the high solar irradiation, particularly during the summer season. Figure 4.2 depicts the real load profile data for the period 2011-2015 and the monthly average GHI for the period 1994-2012 on the monthly average basis. This indicates that solar energy technologies may be able to provide an adequate alternative source of energy. The solar power is a potential supplement to the primary utility's generation to cope with the massive load.

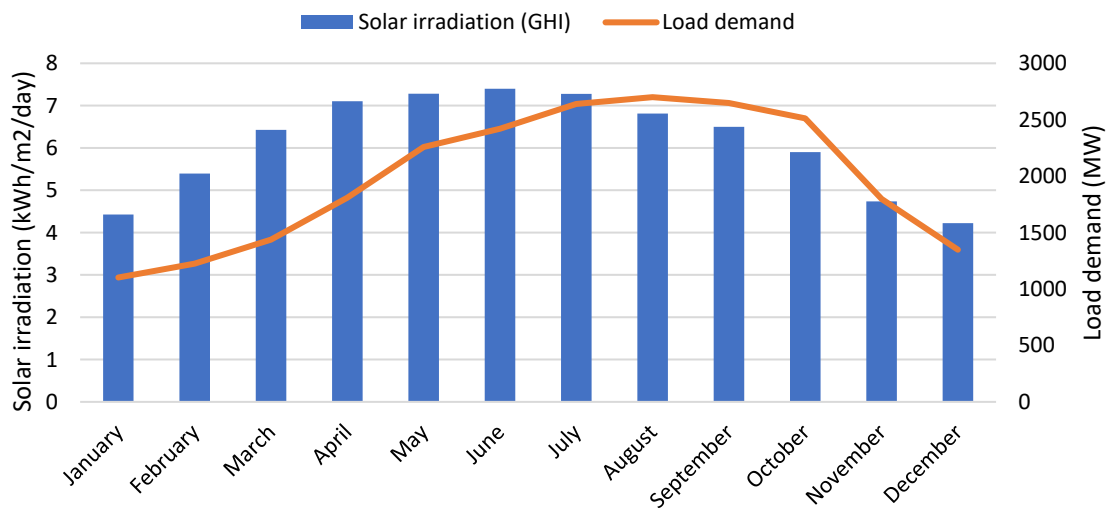


Figure 4.2. The relation between load demand and GHI in Makkah City

One of the key factors in solar PV performance is the angle between the sun rays and the solar PV panels. Accordingly, the main objectives of this chapter are as follows:

- To examine different solar PV tracking system configurations with different time adjustments, including horizontal-axis, vertical-axis, and two-axis systems by studying their impact on the system cost and power generation.
- To design an optimal solar PV grid-connected system based on realistic key inputs including metrological data, user profile data, and economic factors.

4.3. Literature Review

Many research papers studied the techno-economics of PV systems based on off-grid [179], [180], [189]–[191], [181]–[188] or grid-connected settings [192]–[200]. The grid-connected systems are intended to supply power generated by RES into the electric grid. Such schemes could be in a distributed form, serving a particular grid-connected client, or in a centralized form, delivering power into a transmission grid. Hafez in [200] studied different configurations of hybrid renewable energy systems including diesel only, fully RES, diesel-RES mixed and RES-grid-

connected configuration. Using the HOMER software, the load applied was a hypothetical rural community, while the solar data was derived from National Aeronautics and Space Administration (NASA) surface metrology database. The results showed that diesel-RES mixed configuration has the lowest NPC, while the fully RES has the highest NPC with no carbon emissions. A hybrid RES grid-connected system was found to be the most economical option due to the low capital cost. Furthermore, a break-even grid extension distance from the microgrid was analyzed.

Anwari and Ayong in [192] studied the technical feasibility of off-grid PV that generated 2.5% of load requirement of Makkah city in Saudi Arabia based on solar irradiance using HOMER software. The load profile with random variability factors was assumed based on the load pattern in Makkah with no grid connection consideration. In [193], they applied grid-connected solar PV to the same case. Similarly, Adaramola examined the feasibility of grid-connected solar PV in Jos, Nigeria, investigating the technical and economic performance of the system [194]. The load profile was assumed based on the pattern of the energy consumption in Jos. He concluded that the solar PV system could provide for around 40% of the annual electricity consumption, whereas, aside from the amount of solar irradiation, the initial cost of the scheme plays a significant role in electricity price. Tomar and Tiwari in [195] studied demand-side management to obtain an optimal design of solar PV system for a decentralized application in New Delhi, India. They concluded that a grid-connected solar PV system without battery storage is a technically and economically viable option for decentralized applications. Mondal et al. [196] examined the economic feasibility of grid-connected solar PV for Bangladesh employing a proposed 1MW solar PV system. All sites showed favorable condition for development of the proposed solar PV system. Liu et al. [197] simulated and optimized a grid-connected PV system of residential power supply in Queensland, Australia. It is found that the PV system is an effective way to decrease electricity bills and mitigate

CO₂ emissions. Raturi et al. [198] described the current status of grid-connected PV systems in the Pacific region and reviewed some challenges associated with the power utilities which are completely dependent on diesel generators and hydropower. The results obtained reveal that both grid-connected and stand-alone solar PV are economically attractive to tackle these challenges. Kim et al. [201] examined hybrid PV-wind-battery systems by simulating a system composed of a renewable energy grid system and a diesel generator on Jeju Island in South Korea. This study found that the grid-connected PV-wind-battery hybrid system is the most economically feasible system. Furthermore, comprehensive reviews of different aspects of grid-connected PV systems, along with highlights on technical and economic constraints that may hinder the solar energy projects, were provided in [202], [203].

In promoting RES, the REFIT mechanism has been applied the most extensively and it has proven to be an efficient system offering substantial benefits to both RES project developers and consumers [204]. REFIT has prevailed as a fruitful policy approach to spur renewable energy penetrations, which obligates the public power entities to purchase the power generated from RES. Lau in [199] analyzed the effects of such policy and economic factors on grid-connected PV systems in Malaysian residential sector. The effect of varying interest rates, electricity tariffs, and the carbon tax was discussed. The grid-connected system with no battery showed to be the most feasible alternative, as introducing a battery increases the system's NPC. As of 2016, more than 100 countries and provinces enacted feed-in-tariff policies [4]. The REFIT is considered to be the most commonly adopted regulatory mechanism to prompt RES.

The performance of solar panels is primarily dependent on the amount of solar irradiation received. Hence, a mechanical system that tracks the sunlight and enables orienting the panel towards being perpendicular to the light beam leads to capturing more solar irradiation, which

accordingly advances the system performance. A tracking system for a PV array can increase the array's annual energy production up to 27% using a single-axis tracker and 40% for dual-axis trackers [205]–[207]. A single-axis tracker adjusts either the azimuth or the tilt angle, while dual-axis tracking can adjust both angles. The tilt angle is the vertical angle between the horizontal plane and the solar panel surface (typically towards the south if PV site located in north hemisphere). The azimuth angle is the deviation angle between the surface and the south direction horizontally, as illustrated in Figure 4.3.

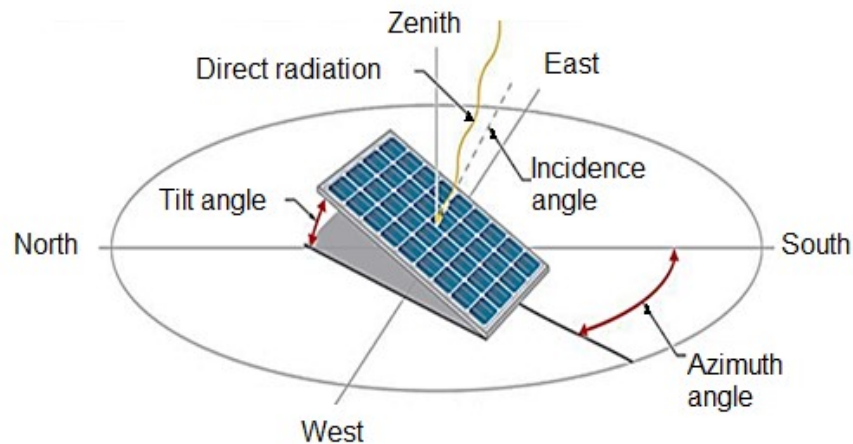


Figure 4.3. The tilt and azimuth angles of the solar panel [208]

Typically, PV panels are installed with fixed tilt and no tracking system, as in the cases studied in [20], [194], [209]–[214]. Nevertheless, single-axis and dual-axis trackers have recently undergone intense research. In addition to the daytime movement of the sun rays from morning to evening, their direction also varies across the seasons throughout the year.

Compared to fixed systems, the advantage of the tracking systems is the significant boost in power production. In high irradiation areas, one-axis tracking has dominated for utility-scale PV systems, with benefits greater than the costs [215]. Lazaroiu et al. [216] examined the daily energy production of a fixed system and the sun-tracking PV systems and found that sun tracker systems

generated 12–20% more power than the fixed system. Based on both technical and economic criteria, Alexandru [217] determined that a single axis tracking system is preferable to dual-axis tracking for the area of Brasov, Romania. Mehrtash et al. [218] investigated the performance of solar tracking PV systems in Toronto, Canada with four different tracking systems: fixed tilted, fixed horizontal, single-axis and dual-axis tracking. The study showed that dual-axis tracking received 33% more irradiation and generated 36% more electricity than the tilted system.

A review of sun-tracking methods by Mousazadeh et al.[219] concluded that using two-axis sun-trackers can increase the energy production by 30–40% yearly. Eke and Senturk in [220] compared double-axis sun tracking versus a fixed PV system and found that 30.79% more electricity is obtained with double-axis sun-tracking. Similarly, Ismail et al. [221] found that dual axis tracker achieved 20.4% more in annual energy production compared to a fixed system. Salah [222] studied four tracking systems including dual-axis, one axis vertical, one axis east-west and one axis north-south. The results revealed that each of the four trackers was superior to the fixed system. The electrical power gain was 44%, 38%, 34% and 16% for the two axes, east-west, vertical and north-south tracking, respectively. The above-mentioned studies reveal that solar PV tracking systems are superior to the fixed systems when it comes to power generation. However, there is no study investigating the techno-economic aspects of different PV tracking system configurations with different time adjustments, including fixed system, horizontal-axis, vertical-axis, and two-axis for a grid-connected solar PV.

4.4. System under Consideration

To achieve the above objectives, simulation and optimization processes are used. The major inputs to the simulation and optimization model consist of the key factors affecting the performance of a PV system. The model inputs are electrical load, solar irradiation, air temperature, components

cost, and energy prices. In contrast to studies [192] and [204], real-data including metrological data, load profile, and the technical and economic characteristics of the equipment are used in this chapter. Figure 4.4 shows the major research steps. In previous work [223], the authors considered different costs inputs as well as different technical and economic measures. In this chapter, we extend this work by adding a comprehensive analysis to each tracking system performance under feed-in-tariff mechanism with a detailed investigation of the local conditions. Moreover, an additional economic measure, ROI, has been examined and compared among different tracking designs. The following sub-sections describe the system design components with their specifications applied in this study.

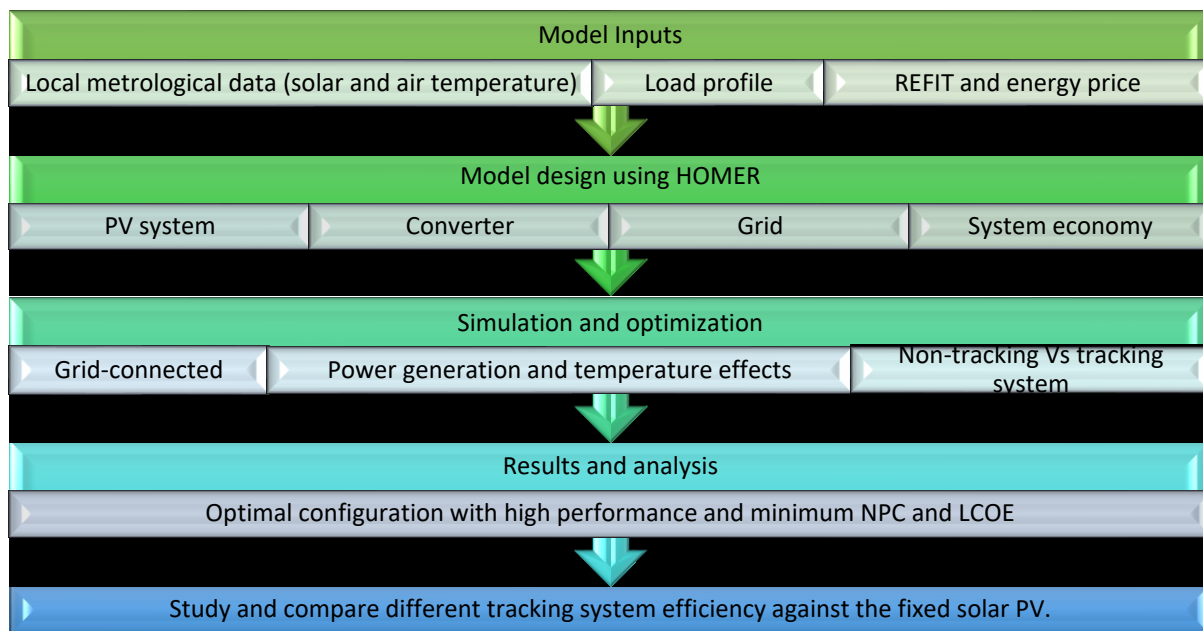


Figure 4.4. Proposed steps for optimal sizing of PV grid connected system

4.4.1. Metrological data

Solar irradiation and the ambient temperature of the PV array affects the amount of energy that a PV system generates. Accordingly, HOMER uses the monthly average global horizon irradiance and the monthly average temperature among its inputs. These inputs are defined in the

HOMER resources, and their effects on the output performance of the PV system are described.

The following points give more detail about the data used in this study for these two variables:

- **The solar irradiation:** the monthly average GHI of Makkah (Latitude 21.42 N, Longitude 39.82 E) is downloaded from K.A.CARE. It is based on GeoModel Solar for the period 1994 – 2012 with 3 km resolution. An extensive comparison study for 18 validation locations in Europe and the Mediterranean region, authored by Ineichen, concluded that Geomodel data has the lowest overall bias [224]. The solar irradiation ranges between 4.22 kWh/m²/day and 7.4 kWh/m²/day, whereas the annual average solar irradiation for this region is 6 kWh/m²/day as depicted in Figure 4.5. From March to September, the GHI rises above the average, with a peak in June. The remaining months particularly January, December, and November have relatively low solar irradiation.

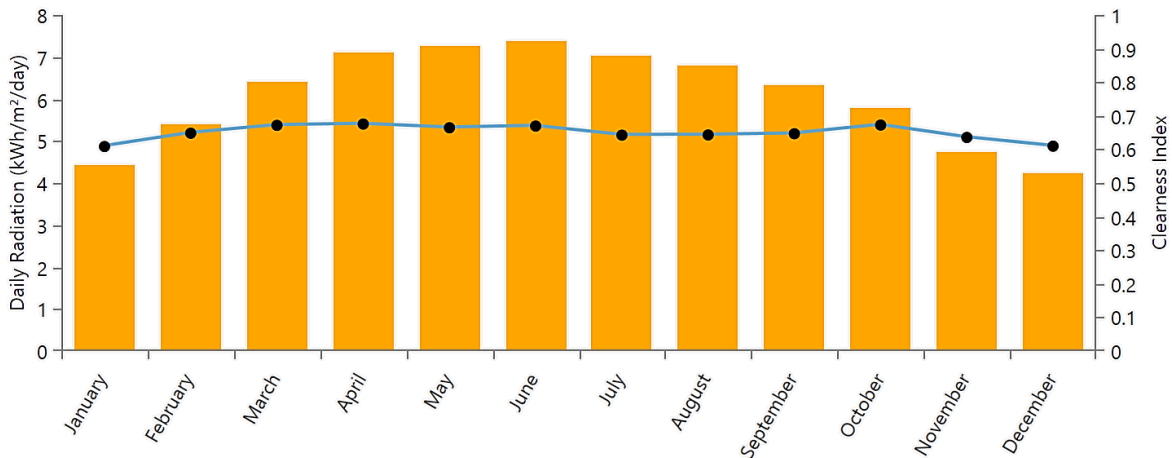


Figure 4.5. The monthly average GHI in Makkah

- **The air temperature:** the monthly average temperature for years 2011-2015 using a 1-hour time step, is depicted in Figure 4.6. The average annual temperature is 31°C, and the long summer season with even higher temperatures is from May until September. This ambient temperature profile will be considered in determining the PV power efficiency, as

HOMER software can calculate the power output of a PV array utilizing the cell temperature in each time step. Figure 4.7 shows the temperature data frequency distribution with a normal shape.

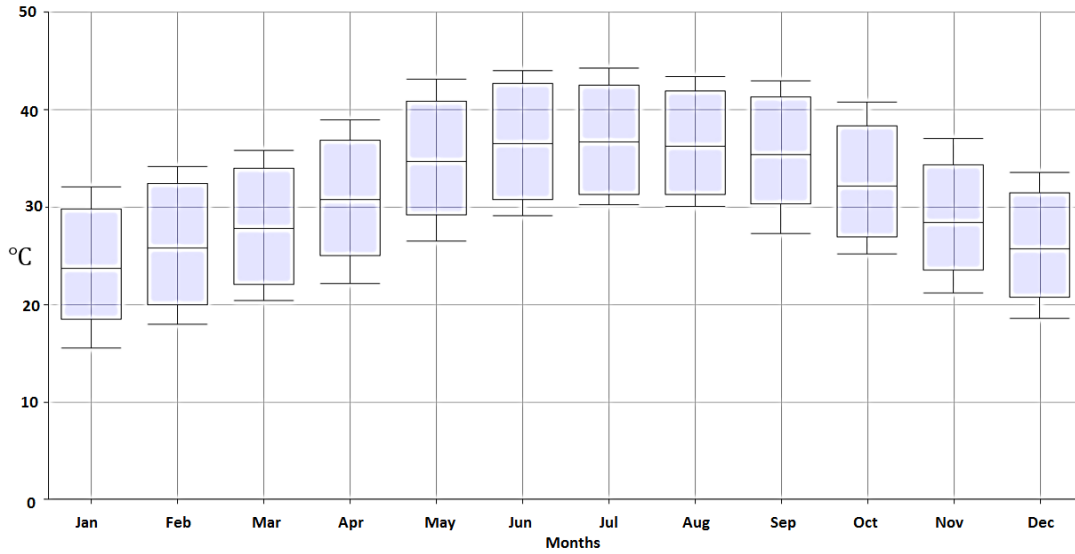


Figure 4.6. The monthly average temperature

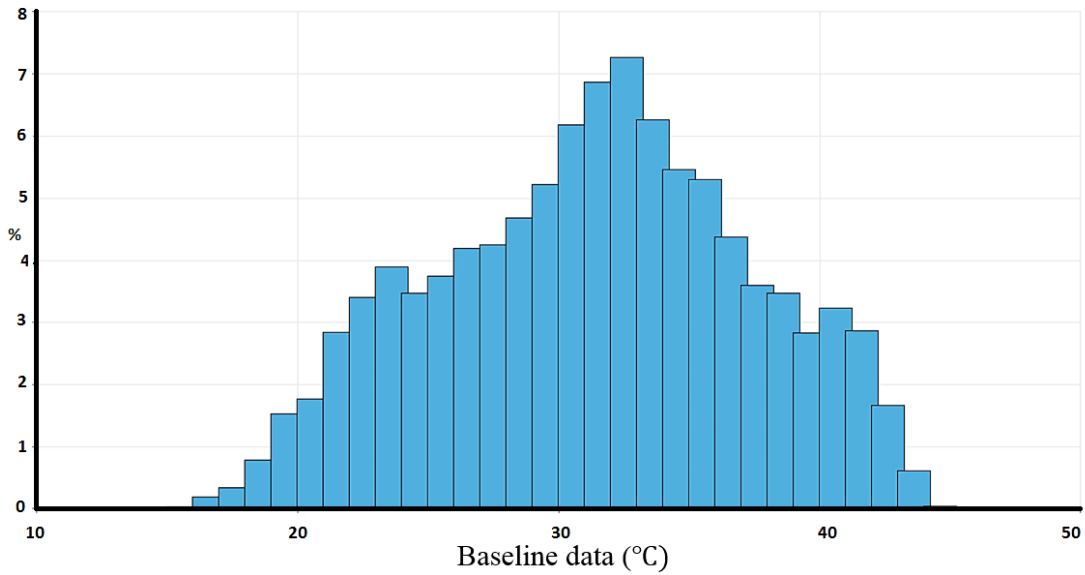


Figure 4.7. Histogram graph of temperature data of Makkah

4.4.2. Load profile

From the demand perspective, the load profile of any study area is the most significant factor in the optimization process. The load profile is critical for accurately designing an optimal system, which means to satisfy the power demand at any given time and avoid extra costs due to overdesign. Compared to other regions in Saudi Arabia, western region has the highest number of consumers and the highest energy sales [171]. The electricity demand of Makkah has significant fluctuations due to several factors including weather variations - an extremely hot summer, religious events such as the month of fasting (Ramadan), and pilgrimage (Hajj), and other special occasions (National day, Eids, etc.) [193]. Figure 4.8 shows the yearly average electrical load profile for years 2011 to 2015 in 1-hour time step size.

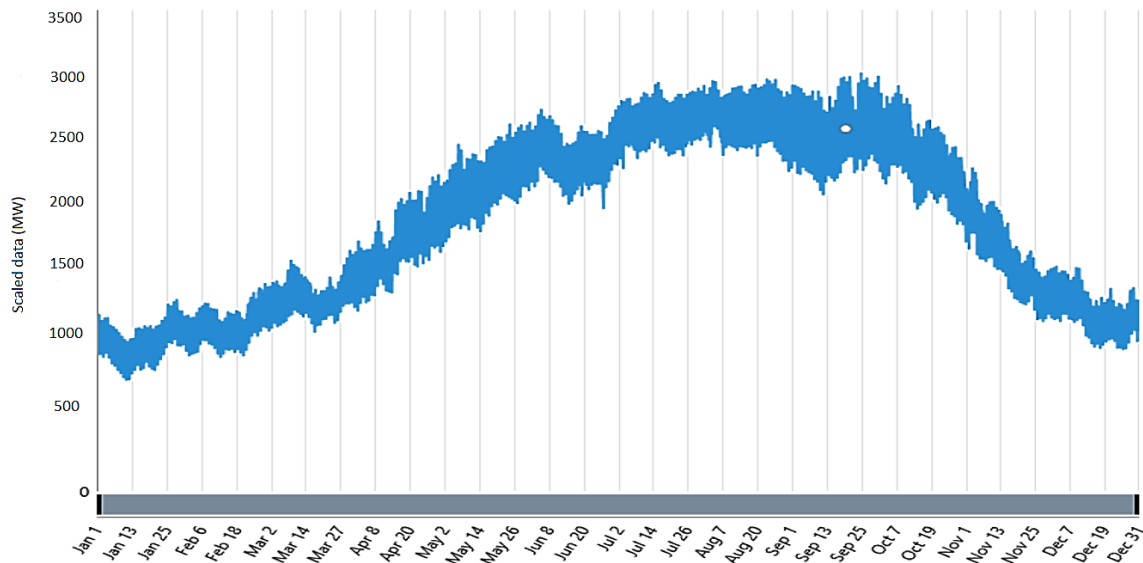


Figure 4.8. The annual average electrical load of Makkah

Figure 4.9 illustrates the monthly average load profile with a peak demand starting in April, continuing during summer season and declining in November. This is mainly due to the overlap of the summer and the Holy Mosque visitors' period. The daily average power consumption is 47,752 MWh/d with a peak of 3,041 MW.

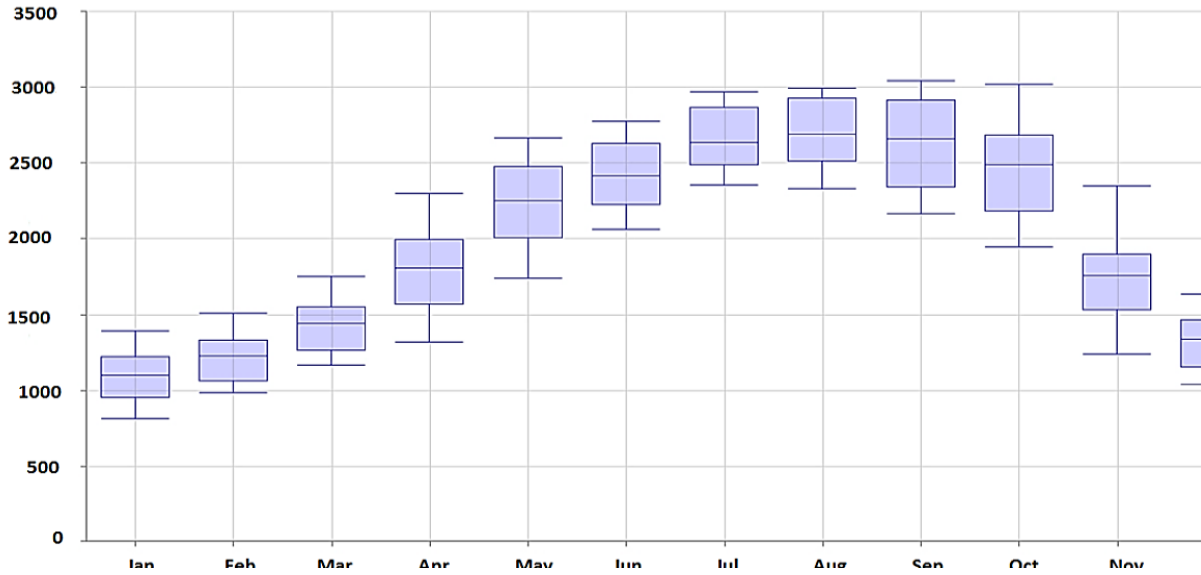


Figure 4.9. The monthly average load profile for Makkah

The histogram in Figure 4.10 shows a bimodal distribution with two relative peaks of power demand (1,200 MW and 2,600 MW). The relative frequency of load consumption reveals that the highest frequency is between 2,000 and 3,000 MW yearly. Another peak is between 1,000 and 2,000 MW with lower frequency. This indicates that different customers utilized a different distribution of power consumption throughout the year.

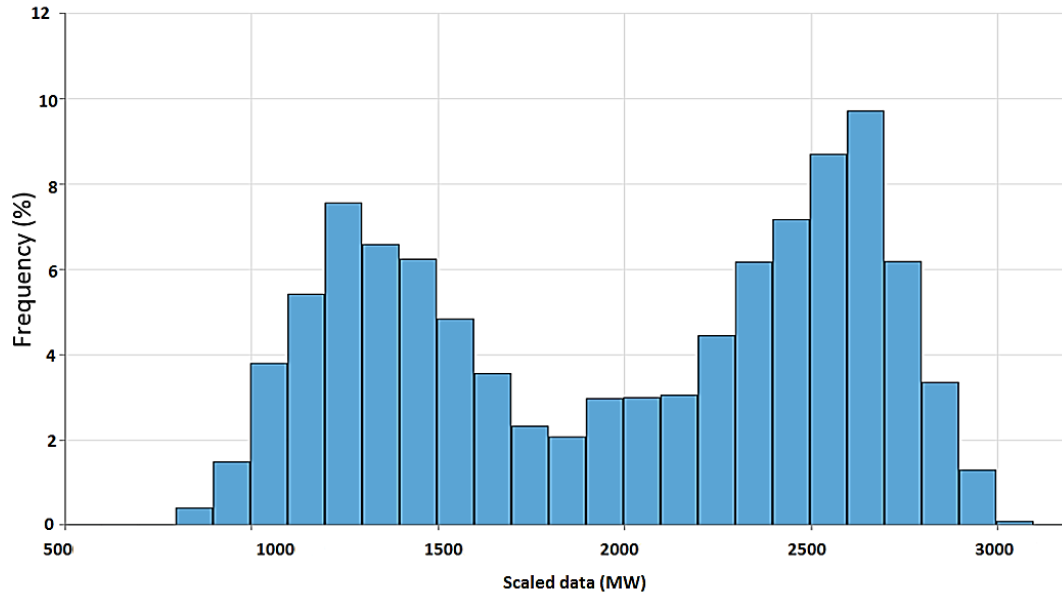


Figure 4.10. Histogram graph of the load profile

4.4.3. Grid and renewable energy feed-in-tariff

The utility grid is the main power supplier, whereas the solar PV system runs in daytime only. However, if the power generated by the solar PV exceeds the primary load demand, the surplus electricity is sold to the grid. Several studies have shown that utilizing the excess energy in this way can significantly reduce the LCOE [225]. The REFIT is a long-term policy agreement with the RES provider to pay for the electricity that the RES system feeds into the grid. Recently, based on an assessment of REFIT and their applications in Europe, Asia, and Africa, Ramli, et al. in [204] concluded that applying fixed REFIT in Saudi Arabia is likely to accelerate the development of its renewable energy sector. Such fixed pricing scheme is market independent, which neglects inflation and is not affected by the fossil fuel prices. Accordingly, the residential rate in Saudi Arabia (see Table 4.1) is utilized to design a scheduling rate that permits fixed prices at each time of day and month as presented in Figure 4.11.

Table 4.1. Consumption rates for residential category in Saudi Arabia [173]

Consumption categories (kWh)	Residential rate (¢/kWh)
1 – 2000	1
2001 – 4000	3
4001 – 6000	5
6001 – 8000	8
> 8000	

Figure 4.11 shows the daily grid scheduled rates divided into five intervals based on the peak load period, where each column presents the daily hours starting at 00:00 [193]. The rates include off-peak, shoulder and peak hours whereas their prices are \$0.016/kWh, \$0.027/kWh, and \$0.040/kWh respectively, as shown in Figure 4.12. As a result, the buying/selling of power from/to the grid at a fixed REFIT scheme is possible.

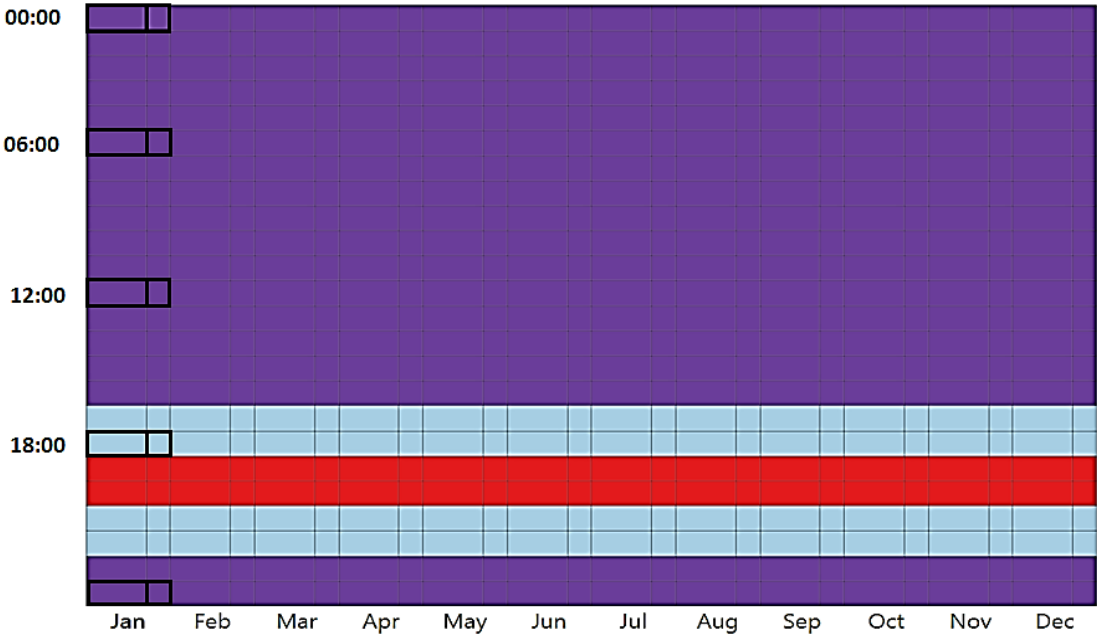


Figure 4.11. The grid scheduling rate during the day in each month




		Price	Sellback		
OFF-PEAK		0.0320	0.0160	Edit	✕
SHOULDER		0.0530	0.0270	Edit	✕
PEAK		0.0690	0.0400	Edit	✕

Figure 4.12. The scheduled rates for different time during the day [193]

4.4.4. Optimal design of solar PV grid-connected system

The design of the system under consideration comprises of four components: solar PV array, direct current (DC) to alternating current (AC) converter, grid system, and primary load as presented in Figure 4.13. Grid-connected PV systems require an inverter to adapt the DC generated by the PV array and supply it to the load side. Since this system has no batteries or external generator, the utility grid will be the main power supplier to the load.

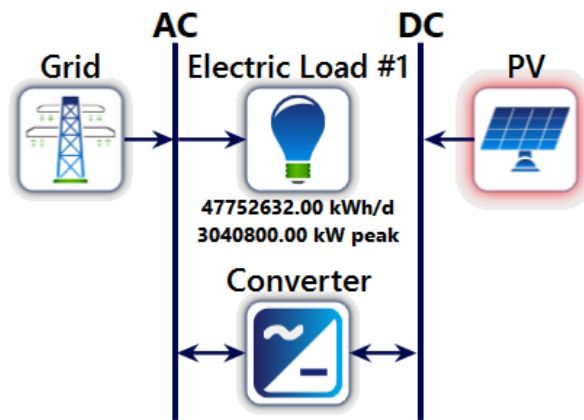


Figure 4.13. Design configuration of PV grid-connected system

4.4.4.1. PV modules

A PV module is a RES integrated into the system, which supplies renewable electricity to the DC line. The size of a PV module depends on the system constraints, including the unmet load permission and the size of other renewable fractions contributing to the system. In this study, the PV system should be sized to deliver the required peak load demand, and this determines the output power requirement of a PV panel system. The output power of a PV system can be calculated using Eq. 4.4 [226].

$$P_{PV} = Y_{PV} * f_{PV} \left(\frac{\bar{G}_T}{\bar{G}_{T,STC}} \right) [1 + \alpha_P (T_c - T_{c,STC})] \quad Eq. 4.4$$

Where:

- P_{PV} = is the generated power from PV system
- Y_{PV} = is the rated capacity of the PV array [kW]
- f_{PV} = is the derating factor [%]
- \bar{G}_T = is the solar irradiation on the PV [kW/m²]
- $\bar{G}_{T,STC}$ = is the incident irradiation at standard test conditions [1 kW/m²]
- α_P = is the temperature coefficient of power [%/°C]
- T_c = is the PV cell temperature [°C]
- $T_{c,STC}$ = is the PV temperature under standard test conditions [25°C]

As illustrated in Eq. 4.3 , the power generated from a PV system is influenced by several factors including the PV cell temperature and the amount of solar irradiation. Table 4.2 presents the financial and technical input data of the PV and inverter types.

Table 4.2. PV and Converter parameters

Component	Size	Lifetime (years)	Cost			Other information	Reference
			Capital (\$)	O & M (\$/year)	Replacement (\$)		
PV	1kW	25	640	10	640	<ul style="list-style-type: none"> • $\alpha_p = -0.40 \text{ \%}/^\circ\text{C}$ • $f_{PV} = 90 \text{ \%}$ • Efficiency = 18% 	[227]
Converter	1 kW	25	375	10	\$375	<ul style="list-style-type: none"> • Efficiency = 97 % 	[228]

4.4.4.2. Solar PV tracking system designs

Nowadays, most of the solar PV arrays are installed on a fixed mounted system, where PV panels may be installed with a fixed tilt angle. Such fixed systems, where panels are installed at a fixed slope and azimuth, have the advantages of simplicity and low-cost. However, they have a significant deficiency in receiving adequate solar irradiation, since the sun moves throughout the day and changes its orbit seasonally. Therefore, a fixed system with no tracking (FT) is considered the base case in this research. Tracking systems are categorized according to their number of rotation axes as shown in Figure 4.14. The following six tracking systems are considered [226]:

1. **Horizontal-axis with monthly adjustment (HMA):** the rotation axis is around the horizontal (east-west), whereas the tilt angle is adjusted each month to have a close-to-perpendicular angle between sun rays and panels at noon time.
2. **Horizontal-axis with weekly adjustment (HWA):** the rotation is around the horizontal, whereas the tilt angle is adjusted every week.
3. **Horizontal-axis with daily adjustment (HDA):** the rotation is around the horizontal, whereas the tilt angle is adjusted each day.
4. **Horizontal-axis with continuous adjustment (HCA):** the rotation of HCA is around the horizontal, while the tilt angle is adjusted continuously.

5. **Vertical-axis with continuous adjustment (VCA):** the system rotates continuously around the vertical (north-south) axis, whereas the tilt is fixed.
6. **Two-axis (TA):** the panels rotate in both axes (horizontal and vertical) continuously in order to maintain the perpendicular angle between PV panels and sun rays.

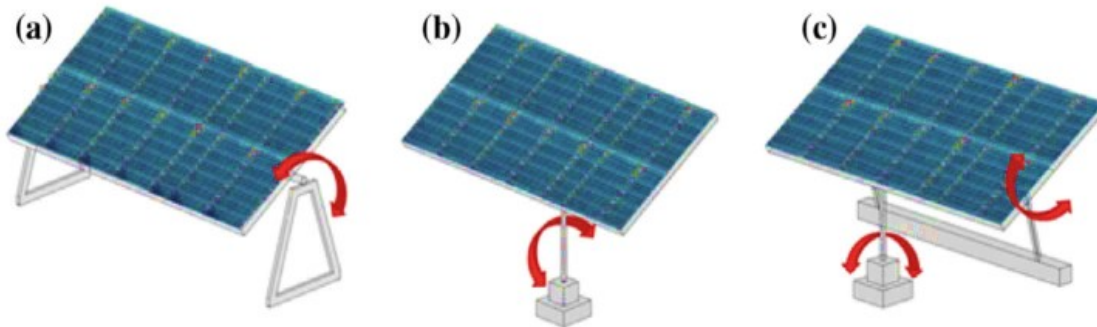


Figure 4.14. (a) Horizontal axis, (b) Vertical axis and (c) Two-axis tracking [229]

A study of each design's impact on the system economic and technical performance is carried out. The cost of the tracking system components excluding the PV module cost are given in Table 4.3.

Table 4.3. Cost inputs for the different tracking systems [229]

No.	Tracking System	Capital cost (\$/kWh)
1	Horizontal-Axis, daily, weekly, and monthly tracking system	563.00
2	Horizontal-Axis, continuous adjustment	870.00
3	Vertical-Axis, continuous adjustment	255.00
4	Two-Axis	1000.00

For moderate latitude locations (less than 30°), which is the case of Makkah, it is generally accepted that the tilt angle is approximately equal to the latitude which typically maximizes the annual PV energy production [230]. Therefore, the tilt angle for the FT system for the location of Makkah is considered equal to 21.39° . This is identical for VCA where the tilt angle is fixed while

the azimuth is changing continuously. The rest of the tracker systems have variable tilt angle as part of each tracker scheme.

4.5. Results Discussion

The results and discussion of different grid-connected solar PV system designs are presented in this section. Seven cases of tracking systems are examined to determine the most efficient alternative in terms of both technical and economic measures. The performance results and analysis of the panel with no FT, as well as the results of HMA, HWA, HDA, HCA, VCA, and TA are investigated in the next subsections.

4.5.1. Impact of various tracking designs on technical performance

For the FT scenario, the annual average electricity production from PV is about 32.11% (5,595,937 MWh/year) of the total generation, while the remainder of the necessary power in this case is purchased from the grid, as shown in Figure 4.15. Therefore the major share of the power is obtained from the grid to meet the load requirement and to keep zero unmet energy by the system.

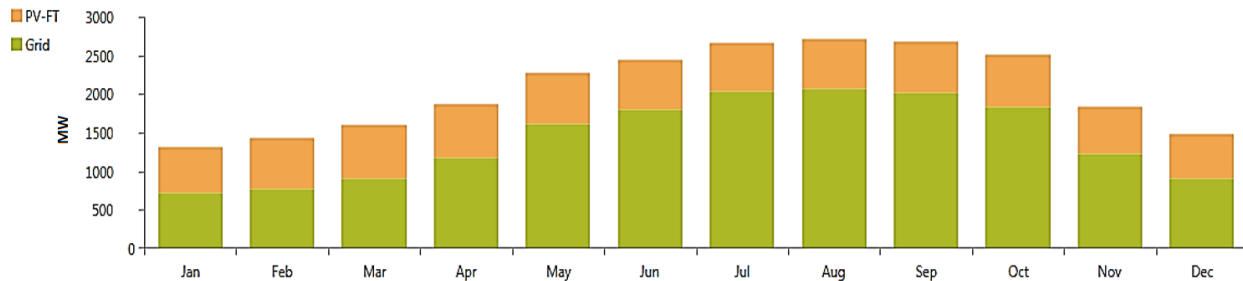


Figure 4.15. The monthly average electric production

The PV system generates power during the daylight period, with a peak output around noon as illustrated in Figure 4.16. The system operates 4,404 hours throughout the year, with an average output of 1,500 MW/day.

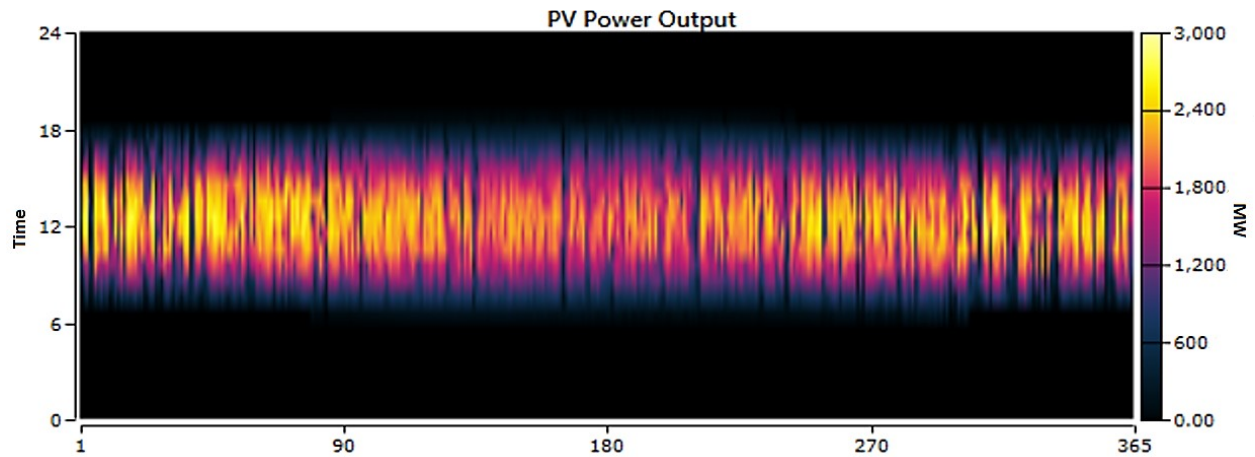


Figure 4.16. PV power output throughout the year and daytime

In order to investigate the air temperature impact on the power generated by the PV system, the yearly average of real air temperature for Makkah was used in addition to the temperature coefficient from Table 4.2 in the PV parameters. Owing to the negative temperature coefficient of solar panels, the power output from the PV system decreases as the temperature increases. As predictable, during the summer season when the average temperature ranges between 30 to 45°C the system efficiency declines as shown in Figure 4.17.

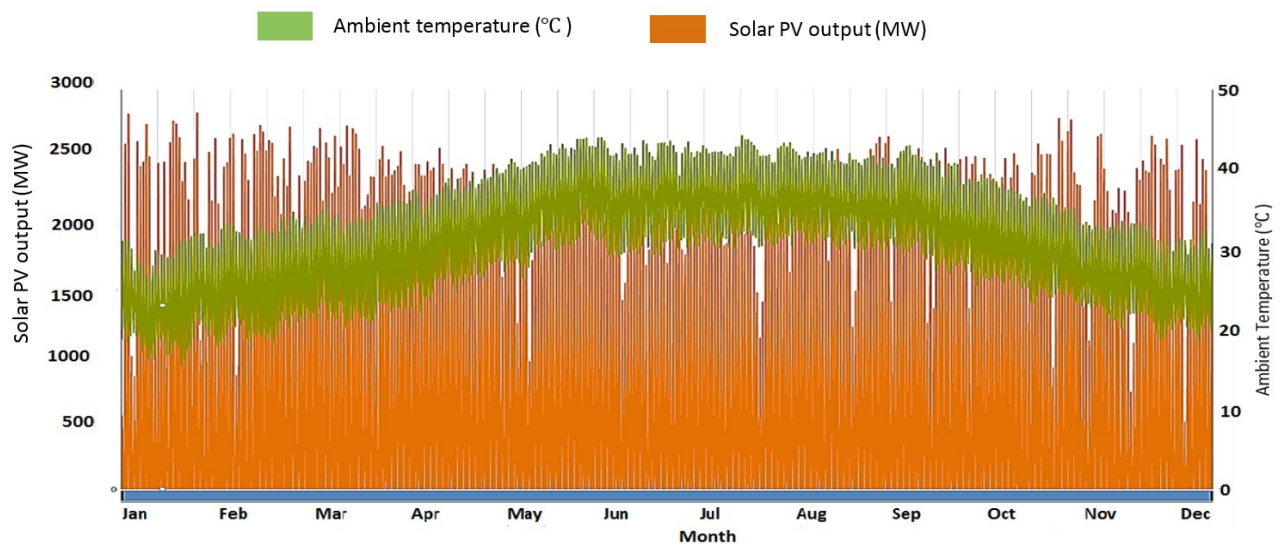


Figure 4.17. Solar PV production versus ambient temperature throughout the year

Undoubtedly, the amount of solar irradiation received by panels is a determining factor for their output. Figure 4.18 illustrates the average output power generated by different tracking designs on a daily basis. It was found that all the tracking systems produce similar amounts of power at noontime while the power density varies noticeably in the morning and evening hours. Obviously, the TA generates considerably more power in the shoulder periods of the day compared to the other trackers, and it was found to provide 34% more electricity than the FT. The TA has a distinctive feature as it can rotate according to the sun direction on a daily and seasonal basis. Consequently, during the morning and evening hours, TA directs the panels towards the sun and captures more irradiation than the other trackers. On the other hand, FT shows the lowest daily output power whereas the HDA, HWA, HMA generate similar amounts of power. HCA produces 2.4% more power than the other three horizontal trackers. This slight improvement is owing to the continuous adjustment of the panels from morning to evening. The simulation shows a significant amount produced by VCA, 20% more than FT.

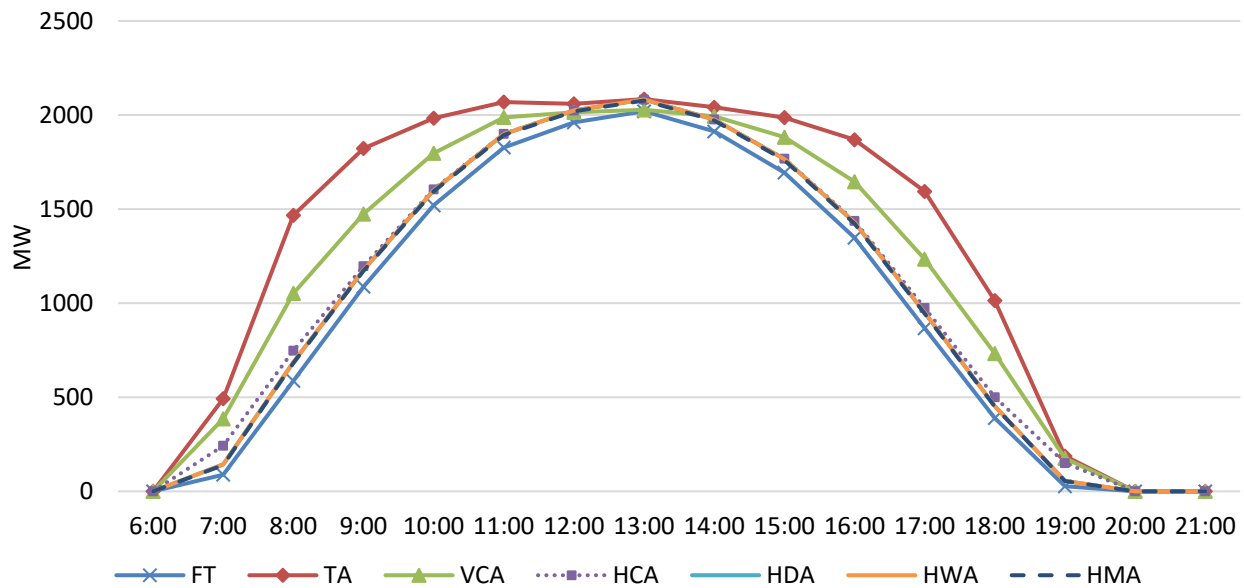


Figure 4.18. Average daily power graph of the different tracking systems

The excess electricity production occurs when total production of solar PV surpasses the amount of consumption. The surplus power is normally dumped or curtailed. However, in the proposed system, the excess power will be sold back to the grid at the rates previously described in Figure 4.12. Such grid-connected scheme can take advantage of the unused power and gain additional revenues for the system. As shown in Figure 4.19, FT yields the lowest excess power (37,923 MW/year), whereas all the horizontal axis tracker designs (HMA, HWA, HDA, and HCA) give similar amounts of excess electricity (around 66,000 MW/year). On the other hand, TA gives the highest amount of excess electricity, almost 400% more than FT. VCA presents a reasonable amount of excess electricity compared to the other trackers.

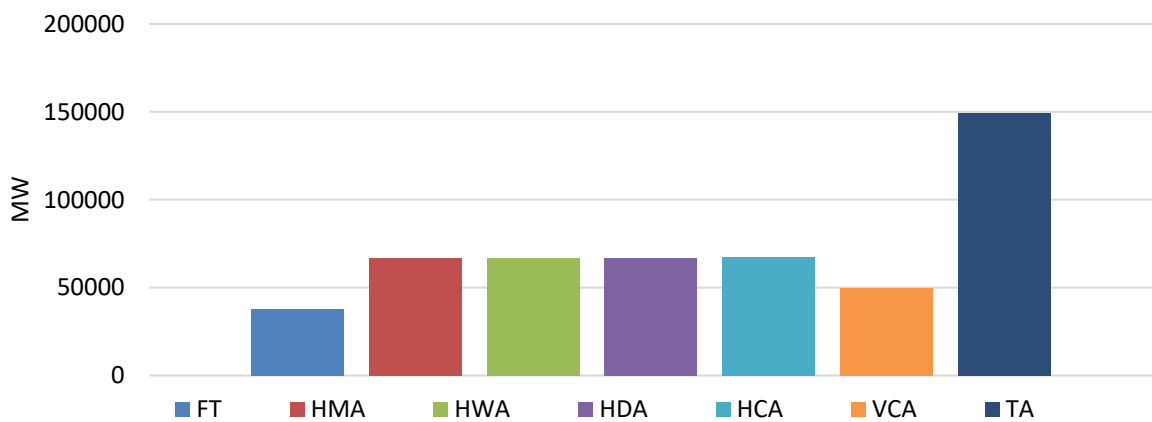


Figure 4.19. The excess electricity of different trackers per year

Through comparative analysis of the six tracking designs in terms of monthly power generation, the variance in the efficiency of various tracking systems is illustrated in Figure 4.20. TA design shows the highest power generated from the PV system, with a maximum of 912.4 MW in April and the minimum in December. Furthermore, HMA, HWA, and HDA show very similar production. However, from May to June, HDA and HWA were able to generate 2.5% (17.8 MW) more power than HMA as shown in Figure 4.21. FT demonstrated the lowest performance during

summer period, as a result of the movement of sun's orbit to the north in addition to the high-temperature impact. This highlights the significance of adjusting the tilt angle regularly.

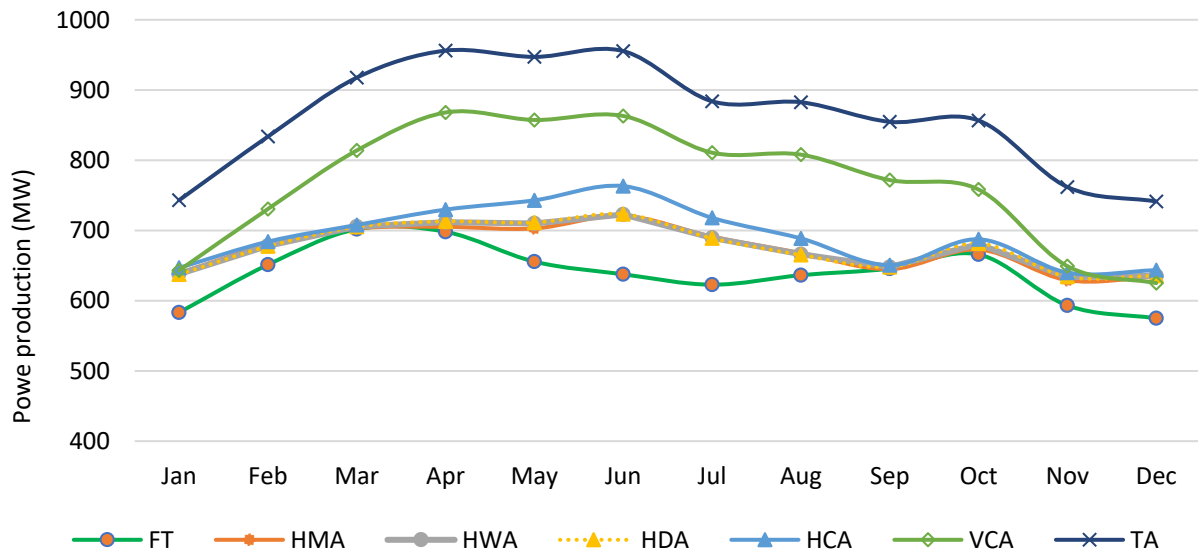


Figure 4.20. Monthly power generation from various tracking systems

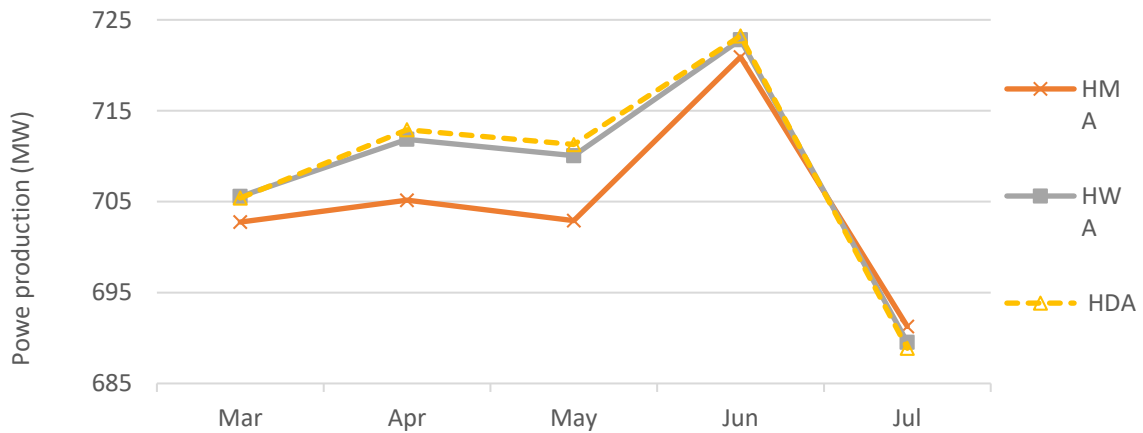


Figure 4.21. Horizontal trackers performance from March to July

The percentage difference in electricity generation by different tracking systems in comparison to the FT is shown in Table 4.4. It can be noted that TA generates the highest power output, with an hourly average of 861.3 MW which exceeds the FT system production by 34.84%. It should also

be noted that PV panels mounted with horizontal-axis (HCA, HDA, HWA, and HMA) show relatively small differences in capacity, with a slight improvement compared to FT system (5-8%). Power generated with VCA trackers was 20% more than power generated with FT due to increased production during daily tracking.

Table 4.4. Hourly power production along with comparison to non-tracking system

Tracking System	FT	TA	VCA	HCA	HDA	HWA	HMA
Hourly average power (MW)	638.8	861.3	766.8	691.9	676.7	676.6	674.2
PV power output Vs FT (%)	0	34.84	20.04	8.32	5.94	5.92	5.54

As the output power generated by a PV system increases, the power purchased from the grid declines instantaneously. As shown in Figure 4.22, the sum of the PV power and the grid power is equivalent to the total electrical load served, which means that the system has delivered the right amount of power with zero unmet power demand.

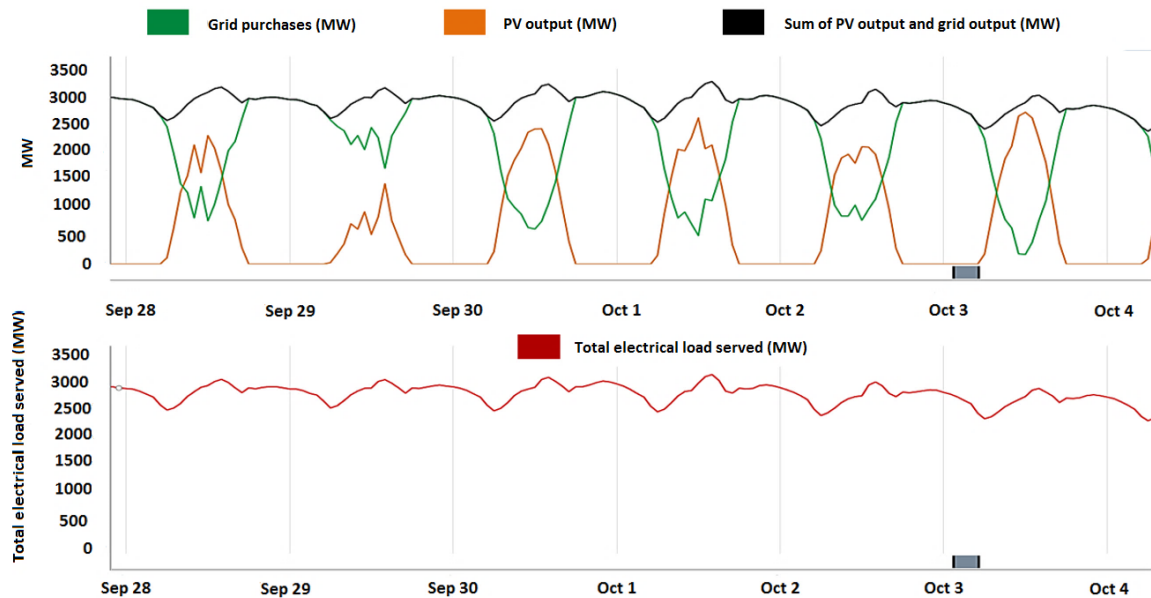


Figure 4.22. The production of PV system along with grid to maintain load demand

4.5.2. Impact of various tracking designs on system economics

By applying Eq. 4.1 and Eq. 4.2, HOMER calculates NPC and LCOE for the entire system. Figure 4.23 shows the cost summary of FT scheme by components. The power purchased from the grid, which is considered an operation cost, represents the highest cost. It amounts to \$6,361 million with a constraint of no unmet power. The total NPC of the system is \$10,233 million whereas the LCOE is \$0.0441/kWh. Since there is no tracking, the PV component cost of \$2,339 million has a moderate cost compared to other tracking systems scenarios.

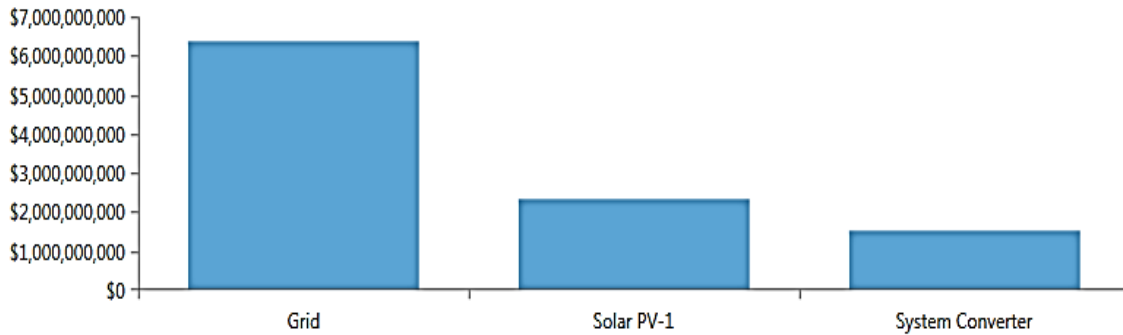


Figure 4.23. Simulation results of net present cost of FT system

It is interesting to discuss the purchasing and selling periods throughout the year. The power flow during the year to and from the grid for the tracking scenario FT is depicted in Figure 4.24, where three periods can be distinguished. In the first three months of the year (period 1), the air temperature and the customer load are lowest. Consequently, the system shows the highest amount of power sold to the grid, reaching 1,000 MW. However, during most of the year (period 2) the system becomes more reliant on the grid due to high demand in addition to the rising temperatures (over 40°C). Finally, in period 3, the system resumes generating more power than required by the load and selling the surplus to the grid. Power purchasing from the grid is continuous throughout the year, with a maximum of 2,931 MW during August and September.

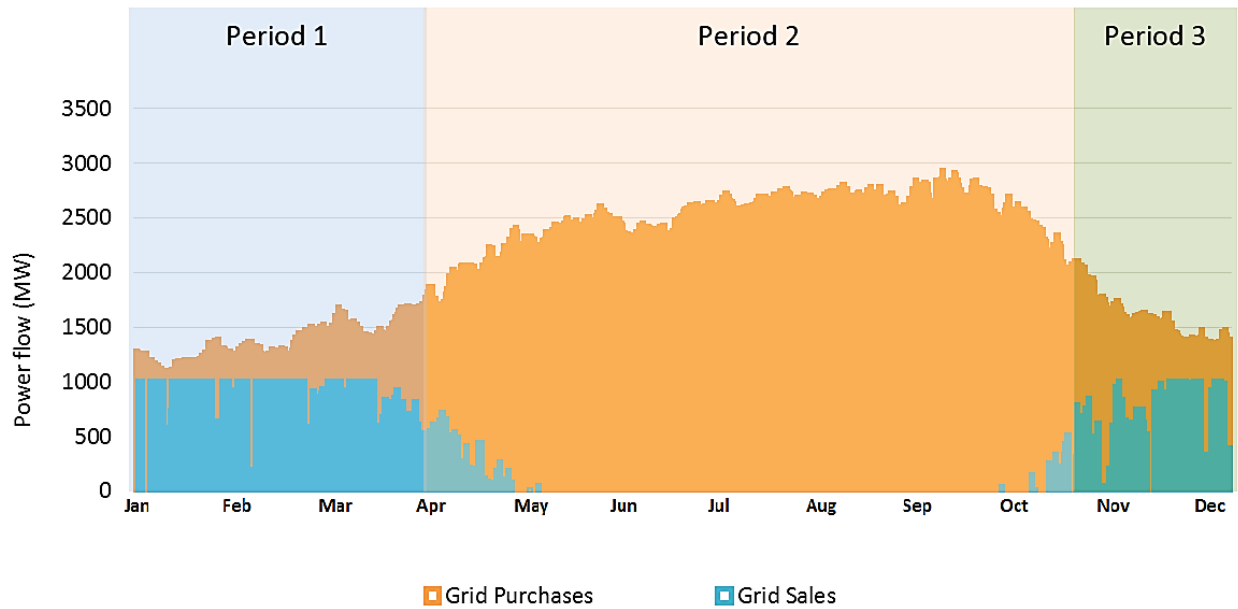


Figure 4.24. Energy purchased from grid and energy sold to grid

The findings of the different tracking simulations show that FT has the lowest NPC and LCOE as shown in Figure 4.25. This is due to the relatively low power generation cost along with the low cost of the simple system. Conversely, HCA demonstrated the highest NPC and LCOE of \$12,662 million and 0.05434 \$/kWh respectively. Despite the daily and weekly adjustment of the tilt angle in HWA and HDA, results presented almost the same as each other in terms of LCOE and NPC values. Moreover, there are no significant differences between HMA, HWA, and HDA regarding LCOE, whereas HCA had the highest LCOE followed by TA. On the other hand, the VCA tracking system showed enhanced performance. Consequently, in this scheme less power is purchased from the grid, which reduces its NPC (10,470 million) and LCOE (0.04475 \$/kWh). In spite of the high contribution of renewable energy to the system by HCA and TA, the high costs of grid purchases and the tracking system components boost the LCOE for these two systems compared to other trackers.

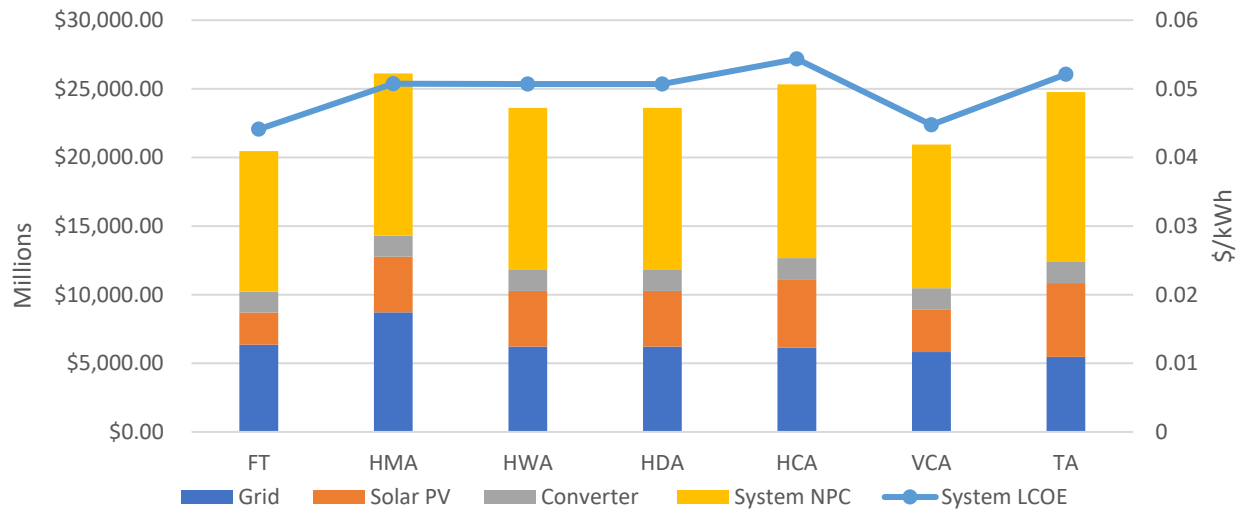


Figure 4.25. NPC and LCOE for various scenarios of tracking systems

Due to the differences in cost of solar tracking systems and in solar irradiation, the optimal solar tracking design may vary for different locations. The results obtained using HOMER software in this research could be compared with the results from existing projects with similar solar irradiation. In the United States, more than 50% of the utility-scale operating solar PV (which account for 60% of the total solar PV unit capacity) use either single-axis or dual-axis form of tracking system [231]. These tracking technologies tend to be located in the Southwest where the solar irradiation ranges from 5 to 6 kWh/m²/day, which is comparable to that in Makkah, Saudi Arabia.

In comparison to the reference case which is the FT, all the horizontal axis trackers demonstrate a negative ROI (-3.3%) as shown in Figure 4.26. This is mainly due to the high capital cost at the year zero of the project. On the other hand, despite the double capital cost of the TA system compared to the reference, the negative impact on the TA's ROI is mitigated by a higher efficiency throughout the project lifetime which is considered as 25 years for all designs. The ROI of the TA is -1.8%. Notably, TA can generate extra power and sell it to the grid. Ultimately, VCA shows a positive ROI (+1.73%) which makes it the best option since it generates a profit in the project

lifetime. We should also bear in mind that solar tracker prices are anticipated to continue falling in the coming years, as the historic drivers including the steadily reducing production costs and the market expansion are likely to continue into the future. Therefore, the ROI of all trackers will increase.

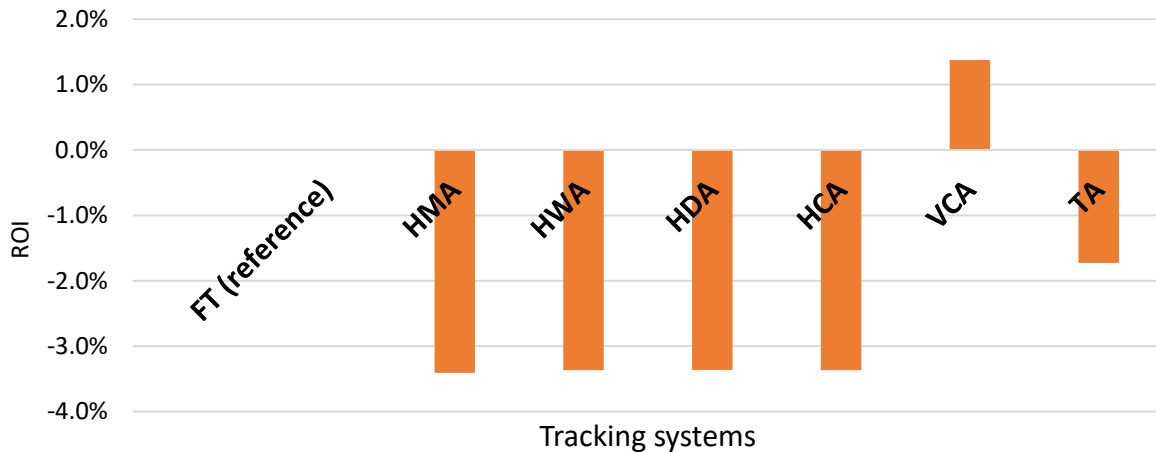


Figure 4.26. Return on investment with FT as the reference case

4.6. Conclusions

The following are the key findings and contributions of this chapter:

- Grid-connected solar PV systems with different tracking system designs, including different time adjustments of the tilt angle, have been examined and compared. An optimal design of a utility size solar-PV grid-connected system for a specific location has been demonstrated. Six tracking designs including FT, HMA, HWA, HDA, HCA, VCA, and TA are considered as viable options for a solar PV grid-connected system. The techno-economic performance of the different tracking schemes was assessed using HOMER simulation tool and discussed.
- In a comparative analysis of daily power generation, all the tracking systems produce similar power output at noontime while the power density varies noticeably in other

periods. The results reveal that TA can produce 34% more power than FT, which was the base case and the lowest producing scheme, while VCA can produce up to 20% more power than FT. The different time adjustments of the tilt angle in HAD, HWA and HMA designs had no significant effect on the amount of power generated compared to each other, whereas HCA produced only 2.4% more than HDA.

- Regarding excess power, TA similarly produced the highest amount, 400% more than FT. All horizontal axes trackers (HMA, HWA, HDA, and HCA) produced similar amounts of excess electricity as each other. VCA produced a reasonable amount compared to other trackers.
- The study findings show that FT design has the lowest NPC and LCOE, \$10,233 million and 0.04907 \$/kWh respectively. This is mainly due to the relatively low power generation cost along with the low cost of a simple system. Moreover, there are no substantial differences between HMA, HWA, and HDA regarding LCOE whereas HCA had the highest costs, followed by TA. VCA is able to sell back excess power produced mainly in low temperature and low demand periods (January – May). It showed less power purchased from the grid than FT and other one-axis trackers which lead to lower the NPC and LCOE.
- In comparison to the fixed system, the tracking systems require higher initial, operation, and maintenance costs. Vertical continuous tracking system presents a high penetration of solar energy to the grid, and it has relatively low LCOE and NPC. Moreover, it introduced the only positive ROI compared to all trackers.
- Considering the high cost of the two-axis tracking system and the low performance of horizontal trackers, the VCA offers a significant technical performance along with feasible economic metrics (LCOE, ROI and NPC). Therefore, VCA can be recommended as the

optimal choice for Makkah city, to enhance the electricity generation of grid-connected solar PV.

- The proposed system design and evaluation of tracking systems could be applied to any location worldwide to improve the performance of grid-connected solar PV. However, the simulation results in this study are quite dependent on site metrological conditions, the load profile, and the components cost which may vary by location.
- HOMER software is a powerful tool to evaluate designs of a variety of tracking configurations for grid-connected applications, as it considers the key factors of PV system performance including load profile, component costs, and resource availability.

Chapter 5

Determining Optimal Solar PV Orientation

5.1. Introduction

Solar energy is seen as a promising RESs for future energy generation and fossil fuel [169], [232]. In real-world, various operating conditions and factors affect the performance of the solar PV system. Nowadays, most commercial solar cells are 10-20% efficient (Figure 5.1) [233]. The combination of such effects with the site location and climate conditions determines the power generation potential of the system. Thus, understanding and tackling these external factors is essential for improving the solar PV system performance and increasing the feasibility in both technical and economic aspects. Hence, maximizing the utilization of the system by eliminating or mitigating energy losses will improve the reliability of the PV system and overcome some of the drawbacks of solar PV projects. At a particular site, the power output could be maximized if the panel orientation, including its tilt angle and azimuth angle, are adjusted appropriately. At a given moment, the solar irradiation on a PV panel is highest when the surface of the PV plane points towards the sun capturing the core components of the solar irradiation, which is the direct solar beam. This leads to receiving more solar irradiation and ultimately generating more power from the solar PV system since the power output is almost proportional to photons received by the solar panel. For instance, a solar panel with an area of 1 m^2 and a 15% efficiency will yield 150 W at standard test condition (STC) (solar irradiation 1 kW/m^2 , a cell temperature of 25°C). However, the solar cell generates more power when there is high irradiation and less under shading or in cloudy weather.

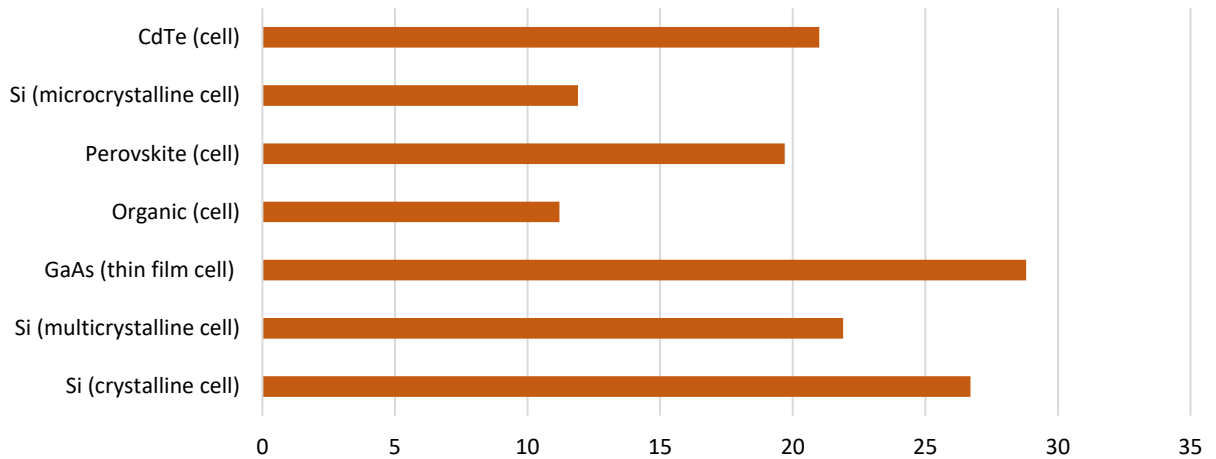


Figure 5.1. Efficiency comparison of some PV technologies

5.2. Problem Statement

The site and weather conditions define the power generation potential of the system. Thus, understanding and tackling these external factors is essential for improving the solar PV system performance. In the same context, the solar PV power output could be maximized if the panel orientation including its tilt angle and azimuth angle, are adjusted appropriately. This leads to receiving more solar irradiation and ultimately generating more power from the solar PV system since the power output is almost proportional to photons received by the solar panel.

As a final phase, by applying a detailed incident solar radiation calculation model, the optimal tilt and azimuth angles will be determined towards generating the maximum energy yield. The orientation adjustment of solar PV panel will lead to more efficient system and can mitigate the challenge of the low cell efficiencies and the high cost to the solar PV system owner. From Chapter 3, the central region of Saudi Arabia was found to have a high suitability index for solar PV [178]. The authors studied and investigated the suitability for the whole country considering different

economic and technical criteria, with the goal of assuring maximum energy yield while minimizing project cost. In this chapter, our objectives are:

1. Consider the permutations of tilt angle between 0 and 90° and azimuth angle between -90° and 90° in one-degree steps to calculate the total power produced monthly and annually for each pair which results in maximum solar irradiation.
2. To investigate the optimal tilt and azimuth angles for 18 cities in Saudi Arabia using real hourly measurements.
3. The air temperature has some effect on the PV performance. Thus, the effective hourly power generated by PV will be considered for more accurate calculations.
4. Due to solar PV cover material, some solar irradiation is lost when the angle of incidence (AOI) is greater than zero. To account for such loss, the incidence angle modifier (IAM) will be used.
5. To validate the results of this chapter with results obtained from Chapter 3 on potential site suitability for utility-scale PV technology in Saudi Arabia.

A detailed incident solar radiation calculation model will be developed to first determine the solar angles and then convert the values of hourly measured solar irradiation components, including GHI, DHI and DNI as well as ambient temperature (T_a) for one year into hourly, monthly and yearly tilted irradiance. These values will be used to find the optimal orientation, consisting of tilt and azimuth, which allow the system to generate the maximum yearly power. Symbols and abbreviations used in this chapter are listed in Table 5.1.

Table 5.1. Symbols and abbreviations

Acronym	definition	Acronym	Definition
GHI	global horizontal irradiation	φ_s	solar azimuth angle
DHI	diffuse horizontal irradiation	β	solar altitude angle
DNI	direct normal irradiation	L	latitude of the site
STC	standard test condition	φ_c	surface azimuth angle
n	day number	τ	tilt angle
Ta	ambient temperature	H	hour angle
AOI	angle of incidence	δ	solar declination
IAM	incidence angle modifier	CT	Clock time
n	day number	Lm	standard meridian
K.A.CARE	King Abdullah City for Atomic and Renewable Energy	Lg	longitude of the site
ρ	ground reflectance	E	equation of time
P_{dc}	Output DC power	θ_{AOI}	AOI angle
P_{dc}	DC power	I_{DNI}	total direct normal irradiation
y	year	I_{DHI}	total diffuse horizontal irradiation
T_C	cell temperature	I_b	total direct normal irradiation on surface
T_a	ambient temperature	I_d	total diffuse irradiation on surface
NOCT	nominal operating cell temperature	I_r	total reflected irradiation
dp	PV temperature coefficient of power		

5.3. Literature Review

Different methods have been proposed for optimizing the tilt angle of solar PV for different sites in various latitudes in the literature [234], [235], [244]–[246], [236]–[243]. Sixteen different analytical formulae have been developed for calculating the optimum PV tilt angle for each month by Nijegorodov et al. [235]. Cheng et al. [240] conducted a study for south oriented tilted PV panels at 20 different locations in 14 countries, ranging from 0 to 85 latitude, and concluded that more than 98% of the system performance can be achieved by considering the latitude angle as the panel’s yearly optimal tilt angle in the Northern Hemisphere. Elminir et al. [239] concluded that

yearly optimum tilt is approximately altitude ± 15 degrees, where plus and minus signs are for winter and summer seasons, respectively. They studied the case of Helwan, Egypt. Monthly, seasonal, semi-annual and annual optimum tilt angles were determined for two cities in Iran [247]. Their study showed that two-time adjustments led to about 8% annual increase in the total received energy. Benghanem et al. [248] found that the average optimum tilt angle at Madinah, Saudi Arabia is 37° for the winter months and 12° for the summer months, whereas the annual optimum tilt angle is almost equal to the latitude of the site. Rowlands et al. [236] recommend that tilt angle be marginally less than latitude for Ontario, Canada, given a particular pricing regime, while the desired azimuth is close to due south. In [249], additional annual energy achieved by adjusting the PV surfaces at monthly, seasonal, semi-yearly and yearly optimum tilt angle can be 23.15%, 21.55%, 21.23% and 13.76%, respectively compared to the no adjustment case. Kaddoura et al. [234] investigated the optimum tilt angles for various cities in Saudi Arabia. For Jeddah city with the latitude of 21.5° N, the optimal tilt angle was found to be 19.28° . The authors concluded that adjusting tilt angles six times per year yields to achieving 99.5% of the solar radiation compared to daily adjustment.

By optimizing solar panel tilt angles in a solar tree for San Francisco and Paris, Dey et al. [238] demonstrated a power generation increase of 2.04% and 7.38% respectively compared to latitude tilt. Lv et al. [237] concluded that due to a low significant variation in total solar energy compared to the case without adjustment, it is not recommended to adjust the tilt angle monthly during the heating season in Lhasa, China.

The tilt angle is essential to the performance of solar PV. Improper tilting leads to capturing less available solar power. A rule of thumb that the tilt angle should be equal to the latitude of the location and that the azimuth angle should be towards the south for a maximum annual energy has

been considered in many studies [239], [250], [251]. However, the solar irradiation availability varies through its annual cycle. The rule-of-thumb approach may be appropriate for specific locations. However, it may result in increased system costs or in oversizing of systems if considered without proper analysis. The consequences are particularly notable for utility-scale solar power plants [252]. In comparison to the earlier studies, this chapter demonstrates that measured data-driven determination of panel tilt and azimuth angles is crucial to maximizing the incident solar radiation on a panel at a particular site, and that simply accepting panel tilt to be equal to location latitude might not be the best approach for all places.

5.4. Methodology

Figure 5.2 presents the proposed methodology. It consists of three steps; the first step comprises of weather data collection for the study region. The second step presents the solar angles equations while the third step computes the impact of solar irradiation on solar PV. The methodology applied in this chapter examines every optimization loop to find the decision variables, including the tilt and azimuth angles, that lead a tilted solar PV panel to capture the maximum solar irradiation in monthly, seasonally and yearly adjustments. These steps are explained in detail as follows:

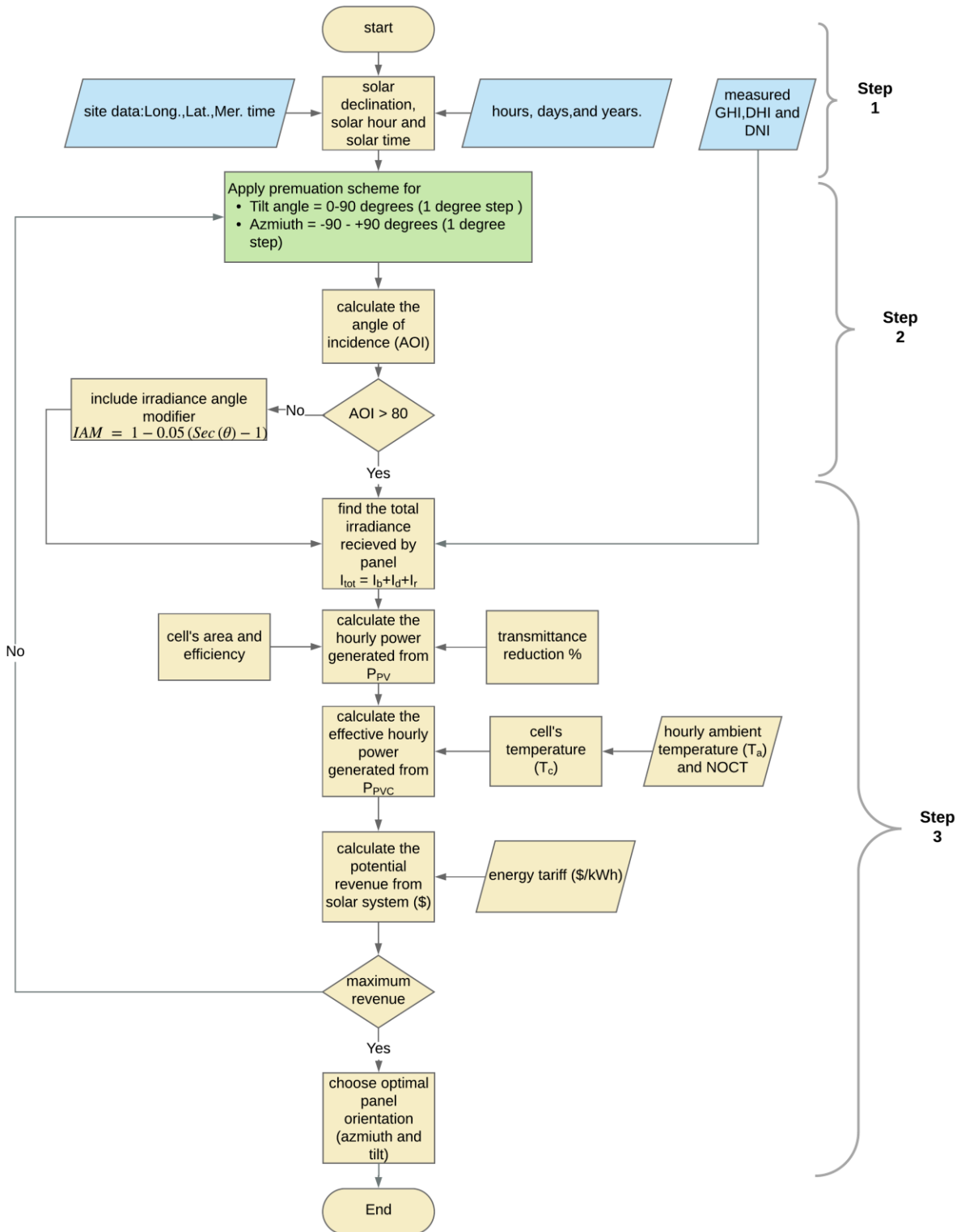


Figure 5.2. Flowchart of the developed methodology for a maximum solar irradiation

5.4.1. Input data

Hourly measured weather data including GHI, DNI, DHI and T_a for the Riyadh city (latitude=24.91 and longitude = 46.40) in central Saudi Arabia were obtained from K.A.CARE. K.A.CARE as the lead organization working to develop a RESs mix portfolio, has established the renewable resource monitoring and mapping (RRMM) solar measurement network, which is deployed over Saudi Arabia with 50 metrological stations classified in three tiers. For this study, a tier-1 RRMM weather station, which is considered as a research type station provided the highest quality data with low uncertainty (in the range of $\pm 2\%$ sub-hourly). This station is maintained and cleaned on a daily basis and provides 1-minute level data. The data from January 2015 to December 2015 was used to investigate the optimal tilt and azimuth angles [253]. Figure 5.3 shows the average monthly GHI and air temperature for Riyadh city.

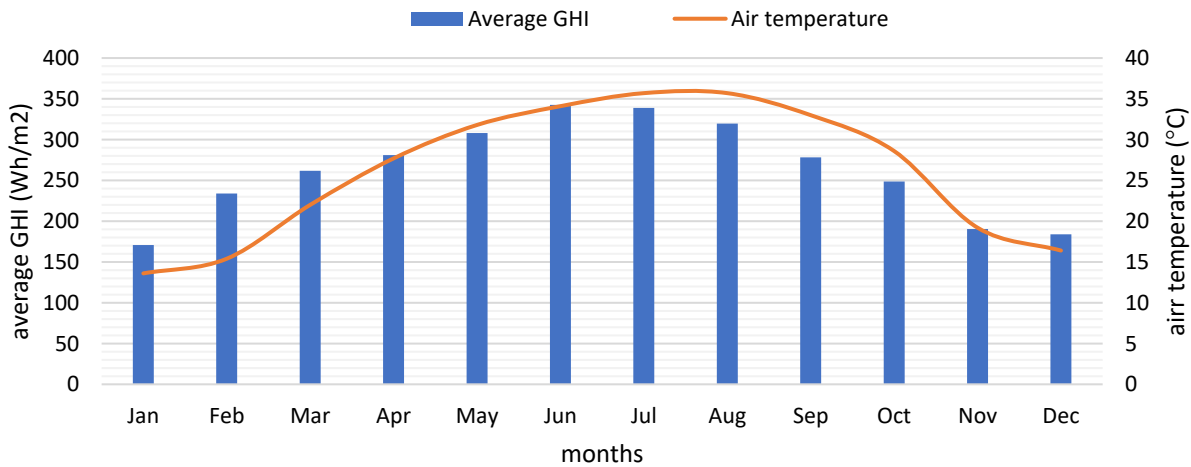


Figure 5.3. Monthly average of GHI on a horizontal surface and air temperature for Riyadh

5.4.2. Solar angles equations

The solar declination (δ) defines the angle between the plane of the equator and a line drawn from the center of the sun to the earth's center, which varies between $+23.45^\circ$ and -23.45° . The

following equation defines the relation between the day number (n) and the declination angle assuming 365-day year and spring equinox on day number 81.

$$\delta = 23.45 \sin \left[\frac{360}{365} (n - 81) \right] \quad \text{Eq. 5.1}$$

At any time of day (n), the sun location can be defined in terms of its altitude angle β and its azimuth angle φ_s as shown in Figure 5.4 [254].

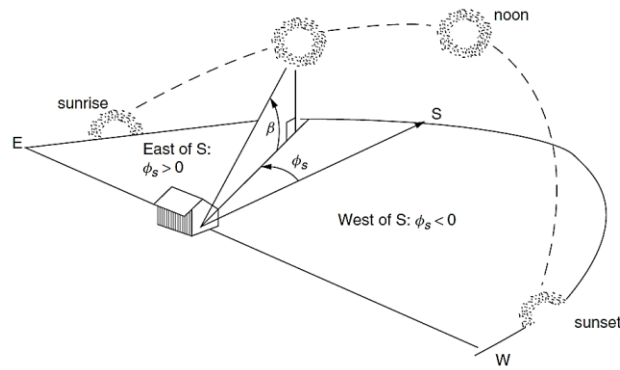


Figure 5.4. The sun's position with solar altitude and azimuth angles

The time of the day, the day number and the site latitude determine the solar azimuth (φ_s) and solar altitude angles β . The following equations can be used to calculate these sun's angles.

$$\sin \beta = \cos L \cos \delta \cos H + \sin L \sin \delta \quad \text{Eq. 5.2}$$

$$\sin \varphi_s = \frac{\cos \delta \sin H}{\cos \beta} \quad \text{Eq. 5.3}$$

The solar azimuth angle is considered positive before noon, when the sun is in the east, and negative in the afternoon when the sun in the west. The hour angle is the number of degrees that earth must rotate before the sun can reach the local meridian (longitude). The hour angle (H) can be calculated as follows considering the earth turns 360° in 24 hours or $15^\circ/\text{hour}$:

$$\text{Hour angle } (H) = \left(\frac{15^\circ}{\text{hour}} \right) \cdot (\text{hours before solar noon}) \quad \text{Eq. 5.4}$$

The solar azimuth could be obtained using Eq. 5.3. However, in summer and spring seasons, the magnitude of the solar azimuth will reach more than 90° or less than -90° away from the south in mornings and afternoons. A test is required to verify the position of the sun as the arcsine is ambiguous. This test should be done to check whether the angle is less or greater than 90° .

$$\text{if } \cos H \geq \frac{\tan \delta}{\tan L}, \text{ then } |\varphi_s| \leq 90^\circ; \quad \text{otherwise } |\varphi_s| > 90^\circ \quad \text{Eq. 5.5}$$

The sun path including solar altitude and solar azimuth could be depicted in a graphical form for a given latitude, to help visualize the sun's position at any time. The sun path diagram can be utilized to avoid locations shaded by trees, buildings or other obstructions at a potential site. In the northern hemisphere, the solar path is high in altitude during summer and low on the horizon during winter. Consequently, summer days are longer while winter days are shorter. Patterns are opposite in the southern hemisphere. All these variations result in varying geometry of the sun position at a particular place [141]. From the above equations, the solar altitude angle β and solar azimuth φ_s can be calculated and graphed at any given latitude. Figure 5.5 illustrates the sun's path in altitude and azimuth angles for Riyadh's latitude of (24.91°) for 21st day of each month from 5:00 a.m. to 7:00 p.m. local time. The positive side (east of φ_s) represents the sun path before noon, while the negative side (west) represents the afternoon path. At the center is the azimuth of zero at noontime. In summer and spring months, the φ_s takes values beyond the $\pm 90^\circ$ with high β . This understanding is essential for analyzing and modelling solar irradiation components as shown in next section.

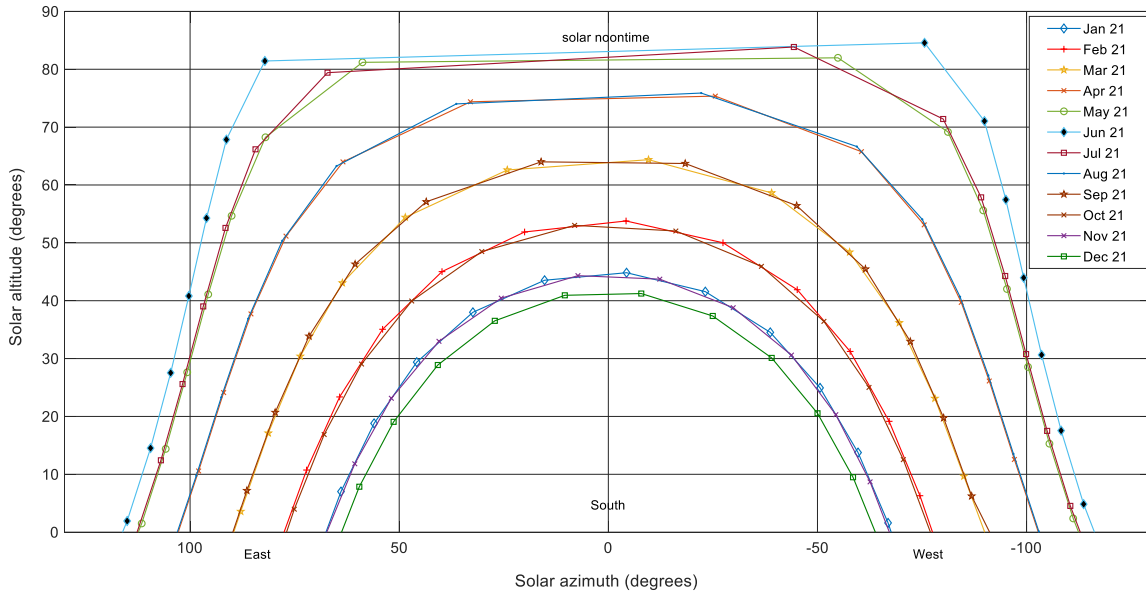


Figure 5.5. Sun path presents altitude and azimuth angles in standard time for 24.91° N

The solar time (ST) is a time expression representing a time relative to solar noon. This is different from the local time or civil time (CT) where the world regulates clocks and time according to the coordinated universal time (UTC) standard. Two equations are required to adjust the ST as follows:

$$\text{Equation of time (E)} = 9.87 \sin 2B - 7.53 \cos B - 1.5 \sin B (\text{minutes}) \quad \text{Eq. 5.6}$$

$$\text{where } B = 360/365 * (n - 81) (\text{degrees})$$

The final relationship between the ST and CT in minutes is:

$$\text{Solar time (ST)} - \text{CT} = (4 * (Lm - Lg) + E) \quad \text{Eq. 5.7}$$

Where Lm is the standard meridian and Lg is the longitude of the site. The equation of the time is a function of time of the year as depicted in Figure 5.6.

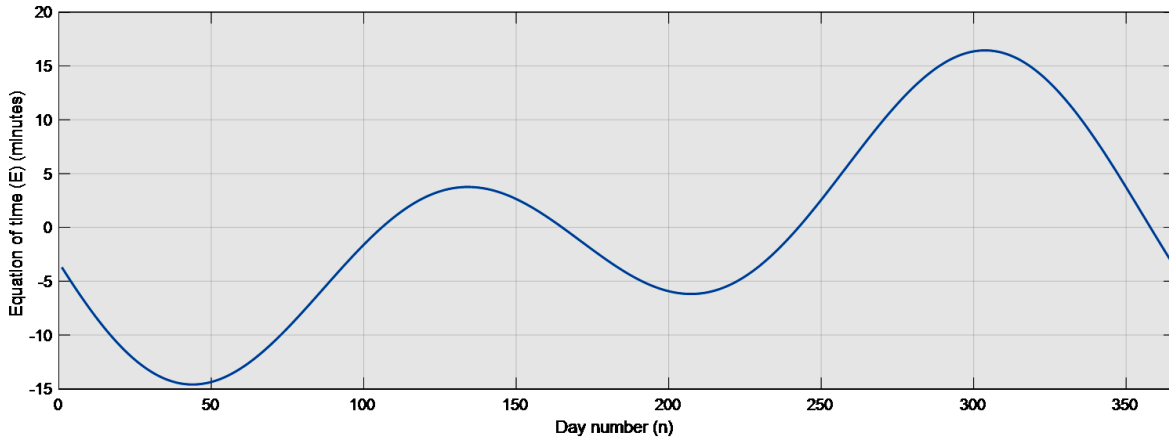


Figure 5.6. The equation of time (E) in minutes as a function of day number (n)

5.4.3. Computing the impact of solar irradiation on solar PV

The solar irradiation received by the solar panel is a combination of its components: direct beam irradiation (I_b), diffuse irradiation (I_d) and reflected irradiation (I_r) as shown in Figure 5.7. Using geometric calculation, the estimation of the DNI insolation on a PV panel is easy and highly accurate compared to DHI and reflected irradiation. The translation of I_{DNI} into direct irradiance hitting the surface (I_b) is a function of AOI and given by:

$$I_b = I_{DNI} \cos(\theta_{AOI}) \quad Eq. 5.8$$

Where θ_{AOI} is the angle of incidence, between the direct beam array and normal to the panel. On a fixed solar PV, I_{DNI} will not be normal to the panel at all the times during the day, thus when the AOI increases, the reflected irradiance increases because of the PV panel front cover material (usually glass). To tackle such material reflectance, irradiance angle modifier (IAM) will be considered to compute more accurately the irradiation of the panel beneath the protective layer. The American Society of Heating, Refrigerating and Air-Conditioning Engineers (ASHRAE) adopted the following calculation of IAM response of PV panels [255]:

$$IAM = 1 - b_0(\text{Sec}(\theta_{AOI}) - 1) \quad \text{Eq. 5.9}$$

The b_0 value of 0.05 has been recommended to model the glass response. It is recommended to use this equation only for $\theta_{AOI} < 80^\circ$ [256]. The modified I_b components after considering IAM are as follows:

$$I_b = I_{DNI} \text{Cos}(\theta)[1 - 0.05(\text{Sec}(\theta_{AOI}) - 1)] \quad \text{Eq. 5.10}$$

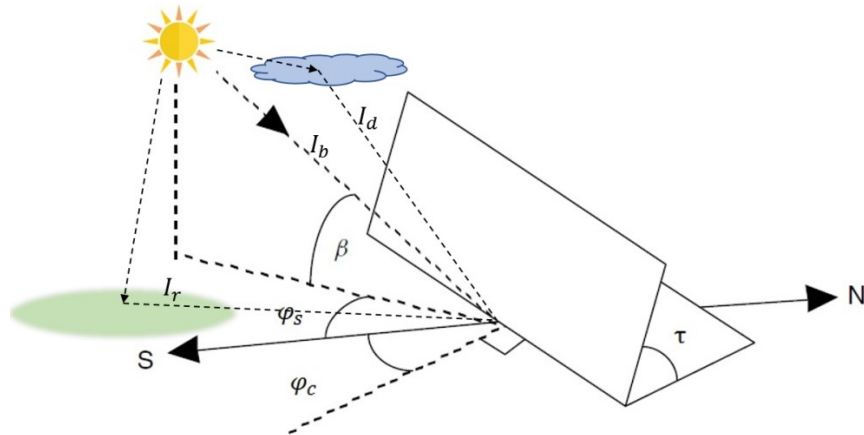


Figure 5.7. Irradiation components received by the panel along with angles

The estimation of scattered solar irradiation (diffuse solar irradiation) I_d due to the diffusion caused by clouds, atmospheric particles or nearby objects is more complicated. For a simple model, the expression for I_d is as follows:

$$I_d = I_{DHI} \left(\frac{1 + \text{Cos}(\tau)}{2} \right) \quad \text{Eq. 5.11}$$

Where τ is the tilt angle of the panel concerning the horizontal surface. On the other hand, I_r is the irradiation reflected from ground, water or snow, received by the panel. The following expression gives the reflected irradiation:

$$I_r = \rho I_{DNI}(\sin(\beta) + I_{DHI})(1 - \cos(\tau))/2 \quad \text{Eq. 5.12}$$

Where ρ is the ground reflectance, which could range from 0.1 for an urban environment to 0.8 for fresh snow. In this study, ρ is estimated as 0.2 [257]. The total irradiance received by a PV panel is:

$$I_t = I_b + I_d + I_r \quad \text{Eq. 5.13}$$

Like other semiconductor devices, a solar cell is sensitive to the temperature generated from the received sunlight. When the operating temperature of the solar panel increases, the solar cell performance decreases. The conversion rate of solar energy to electrical energy for a typical solar PV module is in the range of 5-25%. Accordingly, the rest of the incident irradiation is converted to heat, which significantly increases the temperature of the module hence lowering the efficiency of the module [258]. Taking into account a typical module efficiency of 16%, and cell area of 1m^2 , the DC power yield resulting from I_t will be as follows:

$$P_{dc} = 0.16 I_t \quad \text{Eq. 5.14}$$

To account for the hourly change in the ambient temperature, the nominal operating cell temperature (NOCT) is considered. NOCT is often provided by the module manufacturer and gives the cell temperature when ambient is 20°C , wind speed is 1 m/s , and solar irradiation is 800 W/m^2 . In this study, the NOCT is assumed to be 45, and the temperature coefficient (dp) is $-0.4\%/^\circ\text{C}$ [259].

$$P_d = P_{dc}(1 + dp(T_C - 25)) \quad \text{Eq. 5.15}$$

$$\text{Where } T_C = T_a + [(NOCT - 20)/800] * I_t \quad \text{Eq. 5.16}$$

The consumption tariff (γ) will be considered as if the power produced by the solar PV system will be injected to the grid with the same tariff. A new electricity tariff of 0.08 \$/kWh was announced on 1/1/2018 in Saudi Arabia, [173]. For each hour in the year, the total of annual potential revenue from such panel orientation is calculated as follows:

$$P_{tot} = \gamma P_d \quad \text{Eq. 5.17}$$

5.5. Results

5.5.1. Annual optimal orientation and energy yield

The proposed approach described in Figure 5.2 was coded in MATLAB to find the optimal orientation for Riyadh. The optimization code was run 16,472 times to investigate the potential solar irradiation and power output for every combination of tilt and azimuth angles in the whole year. The tilt angle ranges from 0° to 90° while azimuth from -90° to 90° in 1°-increments. Figure 5.8 presents a sample of such simulation using surface azimuth (φ_c) from -20° to +20° for each tilt angle range from 0° to 90°. The energy yield swings between 181 to 330 kWh per year. The energy yield output increases as the tilt angle varies from 0° to approximately 30° and then starts to decrease. As the azimuth angles changes from -20 towards zero, the peak energy yield remains almost constant, whereas the power trend starts to decrease as the azimuth increases beyond zero.

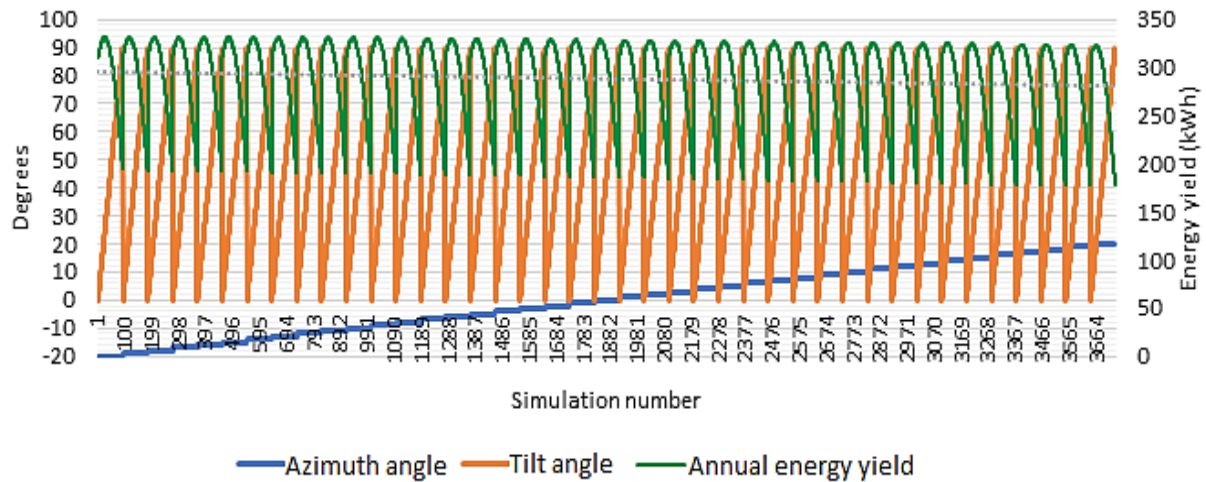


Figure 5.8. Sample of simulation outcome for different azimuth and tilt angles

For a tilted surface, the annual potential solar power has been calculated for different azimuth angles ranging from 90° (east) to -90° (west) in 1° increments, using the MATLAB code. Figure 5.9 shows the annual energy yield for different azimuth angles φ_c ($-60^\circ, -40^\circ, -20^\circ, 0^\circ, 20^\circ, 40^\circ, 60^\circ$). The azimuth angles of $-20^\circ, -40^\circ$ and 0° demonstrate similar potential with their maximum between the tilt of 20° and 30° . The power decreases as the azimuth reaches or exceeds 20° east or 60° west of south-facing. For a panel close to vertical, the -60° azimuth is optimal, as vertical orientation misses the major solar irradiation during noontime, but it can capture more irradiation before sunset by directing the panel towards the west, especially during long summer days.

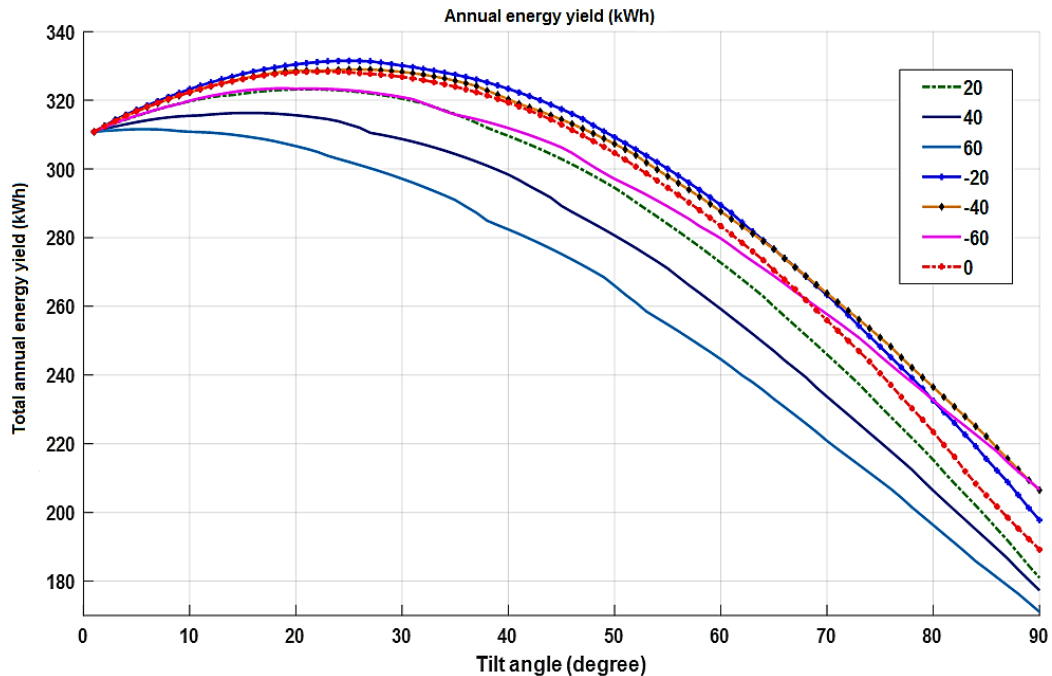


Figure 5.9. The potential annual energy yield versus tilt angles for different azimuth

5.5.2. Monthly orientation adjustments

As discussed in previous sections, the solar power production varies owing to the variations of sun path from one month to another. The monthly energy yield (kWh) is plotted versus tilt angle for each month for a south-facing panel with a fixed azimuth angle (-20°) as depicted in Figure 5.10. As observed from the graphs, the solar energy yield depends on the tilt angle. In January, February, December, and November, it starts at low (15-25 kWh) at the tilt angle of 0° , it increases gradually as the tilt increases to approximately 50° , and then it starts to decrease. In summer months (May, June, July, and August), the energy yield reaches the highest values with low tilt angle near the horizontal, and it declines steeply beyond the tilt angle of 30° . This is due to the high solar altitude during summer. It should be noted that tilt angles higher than 60° give lowest energy yield for any month, and therefore this range need not be considered. It should also be mentioned that the panel

efficiency and air temperature effects are taken into account when calculating the potential solar power.

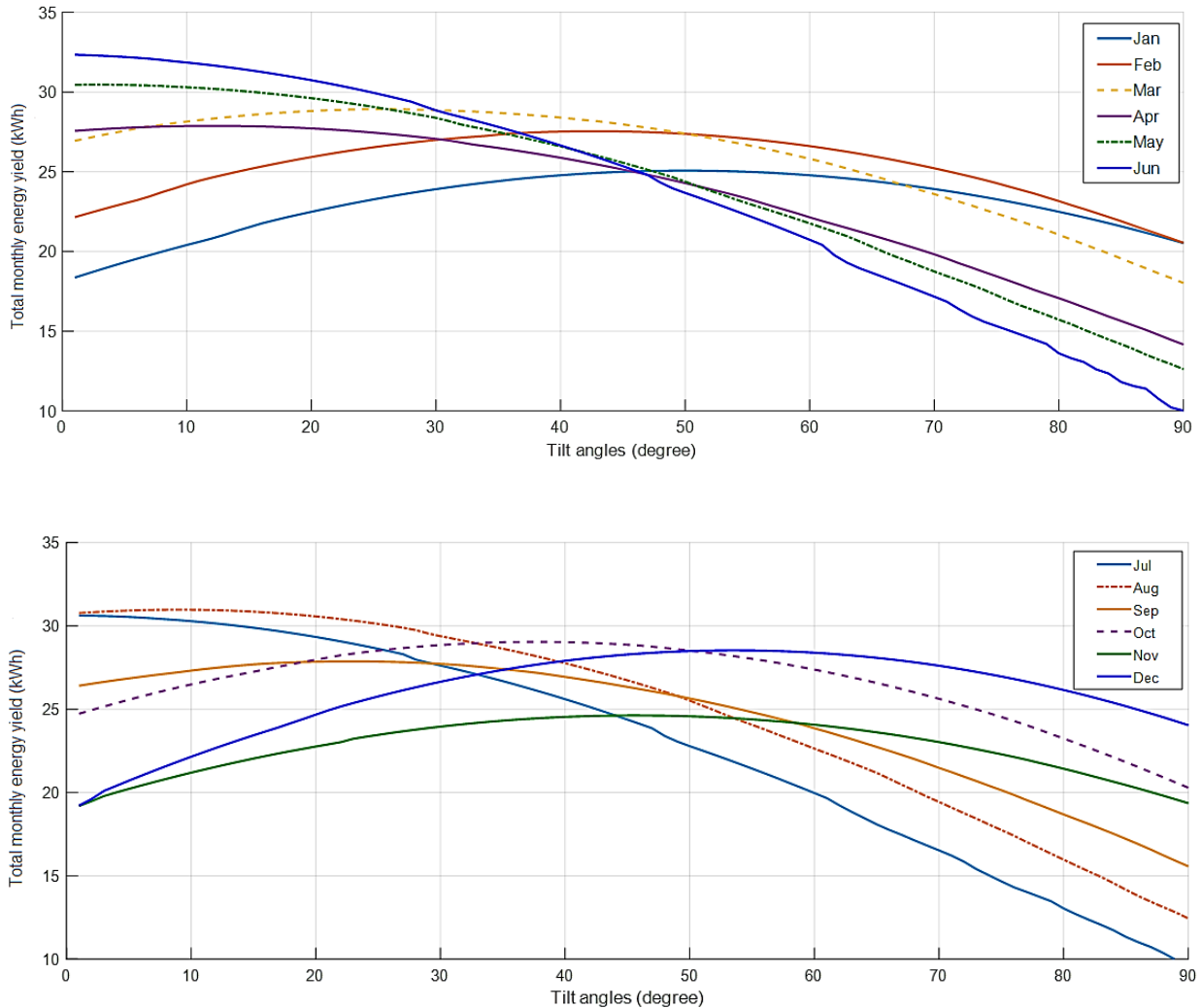


Figure 5.10. Total monthly energy yield versus tilt angle for -20 azimuth angle

Based on the maximum total energy yield in each month, the optimum tilt angle was found for the azimuth angle of -20° as shown in Figure 5.11. Winter months including December, January and February show the highest tilt angles with a peak of 53° in December, which is when the sun is on the Tropic of Capricorn (23.5° south). The average of tilt angles in summer months, i.e., May, June, July, and August, is 9° . For the equinox months (March and September) when the center of

the sun is right over the equator, the tilt angles are 25° and 22° , respectively. Finally, the annual optimum tilt angle was 24° which is very close to the latitude of Riyadh (24.91° N).

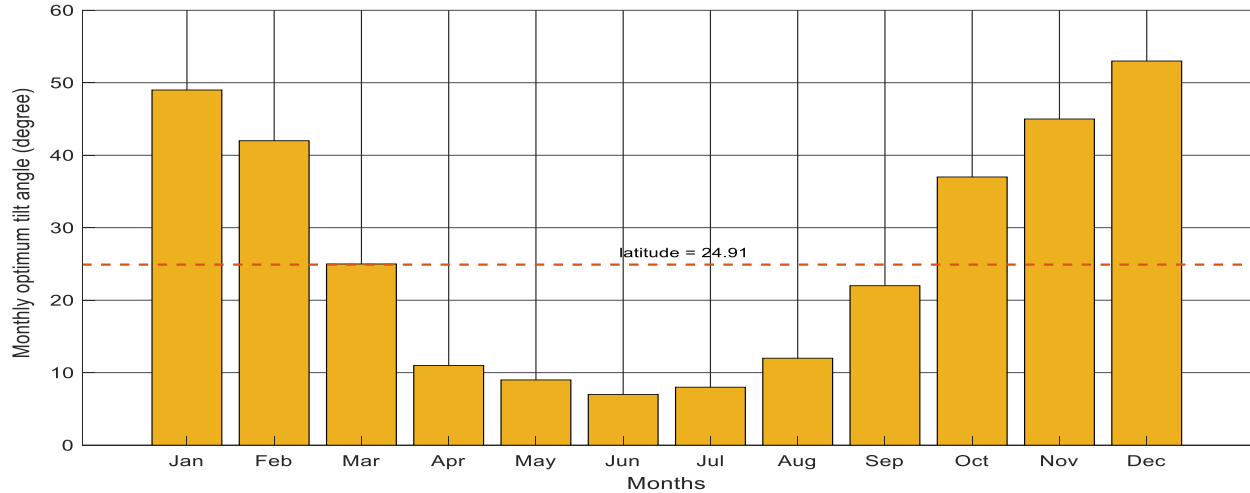


Figure 5.11. The monthly optimum tilt angle for Riyadh

Figure 5.12 shows the total of monthly solar irradiation at the annual optimum tilt angle (24.0° N). For this value of tilt angle, the solar irradiation varies throughout the year. A maximum of 230 kWh/m^2 occurs in July with the azimuth of -40° . During summer months (May, June, and July) the solar irradiation is at the maximum due to the high solar altitude and long days with an average of $225 \text{ kWh/m}^2/\text{month}$. In these summer months, the sunrise is around 6:00 am and the sunset around 7:00 p.m. The surface azimuth between -20° and -40° (towards the west) is suitable in these months, to capture more irradiation. In the equinox months, *i.e.*, March and September the azimuth angles between south-facing and -20° are optimal, with around $200 \text{ kWh/m}^2/\text{month}$. In general, the azimuth of 0° (south-facing) and -20° have similar performance except in summer months when -20° has a higher output due to the solar path. The monthly energy yield has the pattern similar to that of solar irradiation as shown in Figure 5.13. However, due to the air temperature

effect, the energy yield decreases sharply in April and September, while in the summer months the availability of solar irradiation compensates for the air temperature effects (see Figure 5.3).

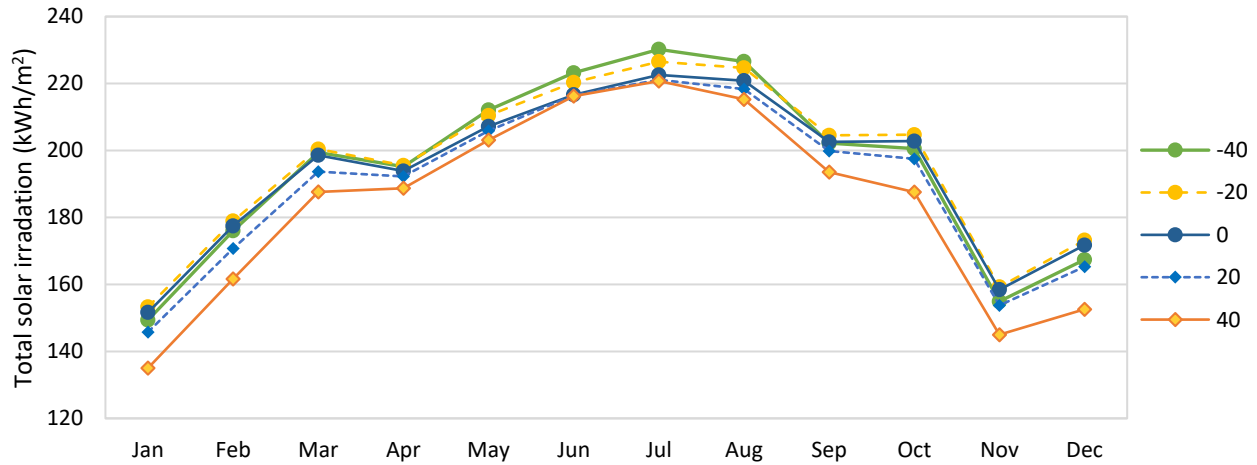


Figure 5.12. Total monthly solar irradiation in kWh/m²

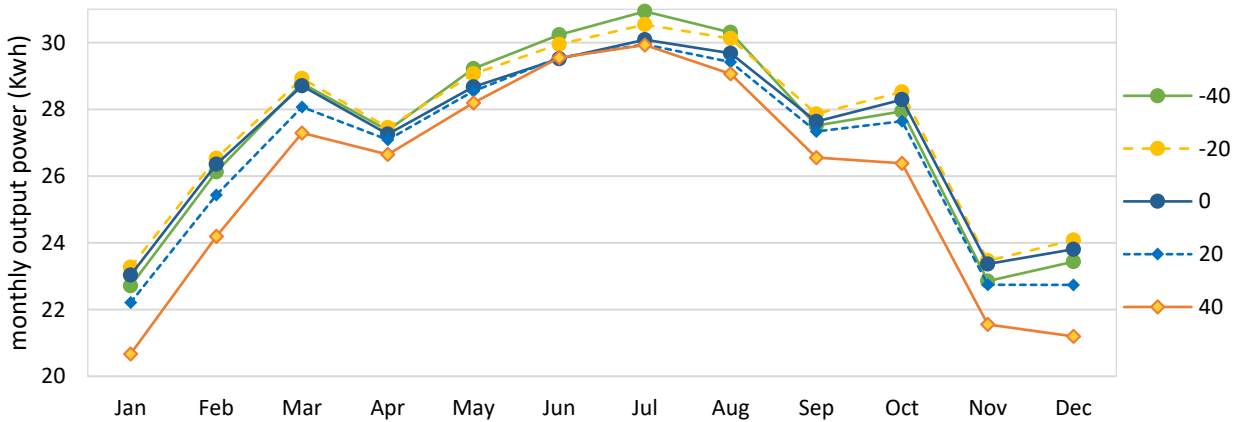


Figure 5.13. Total monthly energy yield for different azimuth

5.5.3. Proposed orientation adjustment scheme

The fixed tilt angle of 24°, which is the same as the Riyadh's altitude, with -20° azimuth would yield the maximum annual power of 331.5 kWh. The azimuth of -20° indicate that the panel will generate more on the west and this is as a result of high solar irradiation is available in the

afternoon. Figure 5.14 presents the daily GHI of each 15th day of each month to highlight the time where high solar irradiation taking place.

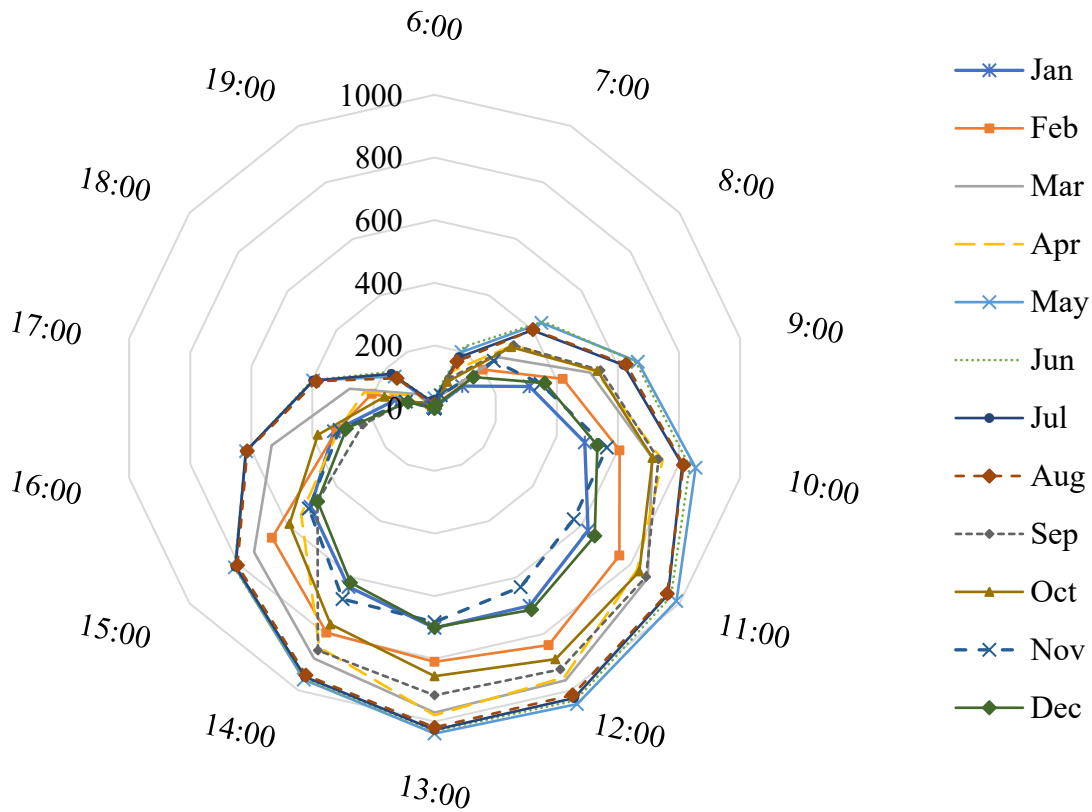


Figure 5.14. Daily GHI of the 15th day of each month

This is in accordance with the general “rules of thumb” that consider the tilt equal to latitude as optimal, and the deviations in the azimuth angle of 10° to 20° from south as having small effects. The optimum monthly tilt and azimuth angles found in this study, with their energy yield are shown in Table 5.2. Moreover, the calculation of energy yield that could be generated by the solar generation system is investigated. It was found that the monthly adjustment increases the harvested solar energy by 4% (13.3 kWh). The monthly adjustment might not be justified considering the cost of manpower and solar trackers for such minor improvement in the system performance. From Figure 5.11 and Table 5.2, it can be noted that the summer tilt angles for May, June, July and August are very close to each other with an average of 9.4°. Moreover, the energy yield differences

between these months are less than 5 kWh. Therefore, there could be one tilt angle for the whole summer season. Similarly, for the winter months of November, December, January, and February there could be one tilt angle of 47.25° .

Table 5.2. The monthly optimum orientation and their corresponding potential energy yield

Month	Optimal (Base, Monthly)		Energy yield (kWh)
	τ°	φ_c°	
Jan	49	-14	25.126
Feb	42	-15	27.5565
Mar	25	-18	28.9332
Apr	11	-24	27.8821
May	9	-90	30.5617
Jun	7	-90	32.4334
Jul	8	-90	30.8385
Aug	12	-64	31.074
Sep	22	-16	27.8855
Oct	37	-15	29.0833
Nov	45	-12	24.7242
Dec	53	-10	28.6875
Annual	24	-20	331.4937

Compared to the study of [234], which considered only tilt angle adjustment, the optimization approach in this study considered both the adjustment of tilt angle and the surface azimuth angle from the east (-90°) to the west ($+90^\circ$) with high accurate solar irradiation data. The monthly optimum tilt angles are very comparable. However, in our study, for the summer season (May to August), the optimum tilt angles were found to be very close to horizontal, while the optimum surface azimuth is in the west direction, at -90° . The case in the previous study shows a tilt angle

with a negative tilt, which means that the surface is oriented towards the north. The azimuth of -90° (west-facing) is owing to the sun path in summer months which is more upwardly concave towards the north especially during morning and late afternoon time as shown in Figure 5.5. Also, due to the clear sky in the afternoon the high availability solar irradiation is existing.

A wider solar modules can range can result in a self-shading issue which may reduce the system performance significantly. For more practical azimuth range besides avoiding wider orientation, modified azimuth angles are proposed. A curve fitting with 4th order polynomial ($R^2 = 0.964$) is applied for better azimuth angles for summer months as depicted in Figure 5.15. The results show that the new azimuths for summer season (May to August) have 98.5% efficiency compared to the obtained optimal azimuth as shown in Table 5.3.

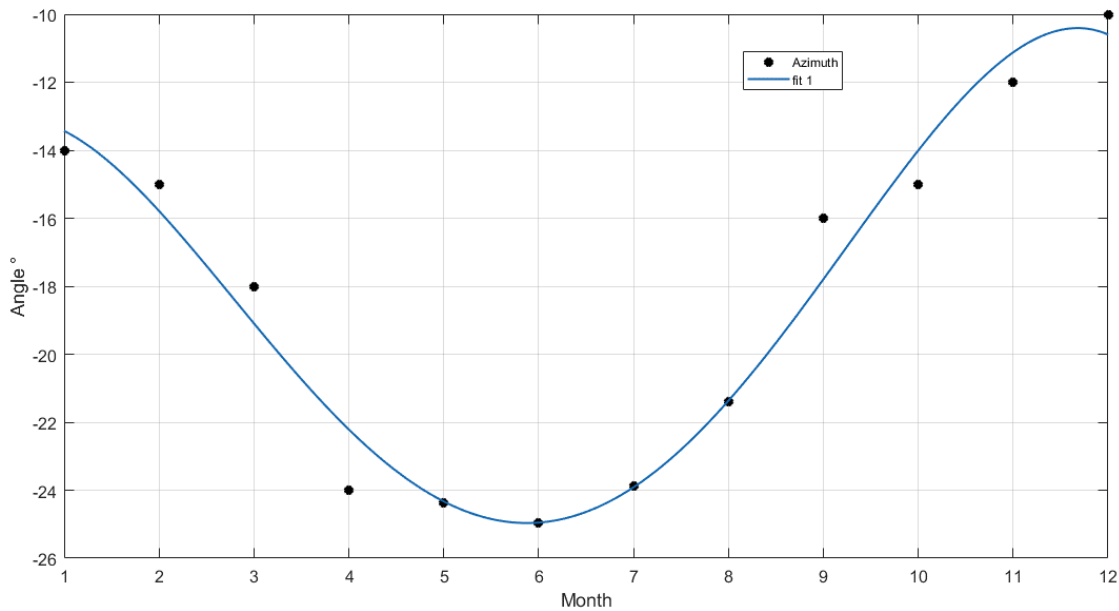


Figure 5.15. Proposed monthly azimuth angle for Riyadh

Table 5.3. Proposed solar PV orientation for summer months

Month	Optimal (Fitted model)		Energy yield (kWh)	Efficiency compared to optimal orientation (%)
	τ°	φ_c°		
May	9	-24.5	30.3195	-0.792
Jun	7	-25	32.0213	-1.270
Jul	8	-24	30.3723	-1.51
Aug	12	-21.5	30.9340	-0.450

The monthly adjustment of solar PV orientation might be quite challenging as it is labor demanding. Therefore, the proposed adjustment schedule for both tilt and azimuth angles is presented in Table 5.4. Adjusting the tilt angles according to the proposed scheme results in harvesting 3.63% more solar energy than with the fixed annual optimum orientation. This scheme should generate almost the same as the case of monthly adjustments (with only 0.366% less) as shown in Table 5.4. The variation of tilt has a significant impact on the energy yield. By considering a monthly tilt of altitude (24°) and fixing the azimuth as shown Table 5.4., the annual energy yield decreases by 4.1% (14 kWh). On the other hand, the impact of the azimuth angle has a minor effect on the energy yield. Using the optimum tilt with zero azimuth (south-facing), the system would generate less by only 0.77% in energy yield (3 kWh).

Table 5.4. Proposed scheme for periodic adjustments and the corresponding energy yield

Period		Optimal (Base, Fitted, Periodic)		Energy yield (kWh)
		τ°	φ_c°	
1	Nov	47.25	-12.75	28.565
	Dec			24.712
	Jan			25.109
	Feb			27.468
2	Mar	25	-18	28.933
3	Apr	9.4	-23.8	27.8707
	May			30.3195
	Jun			31.8736
	Jul			30.3149
	Aug			30.9947
4	Sep	22	-16	27.886
5	Oct.	37	-15	29.083

Figure 5.16 illustrates the impact of varying the panel orientation with respect to the potential energy yield. It can be noticed that both monthly tilt and azimuth angles are presented as concave upward throughout the year. Compared to altitude tilt and due south orientation, the tilt has its peak of more than double (in December) whereas the azimuth has a minimum -20° (in June). In summer months, tilt angles start to decrease while the azimuth tends to move to the west with a maximum of -5° . This will cause the panel to capture high solar irradiation and thus generate more energy yield (exceeding 30 kWh) as displayed in the sharp move in power trend line (see Figure 5.16). From November to February the tilt angle is at high (latitude $+15^\circ$) whereas the azimuth angle is in the range of -10° to -15° . This drives the energy yield to be between 24-28 kWh per month.

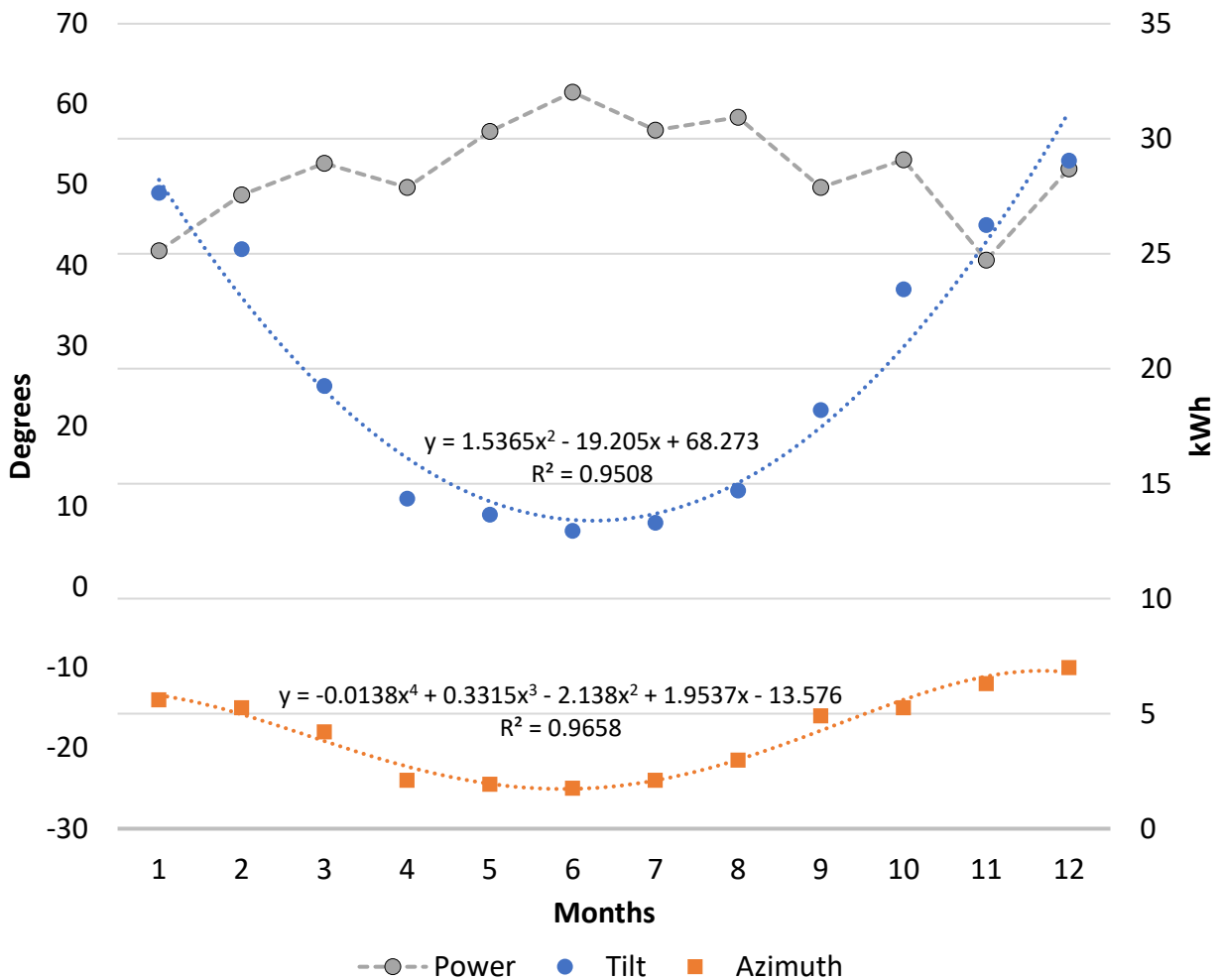


Figure 5.16. The orientation variation with respect to the energy yield

5.5.4. Results validation and optimal annual orientation for 18 cities in Saudi

Arabia

The same optimization procedure was applied for 18 cities in Saudi Arabia using the measurements of RRMM sensors from K.A.CARE from one year, and the results are presented in Table 5.5. Since the data collection project is at its early stages, some stations had missing data. We used the 2015 data, and for the missing data, we used the data for the same hours of the previous or the following year. The annual optimum angles for most of the cities are very close to their respective

latitudes. The highest optimum tilt angles (40 and ° 39°) were found for Tabuk and Alwajh cities, which is consistent with their north locations, with latitudes higher than 26°.

Table 5.5. Annual optimum orientation for 18 cities with energy yield, revenues and suitability

No.	Location	Latitude	Longitude	Annual optimal (Base model)		Annual energy yield (kWh)	Annual potential revenue (\$)	Suitability [178]
				τ°	φ_c°			
1	Abha	18.2227	42.546	22	-25	325.3645	26.0292	Moderate
2	<i>Albaha</i>	<i>20.1794</i>	<i>41.6357</i>	<i>24</i>	<i>-32</i>	<i>330.3742</i>	<i>26.4299</i>	<i>High</i>
3	Aljouf	26.2561	40.02318	33	-54	324.5771	25.9662	-
4	<i>Riyadh</i>	<i>24.90689</i>	<i>46.39721</i>	<i>24</i>	<i>-20</i>	<i>331.4937</i>	<i>26.5195</i>	<i>High</i>
5	Alwajh	26.2561	36.443	39	-56	330.5207	26.4417	-
6	<i>Arar</i>	<i>31.028</i>	<i>40.9056</i>	<i>33</i>	<i>-43</i>	<i>320.679</i>	<i>25.6543</i>	<i>Most</i>
7	<i>Hail</i>	<i>27.39</i>	<i>41.42</i>	<i>28</i>	<i>-33</i>	<i>322.1703</i>	<i>25.7736</i>	<i>High</i>
8	Dammam	26.39497	50.18872	23	-8	309.1162	24.7293	Moderate
9	Al Ahsa	25.34616	49.5956	23	-8	317.0333	25.3627	Moderate
10	Qassim	26.34668	43.76645	25	-30	312.5703	25.0056	High
11	Rania	21.21501	42.84853	24	-32	322.59	25.8072	-
12	Yanbu	23.9865	38.2046	34	-55	320.9651	25.6772	Moderate
13	Al Khafji	28.48	48.48	24	-13	295.5449	23.6436	Moderate
14	<i>Tabuk</i>	<i>28.38284</i>	<i>36.48397</i>	<i>40</i>	<i>-53</i>	<i>343.9283</i>	<i>27.5143</i>	<i>Most</i>
15	Madinah	24.4846	39.5418	32	-50	307.7511	24.6201	Moderate
16	<i>Taif</i>	<i>21.43278</i>	<i>40.49173</i>	<i>26</i>	<i>-35</i>	<i>338.336</i>	<i>27.0669</i>	<i>Most</i>
17	Makkah	21.331	39.949	24	-43	296.139	23.6911	High
18	Wadi Addawasir	20.4301	44.89433	23	-27	328.7003	26.296	Moderate

The results of this study were validated against [178], which offered a high-level overview of potential site suitability for utility-scale PV technology in Saudi Arabia, based on the integration of geographical information system and multi-criteria decision-making tool. A land suitability index is computed to determine potential sites. The locations of the 18 cities are shown on the

suitability map in Figure 5.17. The high suitability areas comprise 50% of all the suitability areas considered, and can be seen mainly spread around the central region.

Tabuk city, with the highest suitability index (Figure 5.17), demonstrates the highest annual potential energy yield of 343.93 kWh and potential yearly revenue of \$27.51 (Table 5.5). This annual energy yield is 9% higher than the annual energy yield when the tilt equals to the latitude and azimuth equals to zero. Also, Taif city which is located in the most suitable area presents the potential of 338.34 kWh and \$27.07. In Riyadh, which has been considered in this study, it shows the third most potential city regarding energy yield. This is due to the high solar irradiation and the mild air temperature year round. From [178], it presents a high suitability index; this is a strong indication that these three locations are the best sites to consider for solar PV. Both studies considered the availability of solar irradiation and the air temperature are the main drivers for ranking the suitability sites.

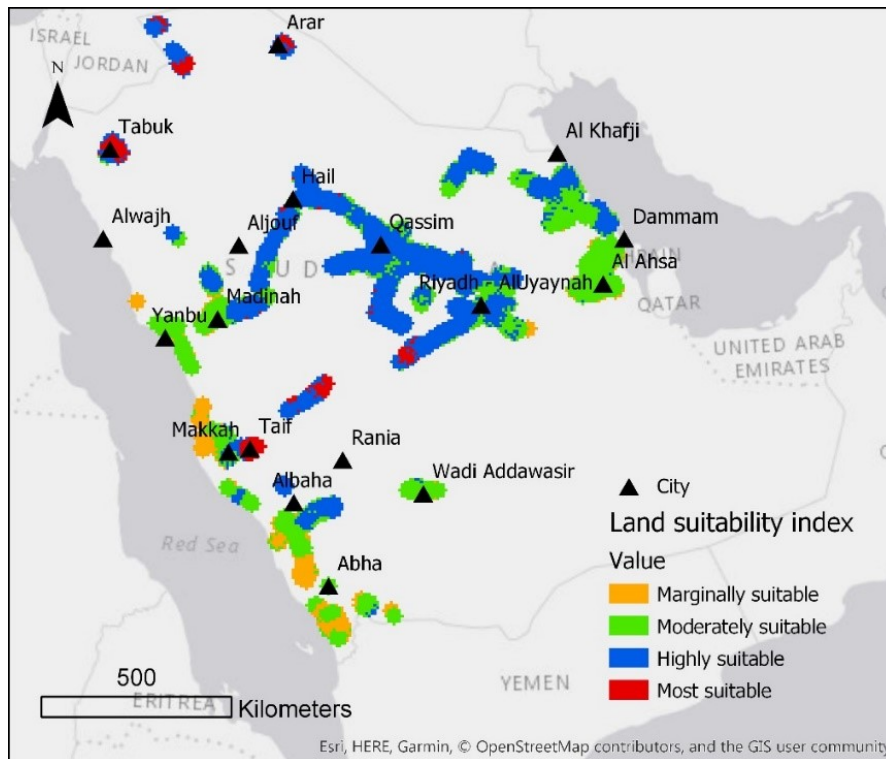


Figure 5.17. Suitability map and solar station sites

Based on both results, high suitability presented in Albaha, Arar, and Hail were associated with a high annual energy yield more than 322 kWh. Tabuk located in the North, Riyadh, Albaha besides Taif city in the West would be the most suitable sites to implement solar PV on a utility-size scale. While these locations account for less than 3% of all the appropriate areas, they offer potential for high-performance solar PV projects regarding energy yield and associated infrastructure costs (see Table 5.5 and Figure 5.17).

5.6. Conclusions

In this chapter, we investigated the impact of the orientation of a fixed solar PV on the energy yield. A case study for Riyadh, Saudi Arabia was conducted. The results of our study show that the monthly adjustment of tilt angle increases the harvested solar energy by 4% compared to the fixed tilt angle. Based on the calculation results, instead of monthly adjustment, it is recommended to adjust the tilt angle five times per year to achieve near-optimal results. This enables harvesting 4% more solar energy than with the fixed annual optimum orientation while minimizing the cost associated with workforce for monthly adjustment or solar trackers. If considering only the fixed direction, the tilt of 24° and azimuth of -20° will lead to the maximum potential power. However, the impact of moving the azimuth from south-facing ($\varphi_c = 0$) to $\varphi_c = -20$ is minor with less than 1% loss in annual potential power.

The optimum orientation, including optimum tilt and azimuth angles of solar panels in 18 cities in Saudi Arabia were studied. Using hourly measured GHI, DHI, DNI and air temperature, a MATLAB detailed model was developed to optimize the tilt and azimuth angles by maximizing the captured solar irradiation and energy yield per square meter.

Chapter 6

Conclusions and Future Directions

6.1. Conclusions

In this thesis, we investigated four interrelated problems towards optimal design and analysis of a grid-connected solar PV system. The first problem tackles the prioritization of RESs under four criteria namely economic, technical, socio-political and environmental. The second problem studies the site suitability of utility-size solar PV system. Then, the design and analysis of solar PV system is examined as the third problem. The fourth and the final problem investigates the optimal orientation of solar PV using a detailed solar irradiation model.

In problem 1, evaluation of five renewable energy resources including solar energy, wind energy, geothermal energy, and biomass energy is performed to examine their potential for electricity generation. Four main criteria (14 sub-criteria) are considered towards prioritization the renewable resources for an energy mix portfolio for Saudi Arabia. The results show solar PV as the most promising alternative (highest weight of 25.6%) followed by solar thermal.

Problem 2 conducts a high-level suitability study of the potential sites for utility-scale PV technology implementation in the study area and defines the degree to which each site is suitable for the placement of PV plants. This suitability was assessed according to the associated criteria and excluding all restrictions. An essential real data of weather including solar irradiation and air temperature are considered in addition to the associated infrastructure data. The approach of integrating the GIS and MCDM effectively excludes the unsuitable sites and produces a land suitability index for potential PV plants where employing utility-size grid-connected PV power

plants varies from the least to the most suitable sites. Chapter 2 and Chapter 3 can be considered as primary stages of installing PV power plants.

Subsequently, in problem 3 of the thesis, we investigate six different designs of tracking system (FT, HMA, HWA, HDA, HCA, VCA, and TA). HOMER software is used for design analysis. A case of Makkah, Saudi Arabia is considered. It was observed that TA can produce 34% more power than FT while VCA can produce up to 20% more power than FT. However, TA requires higher initial, operation, and maintenance costs. VCA presents a high penetration to the grid, low economic costs (LCOE and NPC) and presented a positive ROI compared to all trackers.

Finally, in problem 4 a detailed model was designed to investigate the impact of the fixed solar PV's orientation on the energy yield and to find the optimal tilt and azimuth angles that will generate annual maximum energy yield. This is owing to the emerging discussion of the solar PV orientation and the associated energy losses. The case of Riyadh city is considered. The monthly adjustment of tilt angle increases the harvested solar energy by 4% compared to the fixed tilt angle. Nevertheless, adjusting the panels monthly is associated with challenges such as lack of labor and high costs. Therefore, we propose an adjustment scheme of only five times per year which leads to harvesting almost the same energy as the monthly adjustments scheme with less than 0.5% power losses. The same optimization procedure is applied to calculate the energy yield and system revenue for 18 cities in Saudi Arabia.

The results of this phase were validated against results from Chapter 3, most of the high suitability sites present a high potential for energy yield considering optimal orientation.

6.2. Future Work

This thesis is inspired by the RESs targets set by many countries, and its main objective is to facilitate the decision making towards the deployment of solar PV systems. The chapters of this

thesis narrate how this objective was attained. Yet, some issues still need to be tackled that can be considered as future research works:

- In problem 1 (Chapter 2), further technical and economic sub-criteria could be considered to enrich the model. The accuracy of the model results can be enhanced by using more local data from K.A.CARE.
- In problem 2 more electrical criteria can be noteworthy to consider for determining the best sites including effect on voltage profile on nearby buses, voltage sag/swell, transmission line losses, maximum power injection limits, and maximum power flow rate.
- For the solar PV site suitability problem presented in Chapter 3, tackling hybrid systems including more than one RESs, such as solar PV-wind and solar-biomass could lead to cost effective and technically feasible RES projects. Moreover, applying new techniques as well performing a comparative analysis of such techniques towards an insightful understanding of the best approach, are potential directions for future research. Furthermore, it would be interesting to include other decision criteria to enrich the proposed model, such as population growth, heritage sites, vegetation distribution, and visual impact. Sandstorms, which are a common phenomenon in arid and deserted areas, have a significant impact on PV performance, and therefore avoiding these areas is a crucial factor for more efficient PV systems. Furthermore, considering real long-term data from solar monitoring sensors across the country could enhance the solar irradiation modeling in ArcGIS.
- For the solar PV designs presented in Chapter 4, several limitations can be addressed. First, REFIT can play a vital role in the RES economic viability, and further analysis could be carried out to observe its impact on the economic performance of the system. Moreover, the effect of different models of solar PV with different temperature coefficients and their

effect on power generation, NPC, and LCOE could be investigated. In the future research, a comparative performance analysis of off-grid and grid-connected designs for various locations with different metrological conditions can be investigated. Moreover, hybrid systems such as solar-wind-biomass could be integrated to examine the optimal design.

- Finally, it would be interesting to integrate solar PV into the energy-mix, the demand pattern and market prices in problem 4 (Chapter 5). These factors can play a major role in determining the optimal solar PV panel orientation, as maximizing annual energy yield may not always be appropriate as a sole basis for this determination. Nowadays, various power regulations exist in different countries including time-of-use tariff, peak demand charges and real-time pricing. Accordingly, understanding the load profile of the customer and the associated charges could lead to a proper design to lower the cost on the customer side. In addition, the optimal orientation depends on the site location and climate conditions. However, most of the high solar irradiation regions are hot and arid with low vegetation which can cause dust accumulation on panels that will hinder solar capturing and alter the optimal orientation of solar panels.

Bibliography

- [1] International Renewable Energy Agency, *REthinking Energy 2017: Accelerating the global energy transformation*, vol. 55, no. July. Abu Dhabi, 2017.
- [2] T. Foley, K. Thornton, R. Hinrichs-rahlwes, and S. Sawyer, *Renewables 2015 Global Status Report*. 2015.
- [3] “Data and Statistics - IRENA REsource.” [Online]. Available: <http://resourceirena.irena.org/gateway/dashboard/?topic=4&subTopic=19>. [Accessed: 25-Apr-2018].
- [4] REN 21, “Renewables 2017: global status report 2017,” Paris, France, 2017.
- [5] “Solar PV grew faster than any other fuel in 2016, opening a new era for solar pow.” [Online]. Available: <https://www.iea.org/newsroom/news/2017/october/solar-pv-grew-faster-than-any-other-fuel-in-2016-opening-a-new-era-for-solar-pow.html>. [Accessed: 25-Apr-2018].
- [6] R. Ferroukhi, D. Gielen, G. Kieffer, M. Taylor, D. Nagpal, and A. Khalid, “REthinking Energy: Towards a new power system,” The International Renewable Energy Agency (IRENA), 2014.
- [7] IEA, “Trends 2016 In Photovoltaic Applications, Survey Report Of Selected Iea Countries Between 1992 And 2015,” 2016.
- [8] World Bank, “World Development Indicators,” 2016. [Online]. Available: <http://databank.worldbank.org/data/home.aspx>. [Accessed: 01-Jan-2016].
- [9] EIA, “Saudi Arabia was world’s largest petroleum producer and net exporter,” 2012. [Online]. Available: <https://www.eia.gov/todayinenergy/detail.cfm?id=10231>. [Accessed: 29-Mar-2016].
- [10] “Independent Statistics and Analysis-Saudi Arabia,” 2014. [Online]. Available: <http://www.eia.gov/countries/cab.cfm?fips=SA#note>. [Accessed: 13-Nov-2014].
- [11] “Saudi Energy Efficiency Center,” 2015. [Online]. Available:

- <http://www.seec.gov.sa/?lang=en>. [Accessed: 03-Nov-2015].
- [12] A. DiPaola, “Saudi Arabia Delays \$109 Billion Solar Plant by 8 Years - Bloomberg Business,” 2015. [Online]. Available: <http://www.bloomberg.com/news/articles/2015-01-20/saudi-arabia-delays-109-billion-solar-plant-by-8-years>. [Accessed: 09-Nov-2015].
- [13] “Activities and Achievements of the Authority,” Electricity and Cogeneration Regulatory Authority, Riyadh, Saudi Arabia, 2013.
- [14] M. A. Meleeh, “SEC spends nearly SAR 40-60bn annually on projects.,” 2015. [Online]. Available: <http://english.mubasher.info/news/2747289/SEC-spends-nearly-SAR-40-60bn-annually-on-projects-Al-Shiha#.VUujSflVhHx>. [Accessed: 09-Jun-2015].
- [15] “Sustainability for Future Generations-The Vision of King Abdullah City for Atomic and Renewable Energy,” 2013. [Online]. Available: http://www.kacare.gov.sa/en/?page_id=84. [Accessed: 13-Nov-2014].
- [16] “Saudi electricity annual report,” Saudi electricity company, 2013.
- [17] O. Alnatheer, “The potential contribution of renewable energy to electricity supply in Saudi Arabia,” *Energy Policy*, vol. 33, no. 18, pp. 2298–2312, Dec. 2005.
- [18] F. G. Montoya, M. J. Aguilera, and F. Manzano-Agugliaro, “Renewable energy production in Spain: A review,” *Renewable and Sustainable Energy Reviews*, vol. 33, pp. 509–531, May 2014.
- [19] A. Hepbasli and Z. Alsuhaibani, “A key review on present status and future directions of solar energy studies and applications in Saudi Arabia,” *Renewable and Sustainable Energy Reviews*, vol. 15, no. 9, pp. 5021–5050, Dec. 2011.
- [20] S. Rehman, M. A. Bader, and S. A. Al-Moallem, “Cost of solar energy generated using PV panels,” *Renewable and Sustainable Energy Reviews*, vol. 11, no. 8, pp. 1843–1857, Oct. 2007.
- [21] S. H. Alawaji, “Evaluation of solar energy research and its applications in Saudi Arabia — 20 years of experience,” *Renewable and Sustainable Energy Reviews*, vol. 5, no. 1, pp. 59–77, Mar. 2001.

- [22] “Validation of SolarGIS GHI and DNI data for the Kingdom of Saudi Arabia Technical note,” GeoModel Solar, 2013.
- [23] “IRENA Data and Statistics,” 2015. [Online]. Available: <http://resourceirena.irena.org/gateway/dashboard/index.html>. [Accessed: 10-Jun-2015].
- [24] T. Hurst, “Renewable Power Costs Plummet,” 2015. [Online]. Available: http://www.irena.org/News/Description.aspx?NType=A&mnu=cat&PriMenuID=16&CatID=84&News_ID=386. [Accessed: 09-Jun-2015].
- [25] M. J. Al-Jawah, “A Decision Aiding Framework for Investing in Cleaning Systems for Solar Photovoltaic (PV) Power Plants in Arid Regions,” George Washington University, Washington, DC, USA, 2014.
- [26] “Technology Roadmap: Solar Thermal Electricity,” International Energy Agency (IEA), 2014.
- [27] “Concentrating Solar Power: Technology Brief,” International Renewable Energy Agency (IRENA), 2013.
- [28] World Wind Energy Association, “Wind Power Capacity reaches 539 GW, 52,6 GW added in 2017,” 2018. [Online]. Available: <https://wwindea.org/blog/2018/02/12/2017-statistics/>. [Accessed: 31-Jul-2018].
- [29] A. M. Eltamaly, “Design and implementation of wind energy system in Saudi Arabia,” *Renewable Energy*, vol. 60, pp. 42–52, Dec. 2013.
- [30] S. M. Shaahid, L. M. Al-Hadhrami, and M. K. Rahman, “Potential of Establishment of Wind Farms in Western Province of Saudi Arabia.,” *Energy Procedia*, vol. 52, pp. 497–505, 2014.
- [31] W. E. Alnaser and N. W. Alnaser, “The status of renewable energy in the GCC countries,” *Renewable and Sustainable Energy Reviews*, vol. 15, no. 6, pp. 3074–3098, Aug. 2011.
- [32] I. Bachellerie, “Renewable Energy in the GCC Countries: Resources, Potential, and Prospects.,” Gulf Research Center, 2012.
- [33] “Annual U.S. and Global Geothermal Power Production Report,” Geothermal Energy Association, 2015.

- [34] D. Chandrasekharam, A. Lashin, and N. Al Arifi, "The potential contribution of geothermal energy to electricity supply in Saudi Arabia," *International Journal of Sustainable Energy*, pp. 1–10, Aug. 2014.
- [35] M. T. Hussein, A. Lashin, A. Al Bassam, N. Al Arifi, and I. Al Zahrani, "Geothermal power potential at the western coastal part of Saudi Arabia," *Renewable and Sustainable Energy Reviews*, vol. 26, pp. 668–684, Oct. 2013.
- [36] M. Al-Dayel, "Geothermal resources in Saudi Arabia," *Geothermics*, vol. 17, no. 2–3, pp. 465–476, Jan. 1988.
- [37] H. M. Taleb, "Barriers hindering the utilisation of geothermal resources in Saudi Arabia," *Energy for Sustainable Development*, vol. 13, no. 3, pp. 183–188, Sep. 2009.
- [38] M. S. M. Khan and Z. Kaneesamkandi, "Biodegradable waste to biogas: Renewable energy option for the Kingdom of Saudi Arabia," *International Journal of Innovation and Applied Studies*, vol. 4, no. 1, pp. 101–113, Sep. 2013.
- [39] F. Cavallaro, "Multi-criteria decision aid to assess concentrated solar thermal technologies," *Renewable Energy*, vol. 34, no. 7, pp. 1678–1685, 2009.
- [40] M. B. Shattan, "An analytic-deliberative process for the selection and deployment of radiation detection systems for shipping ports and border crossings," Massachusetts Institute of Technology, Cambridge, Massachusetts, USA, 2008.
- [41] J. R. S. C. Mateo, *Multi-Criteria Analysis in the Renewable Energy Industry*. Santander: Springer Science & Business Media, 2012.
- [42] B. Brand and R. Missaoui, "Multi-criteria analysis of electricity generation mix scenarios in Tunisia," *Renewable and Sustainable Energy Reviews*, vol. 39, pp. 251–261, Nov. 2014.
- [43] M. Amer and T. U. Daim, "Selection of renewable energy technologies for a developing county: A case of Pakistan," *Energy for Sustainable Development*, vol. 15, no. 4, pp. 420–435, Dec. 2011.
- [44] S. Ahmad and R. M. Tahar, "Selection of renewable energy sources for sustainable development of electricity generation system using analytic hierarchy process: A case of

- Malaysia,” *Renewable Energy*, vol. 63, pp. 458–466, Mar. 2014.
- [45] D. Streimikiene, T. Balezentis, I. Krisciukaitienė, and A. Balezentis, “Prioritizing sustainable electricity production technologies: MCDM approach,” *Renewable and Sustainable Energy Reviews*, vol. 16, no. 5, pp. 3302–3311, Jun. 2012.
- [46] E. Georgopoulou, D. Lalas, and L. Papagiannakis, “A multicriteria decision aid approach for energy planning problems: The case of renewable energy option,” *European Journal of Operational Research*, vol. 103, no. 1, pp. 38–54, Nov. 1997.
- [47] M. Beccali, M. Cellura, and M. Mistretta, “Decision-making in energy planning. Application of the Electre method at regional level for the diffusion of renewable energy technology,” *Renewable Energy*, vol. 28, no. 13, pp. 2063–2087, Oct. 2003.
- [48] D. Diakoulaki and F. Karangelis, “Multi-criteria decision analysis and cost–benefit analysis of alternative scenarios for the power generation sector in Greece,” *Renewable and Sustainable Energy Reviews*, vol. 11, no. 4, pp. 716–727, May 2007.
- [49] Y. Goletsis, J. Psarras, and J.-E. Samouilidis, “Project Ranking in the Armenian Energy Sector Using a Multicriteria Method for Groups,” *Annals of Operations Research*, vol. 120, no. 1–4, pp. 135–157, Apr. 2003.
- [50] S. D. Pohekar and M. Ramachandran, “Application of multi-criteria decision making to sustainable energy planning—A review,” *Renewable and Sustainable Energy Reviews*, vol. 8, no. 4, pp. 365–381, Aug. 2004.
- [51] J.-J. Wang, Y.-Y. Jing, C.-F. Zhang, and J.-H. Zhao, “Review on multi-criteria decision analysis aid in sustainable energy decision-making,” *Renewable and Sustainable Energy Reviews*, vol. 13, no. 9, pp. 2263–2278, Dec. 2009.
- [52] T. L. Saaty and L. G. Vargas, *Models, Methods, Concepts and apps of the Analytic Hierarchy Process*, 2nd Editio. New York: Springer US, 2012.
- [53] C. Kahraman, İ. Kaya, and S. Cebi, “A comparative analysis for multiattribute selection among renewable energy alternatives using fuzzy axiomatic design and fuzzy analytic hierarchy process,” *Energy*, vol. 34, no. 10, pp. 1603–1616, Oct. 2009.

- [54] S. Theodorou, G. Florides, and S. Tassou, "The use of multiple criteria decision making methodologies for the promotion of RES through funding schemes in Cyprus, A review," *Energy Policy*, vol. 38, no. 12, pp. 7783–7792, Dec. 2010.
- [55] A. I. Chatzimouratidis and P. A. Pilavachi, "Multicriteria evaluation of power plants impact on the living standard using the analytic hierarchy process," *Energy Policy*, vol. 36, no. 3, pp. 1074–1089, Mar. 2008.
- [56] Fernando Ribeiro, P. Ferreira, and M. Araújo, "Impact Chains and a Multi-Criteria Decision Tool to Support Electricity Power Planning," *Sustainable Electricity Power Planning*, 2012.
- [57] E. W. Stein, "A comprehensive multi-criteria model to rank electric energy production technologies," *Renewable and Sustainable Energy Reviews*, vol. 22, pp. 640–654, Jun. 2013.
- [58] K. Nigim, N. Munier, and J. Green, "Pre-feasibility MCDM tools to aid communities in prioritizing local viable renewable energy sources," *Renewable Energy*, vol. 29, no. 11, pp. 1775–1791, Sep. 2004.
- [59] T. Kaya and C. Kahraman, "Multicriteria renewable energy planning using an integrated fuzzy VIKOR & AHP methodology: The case of Istanbul," *Energy*, vol. 35, no. 6, pp. 2517–2527, Jun. 2010.
- [60] J. Daniel, N. V. R. Vishal, B. Albert, and I. Selvarasan, "Evaluation of the Significant Renewable Energy Resources in India Using Analytical Hierarchy Process," in *Proceedings Of The 19th International Conference On Multiple Criteria Decision Making*, 2010, vol. 634, pp. 13–26.
- [61] F. Elkarmi and I. Mustafa, "Increasing the utilization of solar energy technologies (SET) in Jordan," *Energy Policy*, vol. 21, no. 9, pp. 978–984, Sep. 1993.
- [62] C. Pappas, C. Karakosta, V. Marinakis, and J. Psarras, "A comparison of electricity production technologies in terms of sustainable development," *Energy Conversion and Management*, vol. 64, pp. 626–632, Dec. 2012.
- [63] E. GÖK, "Renewable Energy Planning in Turkey," Middle East Technical University, 2013.

- [64] M. Troldborg, S. Heslop, and R. L. Hough, "Assessing the sustainability of renewable energy technologies using multi-criteria analysis: Suitability of approach for national-scale assessments and associated uncertainties," *Renewable and Sustainable Energy Reviews*, vol. 39, pp. 1173–1184, Nov. 2014.
- [65] A. Phdungsilp and T. Wuttiornpun, "Decision Support for the Selection of Electric Power Plants Generated from Renewable Sources," *World Academy of Science, Engineering & Technology*, vol. 5, no. 3, pp. 131–136, 2011.
- [66] A. I. Chatzimouratidis and P. A. Pilavachi, "Technological, economic and sustainability evaluation of power plants using the Analytic Hierarchy Process," *Energy Policy*, vol. 37, no. 3, pp. 778–787, Mar. 2009.
- [67] B. A. Akash, R. Mamlook, and M. S. Mohsen, "Multi-criteria selection of electric power plants using analytical hierarchy process," *Electric Power Systems Research*, vol. 52, no. 1, pp. 29–35, Oct. 1999.
- [68] A. H. I. Lee, H. H. Chen, and H.-Y. Kang, "Multi-criteria decision making on strategic selection of wind farms," *Renewable Energy*, vol. 34, no. 1, pp. 120–126, Jan. 2009.
- [69] F. E. Boran, E. Dizdar, I. Toktas, K. Boran, C. Eldem, and Ö. Asal, "A Multidimensional Analysis of Electricity Generation Options with Different Scenarios in Turkey," *Energy Sources, Part B: Economics, Planning, and Policy*, vol. 8, no. 1, pp. 44–55, Jan. 2013.
- [70] N. H. Afgan and M. G. Carvalho, "Multi-criteria assessment of new and renewable energy power plants," *Energy*, vol. 27, no. 8, pp. 739–755, Aug. 2002.
- [71] A. Sadeghi, T. Larimian, and A. Molabashi, "Evaluation of Renewable Energy Sources for Generating Electricity in Province of Yazd: A Fuzzy Mcdm Approach," *Procedia - Social and Behavioral Sciences*, vol. 62, pp. 1095–1099, Oct. 2012.
- [72] R. Mamlook, B. A. Akash, and M. S. Mohsen, "A neuro-fuzzy program approach for evaluating electric power generation systems," *Energy*, vol. 26, no. 6, pp. 619–632, Jun. 2001.
- [73] K. R. Craig, R. L. Bain, and R. P. Overend, "Biomass Power Systems—Where are we, where are we going, and how do we get there? The role of gasification.," in *EPRI*

Conference on New Power Generation Technology, 1995, p. 19.

- [74] S. A. M. Said;, I. M. El-Amin;, and A. M. Al-Shehri, “Renewable Energy Potentials in Saudi Arabia,” in *Beirut regional Collaboration Workshop on energy efficiency and renewable energy technology*, 2004, pp. 76–82.
- [75] R. H. Lasseter, “Smart Distribution: Coupled Microgrids,” *Proceedings of the IEEE*, vol. 99, no. 6, pp. 1074–1082, Jun. 2011.
- [76] A. Ipakchi and F. Albuyeh, “Grid of the future,” *IEEE Power & Energy Magazine*, vol. 7, no. 2, pp. 52–62, 2009.
- [77] R. Palma-Behnke, L. Reyes, and G. Jimenez-Estevéz, “Smart grid solutions for rural areas,” in *2012 IEEE Power and Energy Society General Meeting*, 2012, pp. 1–6.
- [78] N. Abd Malek, H. Hasini, A. A. Rahman, and M. N. Jaafar, “An improved solar PV system for Malaysian rural electrification part I: Design and testing of solar PV with tracker and reflectors,” in *2010 IEEE Student Conference on Research and Development (SCORED)*, 2010, no. SCORED, pp. 452–457.
- [79] F. R. Pazheri, N. H. Malik, a. a. Al-Arainy, E. a. Al-Ammar, A. Imthias, and S. O K, “Smart Grid Can Make Saudi Arabia Megawatt Exporter,” *2011 Asia-Pacific Power and Energy Engineering Conference*, pp. 1–4, Mar. 2011.
- [80] “Annual Energy Review,” U.S. Energy Information Administration (EIA), 2011.
- [81] A. H. Mondal, “Implications of renewable energy technologies in the Bangladesh power sector : Long-term planning strategies,” University of Bonn, 2010.
- [82] A. Brown; and S. Müller, “Deploying Renewables: Best and Future Policy Practice,” International Energy Agency (IEA), 2011.
- [83] “Renewable Energy - RD&D Priorities Insights from IEA Technology Programmes,” International Energy Agency (IEA), 2006.
- [84] “Renewable Energy Investing in energy and resource efficien,” United Nations Environment Programme, 2011.
- [85] P. Burgherr, S. Hirschberg, and M. Spada, “Comparative assessment of accident risks in the

- energy sector,” in *Handbook of Risk Management in Energy Production and Trading*, vol. 199, R. M. Kovacevic, G. C. Pflug, and M. T. Vespucci, Eds. Boston, MA: Springer US, 2013.
- [86] P. Burgherr and S. Hirschberg, “Comparative risk assessment of severe accidents in the energy sector,” *Energy Policy*, vol. 74, pp. S45–S56, Feb. 2014.
- [87] M. Wei, S. Patadia, and D. M. Kammen, “Putting renewables and energy efficiency to work: How many jobs can the clean energy industry generate in the US?,” *Energy Policy*, vol. 38, no. 2, pp. 919–931, Feb. 2010.
- [88] “Capital Cost Estimates for Utility Scale Electricity Generating Plants,” U.S. Energy Information Administration (EIA), 2013.
- [89] S. Müller, A. Brown, and S. Ölz, “Policy Considerations for Deploying Renewables,” International Energy Agency (IEA), 2011.
- [90] D. Komljenovic and V. Kecojevic, “Multi-attribute selection method for materials handling equipment,” *International Journal of Industrial and Systems Engineering*, vol. 4, no. 2, pp. 151–173, Mar. 2008.
- [91] “Central Department Of Statistics & Information,” 2014. [Online]. Available: <http://www.cdsi.gov.sa/english/>. [Accessed: 10-Jun-2015].
- [92] J. Arán Carrión, A. Espín Estrella, F. Aznar Dols, M. Zamorano Toro, M. Rodríguez, and A. Ramos Ridaó, “Environmental decision-support systems for evaluating the carrying capacity of land areas: Optimal site selection for grid-connected photovoltaic power plants,” *Renewable and Sustainable Energy Reviews*, vol. 12, no. 9, pp. 2358–2380, Dec. 2008.
- [93] International Finance Corporation, “Utility-Scale solar photovoltaic power plants - a project developer’s guide,” Washington, D.C, 2015.
- [94] A. Lopez, B. Roberts, D. Heimiller, N. Blair, and G. Porro, “U.S. Renewable Energy Technical Potentials : A GIS-Based Analysis U.S. Renewable Energy Technical Potentials : A GIS- Based Analysis,” Washington, D.C, 2012.
- [95] E. Kaijuka, “GIS and rural electricity planning in Uganda,” *Journal of Cleaner Production*,

- vol. 15, no. 2, pp. 203–217, Jan. 2007.
- [96] J. R. Janke, “Multicriteria GIS modeling of wind and solar farms in Colorado,” *Renewable Energy*, vol. 35, no. 10, pp. 2228–2234, Oct. 2010.
- [97] L. D and K. Satish, “GIS based multicriterion site suitability analysis for solar power generation plants in India,” *The International Journal of Science & Technoledge*, vol. 3, no. 3, pp. 197–202, 2015.
- [98] J. M. Sánchez-Lozano, C. Henggeler Antunes, M. S. García-Cascales, and L. C. Dias, “GIS-based photovoltaic solar farms site selection using ELECTRE-TRI: Evaluating the case for Torre Pacheco, Murcia, Southeast of Spain,” *Renewable Energy*, vol. 66, pp. 478–494, Jun. 2014.
- [99] J. M. Sánchez-Lozano, M. S. García-Cascales, and M. T. Lamata, “Comparative TOPSIS-ELECTRE TRI methods for optimal sites for photovoltaic solar farms. Case study in Spain,” *Journal of Cleaner Production*, vol. 127, pp. 387–398, 2016.
- [100] A. Gastli, Y. Charabi, and S. Zekri, “GIS-based assessment of combined CSP electric power and seawater desalination plant for Duqum—Oman,” *Renewable and Sustainable Energy Reviews*, vol. 14, no. 2, pp. 821–827, 2010.
- [101] C. Barrows *et al.*, “Renewable Energy Deployment in Colorado and the West : A Modeling Sensitivity and GIS Analysis,” 2016.
- [102] Y. Noorollahi, R. Itoi, H. Fujii, and T. Tanaka, “GIS model for geothermal resource exploration in Akita and Iwate prefectures, northern Japan,” *Computers and Geosciences*, vol. 33, no. 8, pp. 1008–1021, 2007.
- [103] J. Liu, F. Xu, and S. Lin, “Site selection of photovoltaic power plants in a value chain based on grey cumulative prospect theory for sustainability: A case study in Northwest China,” *Journal of Cleaner Production*, vol. 148, pp. 386–397, 2017.
- [104] M. K. Delivand, A. R. B. Cammerino, P. Garofalo, and M. Monteleone, “Optimal locations of bioenergy facilities, biomass spatial availability, logistics costs and GHG (greenhouse gas) emissions: a case study on electricity productions in South Italy,” *Journal of Cleaner Production*, vol. 99, pp. 129–139, Jul. 2015.

- [105] A. Yousefi-Sahzabi, K. Sasaki, H. Yousefi, S. Pirasteh, and Y. Sugai, “GIS aided prediction of CO₂ emission dispersion from geothermal electricity production,” *Journal of Cleaner Production*, vol. 19, no. 17–18, pp. 1982–1993, Nov. 2011.
- [106] J. M. Sánchez-Lozano, M. S. García-Cascales, and M. T. Lamata, “GIS-based onshore wind farm site selection using Fuzzy Multi-Criteria Decision Making methods. Evaluating the case of Southeastern Spain,” *Applied Energy*, vol. 171, pp. 86–102, Jun. 2016.
- [107] A. Rogeau, R. Girard, and G. Kariniotakis, “A generic GIS-based method for small Pumped Hydro Energy Storage (PHES) potential evaluation at large scale,” *Applied Energy*, vol. 197, pp. 241–253, 2017.
- [108] T. Höfer, R. M. Yasin Sunak, and H. Siddique, “Wind Farm Siting Using a Spatial Analytic Hierarchy Process Approach : A Case Study of the Städteregion Aachen,” vol. 163, no. 16, pp. 1–52, 2014.
- [109] J. Xu, X. Song, Y. Wu, and Z. Zeng, “GIS-modelling based coal-fired power plant site identification and selection,” *Applied Energy*, vol. 159, pp. 520–539, Dec. 2015.
- [110] K. Tisza, “GIS-Based Suitability Modeling and Multi-Criteria Decision Analysis for Utility Scale Solar Plants In Four States in the Southeast US,” Clemson University, 2014.
- [111] D. Mentis *et al.*, “A GIS-based approach for electrification planning—A case study on Nigeria,” *Energy for Sustainable Development*, vol. 29, pp. 142–150, 2015.
- [112] A. Asakereh, M. Omid, R. Alimardani, and F. Sarmadian, “Developing a GIS-based Fuzzy AHP Model for Selecting Solar Energy Sites in Shodirwan Region in Iran,” *International Journal of Advanced Science and Technology*, vol. 68, pp. 37–48, 2014.
- [113] M. Uyan, “GIS-based solar farms site selection using analytic hierarchy process (AHP) in Karapinar region, Konya/Turkey,” *Renewable and Sustainable Energy Reviews*, vol. 28, pp. 11–17, Dec. 2013.
- [114] J. A. Carrión, A. Espín Estrella, F. Aznar Dols, and A. R. Ridao, “The electricity production capacity of photovoltaic power plants and the selection of solar energy sites in Andalusia (Spain),” *Renewable Energy*, vol. 33, no. 4, pp. 545–552, 2008.

- [115] Q. Wang, M. M. M’ikiugu, and I. Kinoshita, “A GIS-based approach in support of spatial planning for renewable energy: A case study of Fukushima, Japan,” *Sustainability (Switzerland)*, vol. 6, no. 4, pp. 2087–2117, 2014.
- [116] A. Massimo, M. Dell’Isola, A. Frattolillo, and G. Ficco, “Development of a Geographical Information System (GIS) for the Integration of Solar Energy in the Energy Planning of a Wide Area,” *Sustainability*, vol. 6, no. i, pp. 5730–5744, 2014.
- [117] M. L. Sabo, N. Mariun, H. Hizam, M. A. Mohd Radzi, and A. Zakaria, “Spatial matching of large-scale grid-connected photovoltaic power generation with utility demand in Peninsular Malaysia,” *Applied Energy*, vol. 191, pp. 663–688, 2017.
- [118] J. M. Sánchez-Lozano, J. Teruel-Solano, P. L. Soto-Elvira, and M. Socorro García-Cascales, “Geographical information Systems and multi-Criteria decision making methods for the evaluation of solar farms locations: Case study in south-eastern Spain,” *Renewable and Sustainable Energy Reviews*, vol. 24, pp. 544–556, Aug. 2013.
- [119] J. M. Sánchez-Lozano, M. S. García-Cascales, and M. T. Lamata, “Evaluation of suitable locations for the installation of solar thermoelectric power plants,” *Computers & Industrial Engineering*, vol. 87, pp. 343–355, Sep. 2015.
- [120] N. Y. Aydin, E. Kentel, and H. Sebnem Duzgun, “GIS-based site selection methodology for hybrid renewable energy systems: A case study from western Turkey,” *Energy Conversion and Management*, vol. 70, pp. 90–106, Jun. 2013.
- [121] H. A. Effat, “Selection of Potential Sites for Solar Energy Farms in Ismailia Governorate, Egypt using SRTM and Multicriteria Analysis,” *Cloud Publications International Journal of Advanced Remote Sensing and GIS*, vol. 2, no. 1, pp. 205–220, 2013.
- [122] J. J. W. Watson and M. D. Hudson, “Regional Scale wind farm and solar farm suitability assessment using GIS-assisted multi-criteria evaluation,” *Landscape and Urban Planning*, vol. 138, pp. 20–31, Jun. 2015.
- [123] A. Kengpol, P. Rontlaong, and M. Tuominen, “Design of a Decision Support System for Site Selection Using Fuzzy AHP: A Case Study of Solar Power Plant in North Eastern Parts of Thailand,” in *Proceedings of PICMET’12: Technology Management for Emerging*

- Technologies (2012)*, 2012, pp. 734–743.
- [124] Y. Charabi and A. Gastli, “PV site suitability analysis using GIS-based spatial fuzzy multi-criteria evaluation,” *Renewable Energy*, vol. 36, no. 9, pp. 2554–2561, Sep. 2011.
- [125] I. Gherboudj and H. Ghedira, “Assessment of solar energy potential over the United Arab Emirates using remote sensing and weather forecast data,” *Renewable and Sustainable Energy Reviews*, vol. 55, pp. 1210–1224, 2016.
- [126] A. Alami Merrouni, A. Mezrhab, and A. Mezrhab, “PV sites suitability analysis in the Eastern region of Morocco,” *Sustainable Energy Technologies and Assessments*, vol. 18, pp. 6–15, 2016.
- [127] W. Yunna and S. Geng, “Multi-criteria decision making on selection of solar–wind hybrid power station location: A case of China,” *Energy Conversion and Management*, vol. 81, pp. 527–533, 2014.
- [128] A. H. I. Lee, H. Y. Kang, C. Y. Lin, and K. C. Shen, “An integrated decision-making model for the location of a PV solar plant,” *Sustainability (Switzerland)*, vol. 7, no. 10, pp. 13522–13541, 2015.
- [129] M. Rumbayan and K. Nagasaka, “Prioritization Decision for Renewable Energy Development Using Analytic Hierarchy Process and Geographic Information System,” in *Advanced Mechatronic Systems (ICAMEchS), 2012 International Conference on. IEEE, 2012.*, 2012, pp. 36–41.
- [130] Y. Charabi, M. Ben Hadj Rhouma, and A. Gastli, “Siting of PV power plants on inclined terrains,” *International Journal of Sustainable Energy*, vol. 35, no. 9, pp. 834–843, 2016.
- [131] E. Borgogno Mondino, E. Fabrizio, and R. Chiabrando, “Site Selection of Large Ground-Mounted Photovoltaic Plants: A GIS Decision Support System and an Application to Italy,” *International Journal of Green Energy*, vol. 12, no. 5, pp. 515–525, 2014.
- [132] T. S. Frank Vignola, Joseph Michalsky, “Solar and Infrared Radiation Measurements,” Boca Raton, FL: CRC Press, 2012, pp. 16–26.
- [133] E. Loken, “Use of multicriteria decision analysis methods for energy planning problems,”

- Renewable and Sustainable Energy Reviews*, vol. 11, no. 7, pp. 1584–1595, Sep. 2007.
- [134] J. P. Huang, K. L. Poh, and B. W. Ang, “Decision analysis in energy and environmental modeling,” *Energy*, vol. 20, no. 9, pp. 843–855, Sep. 1995.
- [135] S. Sener, E. Sener, B. Nas, and R. Karagüzel, “Combining AHP with GIS for landfill site selection: a case study in the Lake Beyşehir catchment area (Konya, Turkey).,” *Waste management*, vol. 30, no. 11, pp. 2037–46, Nov. 2010.
- [136] V. Akbari and M. Rajabi, “Landfill Site Selection by Combining GIS and Fuzzy Multi-Criteria Decision Analysis, Case Study: Bandar Abbas, Iran,” *World Applied Sciences Journal*, vol. 3, no. Supple 1, pp. 39–47, 2008.
- [137] I. A. Chandio, A. N. B. Matori, K. B. WanYusof, M. A. H. Talpur, A.-L. Balogun, and D. U. Lawal, “GIS-based analytic hierarchy process as a multicriteria decision analysis instrument: a review,” *Arabian Journal of Geosciences*, vol. 6, no. 8, pp. 3059–3066, 2013.
- [138] M. M. Mohit, Mohammad Abdul and Ali, “Integrating GIS and AHP for land suitability analysis for urban development in a secondary city of Bangladesh,” *Jurnal Alam Bina*, vol. 8, no. 1, pp. 1–20, 2006.
- [139] M. Izadikhah and R. F. Saen, “A new preference voting method for sustainable location planning using geographic information system and data envelopment analysis,” *Journal of Cleaner Production*, vol. 137, pp. 1347–1367, Nov. 2016.
- [140] M. Herva and E. Roca, “Review of combined approaches and multi-criteria analysis for corporate environmental evaluation,” *Journal of Cleaner Production*, vol. 39, pp. 355–371, Jan. 2013.
- [141] M. Sengupta *et al.*, “Best Practices Handbook for the Collection and Use of Solar Resource Data for Solar Energy Applications,” 2015.
- [142] D. Choudhary and R. Shankar, “An STEEP-fuzzy AHP-TOPSIS framework for evaluation and selection of thermal power plant location: A case study from India,” *Energy*, vol. 42, no. 1, pp. 510–521, 2012.
- [143] J. M. C. Pereira and L. Duckstein, “A multiple criteria decision-making approach to GIS-

- based land suitability evaluation,” *International journal of geographical information systems*, vol. 7, no. 5, pp. 407–424, 1993.
- [144] R. Greene, R. Devillers, J. E. Luther, and B. G. Eddy, “GIS-Based Multiple-Criteria Decision Analysis,” *Geography Compass*, vol. 5, no. 6, pp. 412–432, 2011.
- [145] D. Doljak and G. Stanojević, “Evaluation of natural conditions for site selection of ground-mounted photovoltaic power plants in Serbia,” *Energy*, vol. 127, pp. 291–300, 2017.
- [146] S. Sindhu, V. Nehra, and S. Luthra, “Investigation of feasibility study of solar farms deployment using hybrid AHP-TOPSIS analysis: Case study of India,” *Renewable and Sustainable Energy Reviews*, vol. 73, pp. 496–511, 2017.
- [147] A. Lee, H.-Y. Kang, and Y.-J. Liou, “A Hybrid Multiple-Criteria Decision-Making Approach for Photovoltaic Solar Plant Location Selection,” *Sustainability*, vol. 9, no. 2, p. 184, 2017.
- [148] M. A. Anwarzai and K. Nagasaka, “Utility-scale implementable potential of wind and solar energies for Afghanistan using GIS multi-criteria decision analysis,” *Renewable and Sustainable Energy Reviews*, vol. 71, pp. 150–160, 2017.
- [149] A. Aly, S. S. Jensen, and A. B. Pedersen, “Solar power potential of Tanzania: Identifying CSP and PV hot spots through a GIS multicriteria decision making analysis,” *Renewable Energy*, vol. 113, pp. 159–175, 2017.
- [150] J. Suh and J. R. S. Brownson, “Solar farm suitability using geographic information system fuzzy sets and analytic hierarchy processes: Case study of Ulleung Island, Korea,” *Energies*, vol. 9, no. 8, 2016.
- [151] D. Jun, F. Tian-tian, Y. Yi-sheng, and M. Yu, “Macro-site selection of wind/solar hybrid power station based on ELECTRE-II,” *Renewable and Sustainable Energy Reviews*, vol. 35, pp. 194–204, 2014.
- [152] M. Tahri, M. Hakdaoui, and M. Maanan, “The evaluation of solar farm locations applying Geographic Information System and Multi-Criteria Decision-Making methods: Case study in southern Morocco,” *Renewable and Sustainable Energy Reviews*, vol. 51, pp. 1354–1362, 2015.

- [153] A. Georgiou and D. Skarlatos, “Optimal Site Selection for Sittunga Solar Park using Multi-Criteria Decision Analysis and Geographical Information Systems (GIS),” *Geoscientific Instrumentation, Methods and Data Systems Discussions*, no. March, pp. 1–19, 2016.
- [154] P. Aguayo, “Solar Energy Potential Analysis at Building Scale Using LiDAR and Satellite Data,” University of Waterloo, 2013.
- [155] ESRI, “Modeling solar radiation,” 2016. [Online]. Available: <http://pro.arcgis.com/en/pro-app/tool-reference/spatial-analyst/modeling-solar-radiation.htm>. [Accessed: 04-Apr-2016].
- [156] E. Zell *et al.*, “Assessment of solar radiation resources in Saudi Arabia,” *Solar Energy*, vol. 119, pp. 422–438, Sep. 2015.
- [157] M. El-Metwally, “Sunshine and global solar radiation estimation at different sites in Egypt,” *Journal of Atmospheric and Solar-Terrestrial Physics*, vol. 67, no. 14, pp. 1331–1342, Sep. 2005.
- [158] C. Childs, “Interpolating surfaces in ArcGIS spatial analyst,” *ArcUser, July-September*, vol. 34. ESRI Education Services Editor’s, 2004.
- [159] Y. Kim, K. Shim, M. Jung, and S. Kim, “Accuracy comparison of spatial interpolation methods for estimation of air temperatures in South Korea,” *American Geophysical Union*, 2013.
- [160] Y. Noorollahi, H. Yousefi, and M. Mohammadi, “Multi-criteria decision support system for wind farm site selection using GIS,” *Sustainable Energy Technologies and Assessments*, vol. 13, pp. 38–50, Feb. 2016.
- [161] T. L. Saaty, *The analytic hierarchy process: planning, priority setting, resources allocation*. McGraw-Hill, New York, 1980.
- [162] Systems Research Environmental, “Understanding overlay analysis,” 2011. [Online]. Available: <http://help.arcgis.com/en/arcgisdesktop/10.0/help/index.html#//009z000000rs000000.htm>. [Accessed: 21-Apr-2016].
- [163] T. Mustapha, S. Gauri, and G. Gürbüz, “Mauritania: Renewables Readiness Assessment,”

2015.

- [164] J. Betak, M. Suri, T. Cebecauer, and A. Skoczek, "Solar Resource and Photovoltaic Electricity Potential in EU-MENA Region," in *Proceedings of the 27th European Photovoltaic Solar Energy Conference and Exhibition*, 2012, pp. 2–5.
- [165] Saudi's vision 2030, "Saudi Arabia's Vision 2030," 2016. [Online]. Available: www.vision2030.gov.sa. [Accessed: 01-Jun-2017].
- [166] Saudi Electricity Company, "Solar energy : SEC vision to reduce oil consumption," 2017. [Online]. Available: <https://www.se.com.sa/en-us/pages/newsdetails.aspx?Nid=448>. [Accessed: 18-Aug-2017].
- [167] A. F. Almarshoud, "Performance of solar resources in Saudi Arabia," *Renewable and Sustainable Energy Reviews*, vol. 66, pp. 694–701, 2016.
- [168] V. Fthenakis and H. C. Kim, "Land use and electricity generation: A life-cycle analysis," *Renewable and Sustainable Energy Reviews*, vol. 13, no. 6–7, pp. 1465–1474, Aug. 2009.
- [169] H. Z. Al Garni, A. Kassem, A. Awasthi, D. Komljenovic, and K. Al-Haddad, "A multicriteria decision making approach for evaluating renewable power generation sources in Saudi Arabia," *Sustainable Energy Technologies and Assessments*, vol. 16, pp. 137–150, 2016.
- [170] The U.S. Energy Information Administration (EIA), "Saudi Arabia was world's largest petroleum producer and net exporter in 2012 - Today in Energy - U.S. Energy Information Administration (EIA)," 2013. [Online]. Available: <https://www.eia.gov/todayinenergy/detail.cfm?id=10231>. [Accessed: 01-Jun-2017].
- [171] ECRA, *Annual statistical booklet for electricity and sea water desalination industries*, no. 1. 2014.
- [172] The World Bank Group, "Saudi Arabia, CO2 emissions (metric tons per capita)," 2017. [Online]. Available: <http://data.worldbank.org/country/saudi-arabia>. [Accessed: 01-Jun-2017].
- [173] Saudi Electricity Company, "Consumption tariff," 2017. [Online]. Available:

- <https://www.se.com.sa/en-us/customers/pages/tariffrates.aspx>. [Accessed: 01-Jun-2017].
- [174] Saudi Energy Efficiency Center, “General overview,” 2017. [Online]. Available: <http://www.seec.gov.sa/?lang=en>. [Accessed: 01-Jun-2017].
- [175] S. Bahramara, M. P. Moghaddam, and M. R. Haghifam, “Optimal planning of hybrid renewable energy systems using HOMER: A review,” *Renewable and Sustainable Energy Reviews*, vol. 62, pp. 609–620, Sep. 2016.
- [176] D. Connolly, H. Lund, B. V. Mathiesen, and M. Leahy, “A review of computer tools for analysing the integration of renewable energy into various energy systems,” *Applied Energy*, vol. 87, no. 4, pp. 1059–1082, 2010.
- [177] S. Sinha and S. S. Chandel, “Review of software tools for hybrid renewable energy systems,” *Renewable and Sustainable Energy Reviews*, vol. 32, pp. 192–205, 2014.
- [178] H. Z. Al Garni and A. Awasthi, “Solar PV power plant site selection using a GIS-AHP based approach with application in Saudi Arabia,” *Applied Energy*, vol. 206C, pp. 1225–1240, 2017.
- [179] A. Singh and P. Baredar, “Techno-economic assessment of a solar PV, fuel cell, and biomass gasifier hybrid energy system,” *Energy Reports*, vol. 2, pp. 254–260, Nov. 2016.
- [180] A. Singh, P. Baredar, and B. Gupta, “Computational simulation & optimization of a solar, fuel cell and biomass hybrid energy system using HOMER Pro software,” *Procedia Engineering*, vol. 127, pp. 743–750, 2015.
- [181] S. P. Makhija and S. P. Dubey, “Optimally sized hybrid energy system for auxiliaries of a cement manufacturing unit with diesel fuel price sensitivity analysis,” *International Journal of Ambient Energy*, no. September, pp. 1–12, 2015.
- [182] A. Gheiratmand, R. Effatnejad, and M. Hedayati, “Technical and Economic Evaluation of Hybrid wind / PV / Battery Systems for Off-Grid Areas using HOMER Software,” *International Journal of Power Electronics and Drive System (IJPEDS)*, vol. 7, no. 1, pp. 134–143, 2016.
- [183] M. A. Salam, A. Aziz, A. H. A. Alwaeli, and H. A. Kazem, “Optimal sizing of photovoltaic

- systems using HOMER for Sohar, Oman,” *International Journal of Renewable Energy Research*, vol. 3, no. 2, pp. 301–307, 2013.
- [184] W. M. Amutha and V. Rajini, “Cost benefit and technical analysis of rural electrification alternatives in southern India using HOMER,” *Renewable and Sustainable Energy Reviews*, vol. 62, pp. 236–246, 2016.
- [185] M. K. Shahzad, A. Zahid, T. ur Rashid, M. A. Rehan, M. Ali, and M. Ahmad, “Techno-economic feasibility analysis of a solar-biomass off grid system for the electrification of remote rural areas in Pakistan using HOMER software,” *Renewable Energy*, vol. 106, pp. 264–273, Jun. 2017.
- [186] A. Kaabeche, M. Belhamel, and R. Ibtouen, “Sizing optimization of grid-independent hybrid photovoltaic/wind power generation system,” *Energy*, vol. 36, no. 2, pp. 1214–1222, 2011.
- [187] L. M. Halabi, S. Mekhilef, L. Olatomiwa, and J. Hazelton, “Performance analysis of hybrid PV/diesel/battery system using HOMER: A case study Sabah, Malaysia,” *Energy Conversion and Management*, vol. 144, pp. 322–339, Jul. 2017.
- [188] A. Singh, P. Baredar, and B. Gupta, “Techno-economic feasibility analysis of hydrogen fuel cell and solar photovoltaic hybrid renewable energy system for academic research building,” *Energy Conversion and Management*, vol. 145, pp. 398–414, Aug. 2017.
- [189] F. Baghdadi, K. Mohammedi, S. Diaf, and O. Behar, “Feasibility study and energy conversion analysis of stand-alone hybrid renewable energy system,” *Energy Conversion and Management*, vol. 105, pp. 471–479, Nov. 2015.
- [190] I. Yahyaoui, M. Chaabene, and F. Tadeo, “Evaluation of Maximum Power Point Tracking algorithm for off-grid photovoltaic pumping,” *Sustainable Cities and Society*, vol. 25, pp. 65–73, Aug. 2016.
- [191] I. Yahyaoui, A. Atieh, A. Serna, and F. Tadeo, “Sensitivity analysis for photovoltaic water pumping systems: Energetic and economic studies,” *Energy Conversion and Management*, vol. 135, pp. 402–415, 2017.
- [192] M. Anwari and Ayong Hiendro, “Performance analysis of PV energy system in western

- region of Saudi Arabia,” *Engineering*, vol. 05, no. 01, pp. 62–65, 2013.
- [193] M. a. M. Ramli, A. Hiendro, K. Sedraoui, and S. Twaha, “Optimal sizing of grid-connected photovoltaic energy system in Saudi Arabia,” *Renewable Energy*, vol. 75, pp. 489–495, 2015.
- [194] M. S. Adaramola, “Viability of grid-connected solar PV energy system in Jos, Nigeria,” *International Journal of Electrical Power & Energy Systems*, vol. 61, pp. 64–69, Oct. 2014.
- [195] V. Tomar and G. N. Tiwari, “Techno-economic evaluation of grid connected PV system for households with feed in tariff and time of day tariff regulation in New Delhi – A sustainable approach,” *Renewable and Sustainable Energy Reviews*, vol. 70, pp. 822–835, 2017.
- [196] M. Alam Hossain Mondal and A. K. M. Sadrul Islam, “Potential and viability of grid-connected solar PV system in Bangladesh,” 2011.
- [197] G. Liu, M. G. Rasul, M. T. O. Amanullah, and M. M. K. Khan, “Techno-economic simulation and optimization of residential grid-connected PV system for the Queensland climate,” *Renewable Energy*, vol. 45, pp. 146–155, 2012.
- [198] A. Raturi, A. Singh, and R. D. Prasad, “Grid-connected PV systems in the Pacific Island Countries,” *Renewable and Sustainable Energy Reviews*, vol. 58, pp. 419–428, 2016.
- [199] K. Y. Lau, N. A. Muhamad, Y. Z. Arief, C. W. Tan, and A. H. M. Yatim, “Grid-connected photovoltaic systems for Malaysian residential sector: Effects of component costs, feed-in tariffs, and carbon taxes,” *Energy*, vol. 102, pp. 65–82, May 2016.
- [200] O. Hafez and K. Bhattacharya, “Optimal planning and design of a renewable energy based supply system for microgrids,” *Renewable Energy*, vol. 45, pp. 7–15, 2012.
- [201] H. Kim, S. Baek, E. Park, and H. J. Chang, “Optimal green energy management in Jeju, South Korea – On-grid and off-grid electrification,” *Renewable Energy*, vol. 69, pp. 123–133, 2014.
- [202] S. Mirhassani, H. C. Ong, W. T. Chong, and K. Y. Leong, “Advances and challenges in grid tied photovoltaic systems,” *Renewable and Sustainable Energy Reviews*, vol. 49, pp. 121–131, 2015.

- [203] M. A. Eltawil and Z. Zhao, “Grid-connected photovoltaic power systems: Technical and potential problems—A review,” *Renewable and Sustainable Energy Reviews*, vol. 14, no. 1, pp. 112–129, 2010.
- [204] M. A. M. Ramli and S. Twaha, “Analysis of renewable energy feed-in tariffs in selected regions of the globe: Lessons for Saudi Arabia,” *Renewable and Sustainable Energy Reviews*, vol. 45, pp. 649–661, 2015.
- [205] S. A. S. Eldin, M. S. Abd-Elhady, and H. A. Kandil, “Feasibility of solar tracking systems for PV panels in hot and cold regions,” *Renewable Energy*, vol. 85, pp. 228–233, 2016.
- [206] International Finance Corporation, *Utility scale solar power plants - a guide for developers and investors*. New Delhi, India: International Finance Corporation, 2012.
- [207] Lindsay Porter, *The renewable energy home handbook*, Illustrate. Dorchester, UK: Veloce Publishing, 2015.
- [208] Basudev Pradhan, “Available energy resources in rural India: Rural energy technology,” Jharkhand, India, 2015.
- [209] R. Sen and S. C. Bhattacharyya, “Off-grid electricity generation with renewable energy technologies in India: An application of HOMER,” *Renewable Energy*, vol. 62, pp. 388–398, Feb. 2014.
- [210] H. Belmili, M. Haddadi, S. Bacha, M. F. Almi, and B. Bendib, “Sizing stand-alone photovoltaic-wind hybrid system: Techno-economic analysis and optimization,” *Renewable and Sustainable Energy Reviews*, vol. 30, pp. 821–832, 2014.
- [211] B. Bogno, M. Sali, and M. Aillerie, “Technical and economic sizing of the energy storage in an autonomous hybrid power generator for rural electrification in sub-equatorial area of Africa,” *Energy Procedia*, vol. 74, pp. 707–717, 2015.
- [212] S. Baek *et al.*, “Optimal renewable power generation systems for Busan metropolitan city in South Korea,” *Renewable Energy*, vol. 88, pp. 517–525, 2016.
- [213] P. A. Shinde and V. B. Virulkar, “Sizing of a stand-alone photovoltaic system at minimum cost for GCOE, Amravati,” in *Electrical, Computer and Communication Technologies*

(ICECCT), 2015 IEEE International Conference on. IEEE, 2015., 2015.

- [214] S. B. Jeyaprabha and a. I. Selvakumar, “Optimal sizing of photovoltaic/battery/diesel based hybrid system and optimal tilting of solar array using the artificial intelligence for remote houses in India,” *Energy and Buildings*, vol. 96, pp. 40–52, 2015.
- [215] International Energy Agency, “Next generation wind and solar power - from cost to value,” Paris, France, 2016.
- [216] G. C. Lazaroiu, M. Longo, M. Roscia, and M. Pagano, “Comparative analysis of fixed and sun tracking low power PV systems considering energy consumption,” *Energy Conversion and Management*, vol. 92, pp. 143–148, 2015.
- [217] Catalin Alexandru, “A comparative analysis between the tracking solutions implemented on a photovoltaic string,” *Journal of Renewable and Sustainable Energy*, 2014.
- [218] M. Mostafa, R. Daniel, and Q. Guillermo, “Effects of surroundings snow coverage and solar tracking on photovoltaic systems operating in Canada,” *Journal of Renewable and Sustainable Energy*, vol. 5, no. 5, 2013.
- [219] H. Mousazadeh, A. Keyhani, A. Javadi, H. Mobli, K. Abrinia, and A. Sharifi, “A review of principle and sun-tracking methods for maximizing solar systems output,” *Renewable and Sustainable Energy Reviews*, vol. 13, no. 8, pp. 1800–1818, 2009.
- [220] R. Eke and A. Senturk, “Performance comparison of a double-axis sun tracking versus fixed PV system,” *Solar Energy*, vol. 86, no. 9, pp. 2665–2672, 2012.
- [221] M. S. Ismail, M. Moghavvemi, and T. M. I. Mahlia, “Analysis and evaluation of various aspects of solar radiation in the Palestinian territories,” *Energy Conversion and Management*, vol. 73, pp. 57–68, 2013.
- [222] S. Abdallah, “The effect of using sun tracking systems on the voltage–current characteristics and power generation of flat plate photovoltaics,” *Energy Conversion and Management*, vol. 45, no. 11, pp. 1671–1679, 2004.
- [223] H. Z. Al Garni and A. Awasthi, “Techno-Economic Feasibility Analysis of a Solar PV Grid-Connected System with Different Tracking Using HOMER Software,” in *2017 the 5th IEEE*

- International Conference on Smart Energy Grid Engineering*, 2017, pp. 217–222.
- [224] P. Ineichen, “Long Term Satellite Global, Beam and Diffuse Irradiance Validation,” *Energy Procedia*, vol. 48, pp. 1586–1596, 2014.
- [225] M. S. Ismail, M. Moghavvemi, T. M. I. Mahlia, K. M. Muttaqi, and S. Moghavvemi, “Effective utilization of excess energy in standalone hybrid renewable energy systems for improving comfort ability and reducing cost of energy: A review and analysis,” *Renewable and Sustainable Energy Reviews*, vol. 42, pp. 726–734, 2015.
- [226] Homerenergy, “HOMER Pro version 3 . 7 user manual,” Colorado, USA, 2016.
- [227] EcoDirect., “Canadian Solar- mono solar panel - black frame,” 2015. [Online]. Available: <http://www.ecodirect.com/Canadian-Solar-CS6K-280M-T4-4BB-280W-Mono-Black-p/cs6k-280m-t4-4bb.htm>. [Accessed: 01-May-2017].
- [228] EcoDirect., “Advanced Energy 260,000 watt 480 volt inverter,” 2015. [Online]. Available: <http://www.ecodirect.com/PV-Powered-PVP280kW-480-260kW-480-VAC-p/pv-powered-pvp260kw-480.htm>. [Accessed: 01-May-2017].
- [229] Sunanda and Chandel, “Analysis of fixed tilt and sun tracking photovoltaic–micro wind based hybrid power systems,” *Energy Conversion and Management*, vol. 115, pp. 265–275, 2016.
- [230] I. Rey-Stolle, “Fundamentals of Photovoltaic Cells and Systems,” in *Solar Energy*, G. M. Crawley, Ed. World Scientific, 2016, pp. 31–67.
- [231] U.S. Energy Information Administration, “More than half of utility-scale solar photovoltaic systems track the sun through the day,” 2017. [Online]. Available: <https://www.eia.gov/todayinenergy/detail.php?id=30912>. [Accessed: 05-Jul-2017].
- [232] D. Yang, J. Kleissl, C. A. Gueymard, H. T. C. Pedro, and C. F. M. Coimbra, “History and trends in solar irradiance and PV power forecasting: A preliminary assessment and review using text mining,” *Solar Energy*, Feb. 2018.
- [233] M. A. Green *et al.*, “Solar cell efficiency tables (version 50),” *Progress in Photovoltaics: Research and Applications*, vol. 25, no. 7, pp. 668–676, 2017.

- [234] T. O. Kaddoura, M. A. M. Ramli, and Y. A. Al-Turki, "On the estimation of the optimum tilt angle of PV panel in Saudi Arabia," *Renewable and Sustainable Energy Reviews*, vol. 65, pp. 626–634, 2016.
- [235] N.Nijegorodov, K.R.S.Devan, P.K.Jain, and S.Carlsson, "Atmospheric transmittance models and an of an absorber plate, variously oriented at any latitude," *Renewable Energy*, vol. 4, no. 5, pp. 529–543, 1994.
- [236] I. H. Rowlands, B. P. Kemery, and I. Beausoleil-Morrison, "Optimal solar-PV tilt angle and azimuth: An Ontario (Canada) case-study," *Energy Policy*, vol. 39, no. 3, pp. 1397–1409, 2011.
- [237] Y. Lv, P. Si, X. Rong, J. Yan, Y. Feng, and X. Zhu, "Determination of optimum tilt angle and orientation for solar collectors based on effective solar heat collection," *Applied Energy*, vol. 219, no. March, pp. 11–19, 2018.
- [238] S. Dey, M. K. Lakshmanan, and B. Pesala, "Optimal Solar Tree Design for Increased Flexibility in Seasonal Energy Extraction," *Renewable Energy*, vol. 125, pp. 1038–1048, 2018.
- [239] H. K. Elminir, A. E. Ghitas, F. El-Hussainy, R. Hamid, M. M. Beheary, and K. M. Abdel-Moneim, "Optimum solar flat-plate collector slope: Case study for Helwan, Egypt," *Energy Conversion and Management*, vol. 47, no. 5, pp. 624–637, 2006.
- [240] C. L. Cheng, C. S. Sanchez Jimenez, and M. C. Lee, "Research of BIPV optimal tilted angle, use of latitude concept for south orientated plans," *Renewable Energy*, vol. 34, no. 6, pp. 1644–1650, 2009.
- [241] M. Z. Jacobson and V. Jadhav, "World estimates of PV optimal tilt angles and ratios of sunlight incident upon tilted and tracked PV panels relative to horizontal panels," *Solar Energy*, vol. 169, pp. 55–66, Jul. 2018.
- [242] E. Abdeen, M. Orabi, and E. S. Hasaneen, "Optimum tilt angle for photovoltaic system in desert environment," *Solar Energy*, vol. 155, pp. 267–280, 2017.
- [243] A. Gharakhani Siraki and P. Pillay, "Study of optimum tilt angles for solar panels in different latitudes for urban applications," *Solar Energy*, vol. 86, no. 6, pp. 1920–1928,

- 2012.
- [244] R. Xu, K. Ni, Y. Hu, J. Si, H. Wen, and D. Yu, "Analysis of the optimum tilt angle for a soiled PV panel," *Energy Conversion and Management*, vol. 148, pp. 100–109, 2017.
- [245] Y. El Mghouchi, E. Chham, M. S. Krikiz, T. Ajzoul, and A. El Bouardi, "On the prediction of the daily global solar radiation intensity on south-facing plane surfaces inclined at varying angles," *Energy Conversion and Management*, vol. 120, pp. 397–411, Jul. 2016.
- [246] S. Soulayman and M. Hammoud, "Optimum tilt angle of solar collectors for building applications in mid-latitude zone," *Energy Conversion and Management*, vol. 124, pp. 20–28, Sep. 2016.
- [247] H. Moghadam, F. F. Tabrizi, and A. Z. Sharak, "Optimization of solar flat collector inclination," *Desalination*, vol. 265, no. 1–3, pp. 107–111, 2011.
- [248] M. Benghanem, "Optimization of tilt angle for solar panel: Case study for Madinah, Saudi Arabia," *Applied Energy*, vol. 88, no. 4, pp. 1427–1433, 2011.
- [249] H. Khorasanizadeh, K. Mohammadi, and A. Mostafaeipour, "Establishing a diffuse solar radiation model for determining the optimum tilt angle of solar surfaces in Tabass, Iran," *Energy Conversion and Management*, vol. 78, pp. 805–814, 2014.
- [250] J. a. Duffie, W. a. Beckman, and W. M. Worek, *Solar Engineering of Thermal Processes, 4th ed.*, 2nd ed., vol. 116. New York, NY, USA, 2003.
- [251] H. Z. Al Garni, A. Awasthi, and M. A. M. Ramli, "Optimal design and analysis of grid-connected photovoltaic under different tracking systems using HOMER," *Energy Conversion and Management*, vol. 155C, pp. 42–57, 2018.
- [252] A. K. Yadav and S. S. Chandel, "Tilt angle optimization to maximize incident solar radiation: A review," *Renewable and Sustainable Energy Reviews*, vol. 23, pp. 503–513, 2013.
- [253] K.A.CARE, "Solar monitoring network summary," 2016. [Online]. Available: <https://rratlas.kacare.gov.sa/RRMMDDataPortal/en/Reports/Home/SolarMonitoringNetworkSummary>. [Accessed: 02-Apr-2018].

- [254] G. M. Masters, *Renewable and Efficient Electric Power Systems*. New Jersey: A John Wiley & sons, inc., publication, 2004.
- [255] Sandia lab., “ASHRAE IAM Model,” 2018. [Online]. Available: <https://pvpmc.sandia.gov/modeling-steps/1-weather-design-inputs/shading-soiling-and-reflection-losses/incident-angle-reflection-losses/ashre-model/>. [Accessed: 10-May-2018].
- [256] Solar First, “Module characterization angle of incidence response of first solar modules,” 2016.
- [257] C. A. Gueymard, “Direct and indirect uncertainties in the prediction of tilted irradiance for solar engineering applications,” *Solar Energy*, vol. 83, no. 3, pp. 432–444, 2009.
- [258] S. Ekici and M. A. Kopru, “Investigation of PV system cable losses,” *International Journal of Renewable Energy Research*, vol. 7, no. 2, 2017.
- [259] A. Z. Sahin, S. Rehman, and F. Al-Sulaiman, “Global solar radiation and energy yield estimation from photovoltaic power plants for small loads,” *International Journal of Green Energy*, vol. 14, no. 5, pp. 490–498, 2017.